1-1-1998

Smectic ordering of rod-like polymers owing to monodispersity of chain length : synthesis and characterization of benzyl and (4-hexadecyloxy)benzyl esters of monodisperse derivatives of poly(a, L-glutamate).

Seungju Yu
University of Massachusetts Amherst

SMECTIC ORDERING OF ROD-LIKE POLYMERS OWING TO MONODISPERSITY OF CHAIN LENGTH: SYNTHESIS AND CHARACTERIZATION OF BENZYL AND (4-HEXADECYLOXY)BENZYL ESTERS OF MONODISPERSE DERIVATIVES OF POLY(α, L-GLUTAMATE)

A Dissertation Presented

by

SEUNGJU YU

Submitted to the Graduate School of the

University of Massachusetts Amherst in partial fulfillment

of the requirements for the degree of

DOCTOR OF PHILOSOPHY

September 1998

Department of Polymer Science and Engineering

SMECTIC ORDERING OF ROD-LIKE POLYMERS OWING TO MONODISPERSITY OF CHAIN LENGTH: SYNTHESIS AND CHARACTERIZATION OF BENZYL AND (4-HEXADECYLOXY)BENZYL ESTERS OF MONODISPERSE DERIVATIVES OF POLY(α, L-GLUTAMATE)

A Dissertation Presented

by

SEUNGJU YU

Approved as to style and content by:

David A. Tirrell, Chair

Thomas P. Russell, Member

Horst H. Winter, Member

Richard J. Farris, Department Head
Department of Polymer Science and
Engineering

ACKNOWLEDGMENTS

The long road to a Ph.D. is never walked alone. Along the way many people have offered me encouragement, support, and guidance. To all of them I give my deepest thanks, especially

My advisor, Professor David Tirrell, for his insight, direction, perspective, and vision.

My masters advisor, Professor Jung-Il Jin, for introducing me into a wonderful world of polymer science.

Professor Vincent Conticello and Dr. Guanghui Zhang, for their early contribution to the project which provided the basis of this thesis.

The rest of my dissertation committee, Professors Thomas Russell and Horst Winter for their comments and suggestions.

Professor Edward Atkins and Dr. Alan Wadon for sharing their X-ray diffraction expertise.

Professor Samuel Gido and his group members for their help and discussion related to microscopy experiments.

My close friends and comrades, for provocative conversation, intellectual stimulation, welcome distraction and occasional commiseration.

My family, for their understanding and patience.

My wife, Junghye, who, more than anyone else, made this all possible with her encouragement, support, and love.

ABSTRACT

SMECTIC ORDERING OF ROD-LIKE POLYMERS OWING TO MONODISPERSITY OF CHAIN LENGTH: SYNTHESIS AND CHARACTERIZATION OF BENZYL AND (4-HEXADECYLOXY)BENZYL ESTERS OF MONODISPERSE DERIVATIVES OF POLY(α, L-GLUTAMATE)

SEPTEMBER 1998

SEUNGJU YU, B. S., KOREA UNIVERSITY

M. S., KOREA UNIVERSITY

PH. D., UNIVERSITY OF MASSACHUSETTS AMHERST

Directed by: Professor David A. Tirrell

Two types of monodisperse rod-like polymers, poly(γ-benzyl α,L-glutamate) (PBLG) and poly(γ-4-(hexadecyloxy)benzyl α,L-glutamate) with backbone sequences of **1** have been prepared by chemical modification of monodisperse poly(α,L-glutamic acid) (PLGA) that was synthesized by recombinant DNA biosynthesis techniques. The monodisperse PLGA (**1**) was produced in *Escherichia coli* as a fusion to mouse dihydrofolate reductase and purified to homogeneity by metal affinity chromatography, CNBr digestion and ion-exchange chromatography.

$$GluAsp(Glu_{17}Asp)_{X}GluGlu \quad x=3, 4, 5, 6 \qquad \mathbf{1}$$

The monodisperse PBLG derived from **1** showed smectic ordering both in solution and in films as characterized by polarized light optical microscopy and X-ray diffraction. The layer spacings of smectic order were nearly identical to the expected length of the rods, given the axial rise per residue of 1.5 Å for the α-helix. X-ray diffraction patterns of magnetically oriented films were consistent with the supramolecular structure in which helical rods are arranged in layers with their helical axes approximately perpendicular to the smectic layers.

Transmission electron microscopy and electron diffraction on the PBLG films revealed a banded morphology with an approximately 120 nm period which provides strong evidence for helical rotation of the director field as in cholesteric order. Detailed examination of the relative orientation of the banding in the morphology image and the reflections in the electron diffraction pattern leads to the conclusion that the structure of the unoriented smectic PBLG is that of a smectic A*.

The monodisperse poly(γ-4-(hexadecyloxy)benzyl α,L-glutamate)s exhibit strong melting transitions at around 40°C; however no ordered melt was observed due in part to the reduced aspect ratio brought about by the long alkyl side groups.

TABLE OF CONTENTS

Page

LIST OF TABLES

LIST OF FIGURES

CHAPTER 1

INTRODUCTION

1.1 Chemical Synthesis vs. Biological Synthesis of Polymers

Polymer science is a science of mixtures. From synthesis to physical properties, many aspects of polymer science are governed by statistics[1]. Synthetic polymers are characterized by heterogeneity in chain length, stereochemistry, comonomer sequence and overall composition. Most synthetic polymers can adopt many different conformations which result from the different conformations of each repeating unit. However, in nature, there exists a class of polymer called proteins that does not seem to follow the rules of statistics shared by most synthetic polymers[2]. Proteins are unique macromolecules that are present in nature as highly controlled polymers both in terms of primary sequence and three dimensional structure. The protein synthesis machinery, machinery that has been refined over a long period of time by evolution, can produce polymer that is so specifically controlled that only a few conformational states are strongly favored. Such well defined molecular architectures are the key ingredient for the activity of enzymes, the best catalysts known.

Even given the remarkable developments in polymerization technique, e.g. living polymerization, the statistical nature of the repeated reactions prerequisite for polymer synthesis limits the absolute control of polymer molecular architecture[3]. The protein synthesis machinery overcomes such statistical limitations by employing template-directed polymerization. DNA, the primary template, is transcribed into messenger ribonucleic acid (mRNA), a secondary template, with remarkable accuracy and mRNA can be translated into polypeptide with very high fidelity (Fig. 1.1).

Continuing progress in the synthesis, cloning and expression of artificial DNA has provided a powerful method for the preparation of structurally homogeneous "synthetic"

polypeptides[5,6]. This development raises important questions about the role of molecular heterogeneity, e.g. polydispersity, in determining the behavior of polymeric substances, and offers the prospect of significant new opportunities in polymer materials science.

1.2 Poly(α-amino acid)s

Typically, poly(α-amino acid)s are prepared by ring-opening polymerization of α-amino acid N-carboxy-anhydrides (NCAs)[7]. The NCAs are commonly prepared from their amino acids by either Leuchs method, which involves cyclization of N-alkoxycarbonyl halogenides, or the Fuchs-Farthing method, a simpler and more widely used method where NCAs are prepared by direct reaction of free amino acids with phosgene. Polymerization of NCAs can occur by two different mechanisms, namely the *amine mechanism* and the *activated monomer mechanism*, depending on the relative nucleophilicity and basicity of the initiator. Rough control of molecular weight is possible when an NCA is polymerized with a primary aliphatic amine initiator, through the amine mechanism, when the monomer to initiator ratio is below 100. Recently, Deming reported discovery of an organonickel initiator that significantly reduced side reactions during NCA polymerization[8,9]. By using this initiator he was able to achieve true living polymerization which allowed him to make well-defined block copolymers of poly(α-amino acids). Relatively easy access to the monomers and straightforward polymerization leading to high molecular weight have made NCA polymerization the method of choice for the synthesis of high molecular weight poly(α-amino acid)s. However none of these synthetic procedures comes even close to the level of control that the protein synthesis machinery provides.

The most important type of conformation found in fibrous proteins is the α-helix. In this structure the polypeptide chain coils in a spiral manner (Fig. 1.2). The helix is held together by intrachain hydrogen bonding. The direction of this hydrogen bond is nearly parallel to the helix axis. It requires 18 residues to complete 5 turns with a pitch of 5.4 Å

and the axial advance per residue is 1.5 Å. Although a right-handed α-helix can form from either D- or L-amino acids (but not from racemic mixture of the two), the right-handed version is more stable with the natural L-amino acids. The stability of the helix is governed by the nature of side-chain groups and their sequence along the chain. Polyalanine, where the side chains are small and uncharged, forms a stable α-helix. However, polylysine does not form a helix at neutral pH since the side chains are charged and electrostatic repulsion between the neighboring ammonium groups disrupts the regular coil and forces the polymer to adopt a random coil conformation. For a similar reason, polyglutamic acid exists as a random coil at pH 7, where the side chain carboxy groups are ionized, and as an α–helix at pH 2, where they are uncharged (protonated). When the side chains of polyglutamic acid are alkylated, the polymer becomes soluble in many organic solvents. In organic solvents, the α-helical conformation is further stabilized because the hydrogen bonds that stabilize the helical structure are less likely to be destroyed. Typically, poly(γ-benzyl α,L glutamate), a benzyl derivative of PLGA, can form an α-helical conformation with a persistence length of more than 900 Å. For this reason, this polymer is considered to be a typical example of a rod-like macromolecule[11].

1.3 Liquid Crystals

In general, matter exists in nature as three different phases- solid, liquid, and gas- with the stability of each phase governed by temperature and pressure. However, there exist in nature compounds which exhibit a thermodynamically stable phase between the solid and isotropic liquid. This fourth state of matter which possesses both the crystalline characteristics of the solid state and the fluidity of the liquid state is called the "liquid crystalline" phase (Fig. 1.3)[12].

The liquid crystalline state was first detected more than 100 years ago by the Austrian botanist and chemist, Friedrich Reinitzer. In 1888, he synthesized several ester

derivatives of cholesterol and found an unusual "double melting" i.e., at a certain temperature the compound changes from the crystalline solid phase to an opaque liquid which transforms at a defined higher temperature to an optically clear liquid. Otto Lehmann, a leading crystallographer at that time, intuitively suggested that the optical anisotropy of these liquids is due to elongated molecules which are oriented, with their long axes, parallel to each other and created the name "Flussige Kristalle" (liquid crystal). Daniel Vorlander was the one of the first scientists to conduct systematic synthetic work in order to find connections between molecular structure and liquid crystallinity and correctly concluded that liquid crystallinity originates from the linear shape of the molecular structure. Today, it is clear that, in principle, this explanation is valid and liquid crystals are being used in a variety of applications ranging from high strength fibers and thermography to optoelectronic displays.

Asymmetry of molecular shape is a common feature to all substances that show liquid crystallinity whether they are rod-like or plate-like. Compounds which exhibit the liquid crystalline phase in a certain temperature interval are called "thermotropic" liquid crystals and compounds showing the liquid crystalline phase in solution are called "lyotropic" liquid crystals. For thermotropic LCs, extensive investigation both in terms of synthesis and application has been performed and a wealth of information is now available for the type of mesogenic compounds, their transition temperatures and latent heats[13]. Lyotropic LCs occur abundantly in nature and their structures are often quite complex. Lamella or micelle-like arrangements of amphiphiles in water and cholesteric phases of synthetic polypeptides, e.g., poly(γ-benzyl α,L- glutamate), in organic solvents are typical examples of lyotropic liquid crystals. Liquid crystals can be categorized into at least four structurally different phases.

Nematic Phase: At present about 20,000 compounds with nematic phases are known[13]. This is the most abundant and most liquid-like LC structure in which, contrary

to isotropic liquids, one or two molecular axes are oriented parallel to one another, resulting in long-range orientational order (Fig. 1.4 a).

Smectic Phase: Rod-like molecules are able to form liquid crystalline phases where, in addition to the orientational order of the molecular long axes, the centers of gravity of the molecules are, on average, arranged in equidistant planes so that a layer-like structure results[14] (Fig. 1.4 b). There are several different types of smectic phases distinguished by the orientation and order of molecules within the smectic layer. In the smectic A phase, the long axes of molecules are perpendicular to the layer plane, and in the smectic C phase, there is a tilt of the molecular long axes with respect to the layer normal. Depending on the type of order within the layer, smectic phases are further divided into smectic B (hexagonal order) and smectic E (orthogonal order).

Cubic Phase: There are a few rod-like compounds which exhibit cubic mesophases[12]. The cubic mesophase has a structure similar to micellar lattice units (cubic arrangement of micelle-like spheres) or complicated interwoven network (Fig. 1.5 a). This phase appears isotropic in a polarized light optical microscope.

Columnar Phase: This phase is observed in solutions and melts of large rod-like polymers, in certain soap phases, as well as with disc-like molecules and is characterized by a set of X-ray reflections that can be indexed to a two dimensional hexagonal lattice (Fig. 1.5 b). However, no long-range order is seen along the column (the direction normal to the two dimensional lattice). Variations of this organization, one with a two dimensional rectangular lattice and the other having average tilt of the molecules with respect to the plane normal to the column axis, are also included among the columnar phases.

1.4 Liquid Crystalline Order in Chiral Compounds

When molecules that form liquid crystalline phases are optically active, a variation in the LC ordering takes place. The cholesteric state is a variant of the nematic state occurring in chiral compounds. The directors of the neighboring quasi-nematic like

molecular organizations are rotated at a constant angle and the LC phase has a twisted structure as shown in Figure 1.6. The first observation of this phase was with cholesterol derivatives from which the term cholesteric phase was coined[23]. The cholesteric phase can be transformed into the nematic phase by use of electric or magnetic fields or by surface interaction. In the case of smectic phases, two types of chiral smectic phases, smectic C* and smectic A* are possible. In the smectic C*, molecules are tilted in the layers as smectic C ordering, however the projection of the tilt on the layer plane rotates from one layer to the next layer so that a twisted arrangement is continued throughout the sample (Fig. 1.7 a). This is the most common chiral smectic phase and the ferroelectric properties of this phase have received much attention for potential fast-response switch and display applications. Smectic A* has been observed only with several thermotropic LCs[22]. The structure of this phase is depicted schematically in Figure 1.7 b. Unlike the smectic C* whose helical axis is normal to the layers, smectic A* has its helical axis parallel to them. The structure can be looked upon as a series of smectic A blocks or grains separated by twist grain boundaries. The director is rotated by a constant angle on going from one grain to the next. This phase is also known as the "twist grain boundary phase".

1.5 Textures of Liquid Crystals

One of the most simple, although not complete, ways to characterize LCs is by polarized light optical microscopy[15]. Each different LC phase has its own distinct optical textures when analyzed with a polarized light optical microscope. These textures originate from defects (point defects and line defects) within the LC samples, which are strongly related to the deformation constants of the corresponding LC phase. Typical textures of LC phases are listed below, however it should be noted that the textures can only serve as a guide for identifying specific LC phases and must be combined with X-ray diffraction analysis for complete description of the LC phase.

Nematic Phase: schlieren (thread-like) texture.

Smectic Phase: focal-conic or fan-like textures.

Cholesteric Phase: fingerprint texture.

Columnar Phase: fan-like texture.

Cubic Phase: optically isotropic.

1.6 Liquid Crystalline Order in Polymers

The liquid crystalline state in polymers was first observed with poly(γ-benzyl α,L-glutamate) (PBLG), a synthetic polypeptide with a rod-like structure[16,17]. A few years later Flory established the simple theoretical foundation for the formation of nematic mesophases from solutions of rigid rod-like particles[18]. However it was only after recognizing the ability of LC polymers to easily transform to highly ordered states, the state that can be used to make materials with good mechanical properties, that the liquid crystalline state of polymers has attracted strong and broad attention of scientists. For example, in the 1970's, Soviet and American scientists engaged in in-depth research on solutions of aromatic polyamides which contain para-linked phenylene groups in the main chain[19].

Liquid crystalline order seems at first impossible for polymeric compounds because polymer chains usually adopt statistical coil conformations whereas LC phases possess orientational and/or positional long-range order. However, polymeric chains can be combined with liquid crystallinity in two ways (Fig. 1.8).

1) Main chain LC polymers: Generally, in the case of non crosslinked polymers, the polymer can be considered as a long chain. If the polymer chain is rigid (long persistence length), then the polymer chain itself may act as mesogenic element. This type of LC polymer is called a "rod-like main chain LC polymer". Often, these phases cannot be observed directly, because melting temperatures of rigid polymers are above the decomposition temperature. In these cases the addition of solvent can lower the melting temperature and allow the observation of the LC phases (lyotropic LC). Otherwise, the

main chain LC polymer can be modified to include flexible components in either the main or side chains to reduce the melting temperature[20].

2) Side chain LC polymers: For side chain LC polymers, the mesogens are attached as a side group to the main chain with flexible spacers which decouple the motion of the side groups from that of main chain allowing both subsystems to follow their inherent oritentation tendencies[21].

In the case of side-chain LC polymers and modified main chain LC polymers, where the mesogenic units are derived from low molecular weight LCs, both nematic and smectic phases have been shown to exist. However, for rod-like main chain polymers, only nematic ordering has been known and smectic ordering is rarely observed. For example, both PBLG and aromatic polyamides, poly(p-benzamide) (PBA) and poly (p-phenylene terephthalamide) (PPTA) (Figure 1.9) are rod-like main chain LC polymers. The rod-like character of PBLG comes from the stable helical conformation, a result of intramolecular hydrogen bonds. PBA and PPTA are characterized by a stable trans-configuration of the amide bond and by a high rotational barrier around aryl carbon bonds. The directions of rotational axes in all the chain units almost coincide. As a result, the entire polymer acquires the shape of crankshaft providing the rod-like character necessary for LC phase formation. For rod-like polymers the polymeric backbones themselves can be considered as the mesogenic unit , thus, their LC properties depend strongly on the molecular weight of the polymers. Since the traditional chemical polymerization methods only afford polydisperse samples, the polydispersity of the samples, which results in heterogeneity of the size of mesogenic units, could have frustrated the formation of smectic ordering of rod-like polymers.

For more than 40 years, PBLG has served as a model compound for rod-like LC polymers, however, the smectic LC phase of PBLG has never been observed. Here, we show that when prepared in monodisperse form, PBLG does exhibit smectic ordering both in solution and in solution cast films.

1.7 Dissertation Plan

Chapter 2 describes the preparation of a series of poly(α,L-glutamate) derivatives using recombinant DNA techniques. Reported in chapter 2 are the details of the genetic design and DNA cloning strategy as well as the corresponding bacterial synthesis, purification and characterization of the poly(α,L-glutamate) derivatives. The monodisperse poly(α,L-glutamate) derivatives are modified chemically to produce monodisperse derivatives of poly(γ-benzyl α,L-glutamate) and poly(γ-(hexadecyloxy)benzyl α,L-glutamate). Synthesis and characterization of these polymers are presented in chapter 3 and 4. Chapter 3 describes the preparation and LC properties of a series of monodisperse poly(γ-benzyl α,L-glutamate) derivatives with different molecular weights. Smectic ordering of these polymers in solutions and in films is evaluated by polarized light optical microscopy and X-ray diffraction . In chapter 4, monodisperse derivatives of poly(γ-(hexadecyloxy)benzyl α,L-glutamate) are prepared and their thermal behavior and molecular ordering are investigated by differential scanning calorimetry, polarized light optical microscopy and X-ray diffraction.

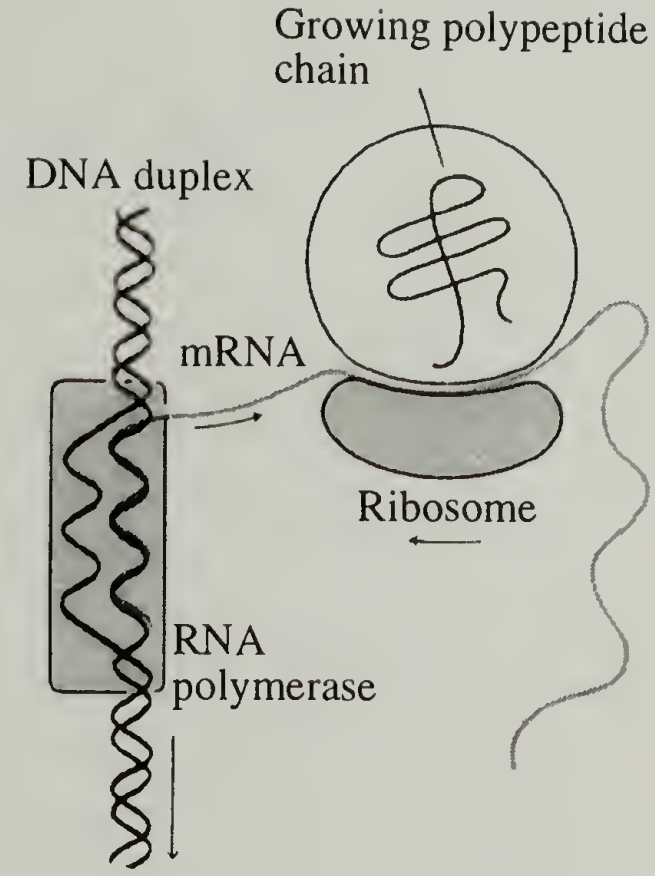

Figure 1.1 Functional complex of DNA, mRNA, RNA polymerase and a ribosome in a bacterial cell. From Ref. 4.

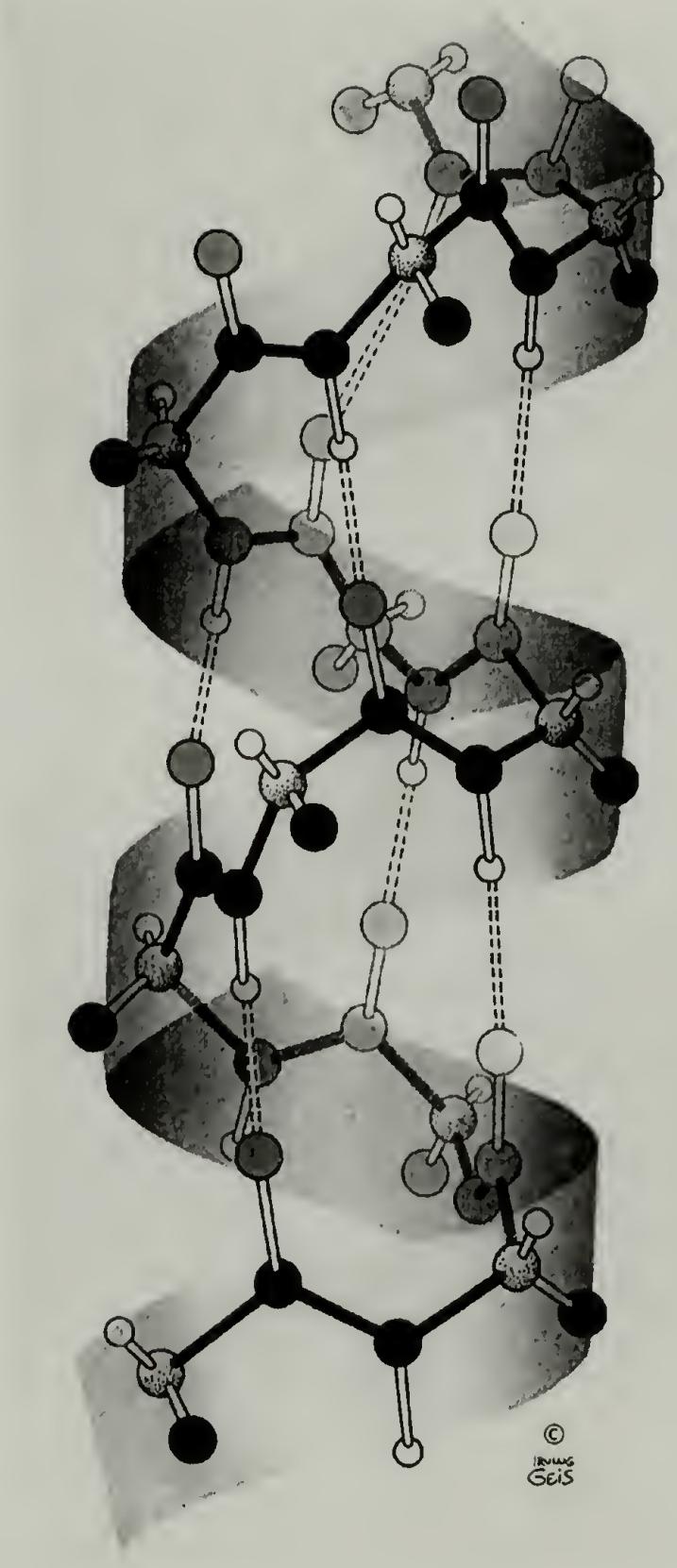

Figure 1.2 Structure of right-handed alpha-helix. Hydrogen bonds are indicated by dashed lines. The direction of hydrogen bonds is nearly parallel to the helix. It requires 18 residues to complete 5 turns with a pitch of 5.4 Å and the axial advance per residue is 1.5 Å. From Ref. 10.

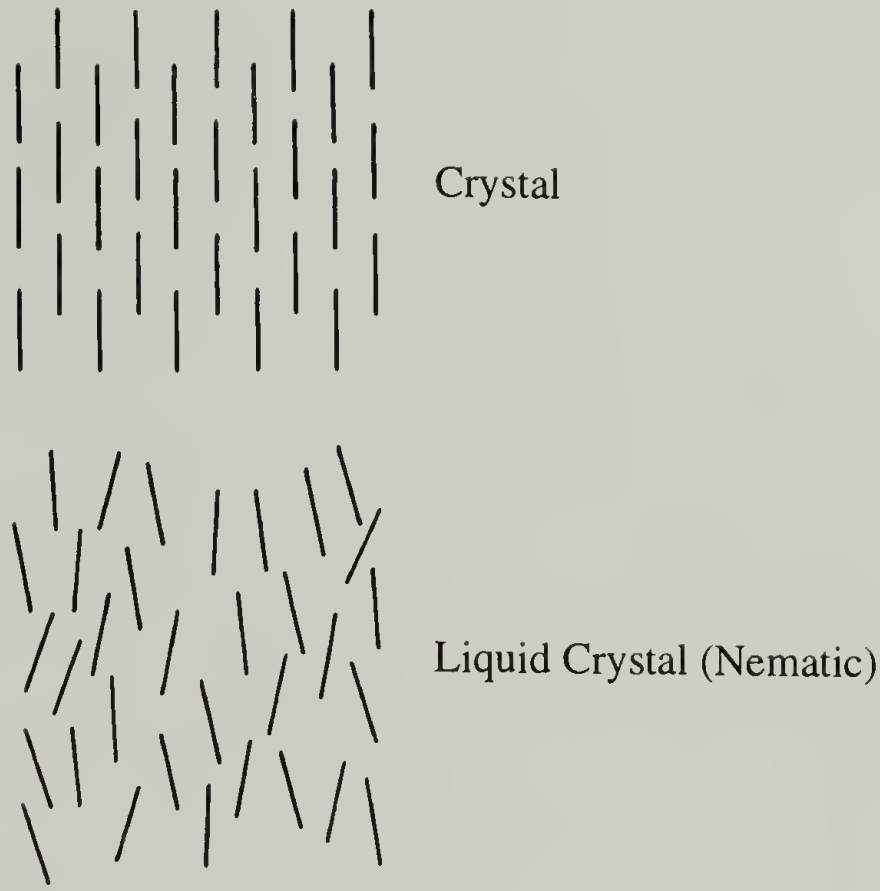

Figure 1.3 Schematic representation of molecular order in the crystalline, liquid crystalline and isotropic phases.

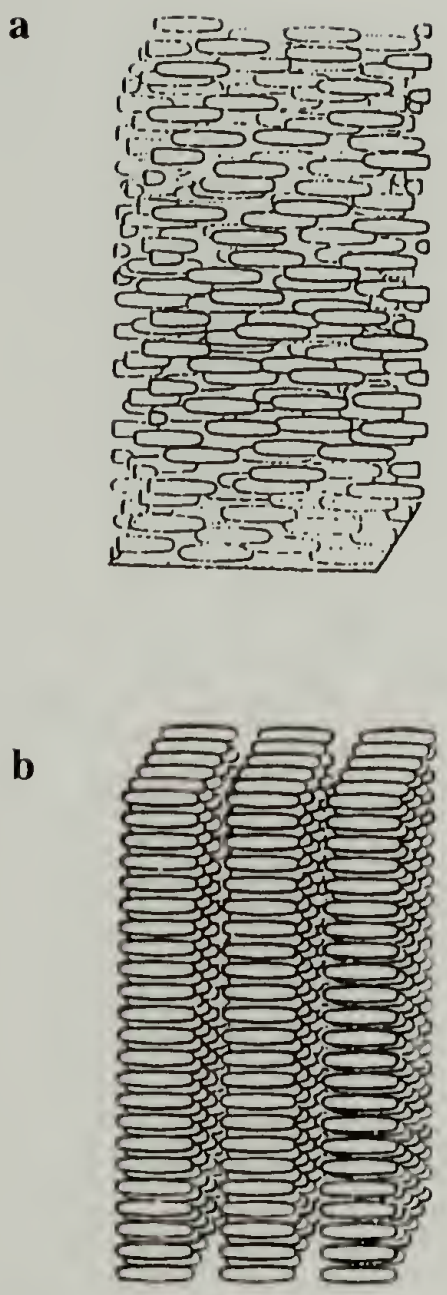

Figure 1.4 Schematic representations of nematic (**a**) and smectic (**b**) liquid crystalline phases. From Ref. 23.

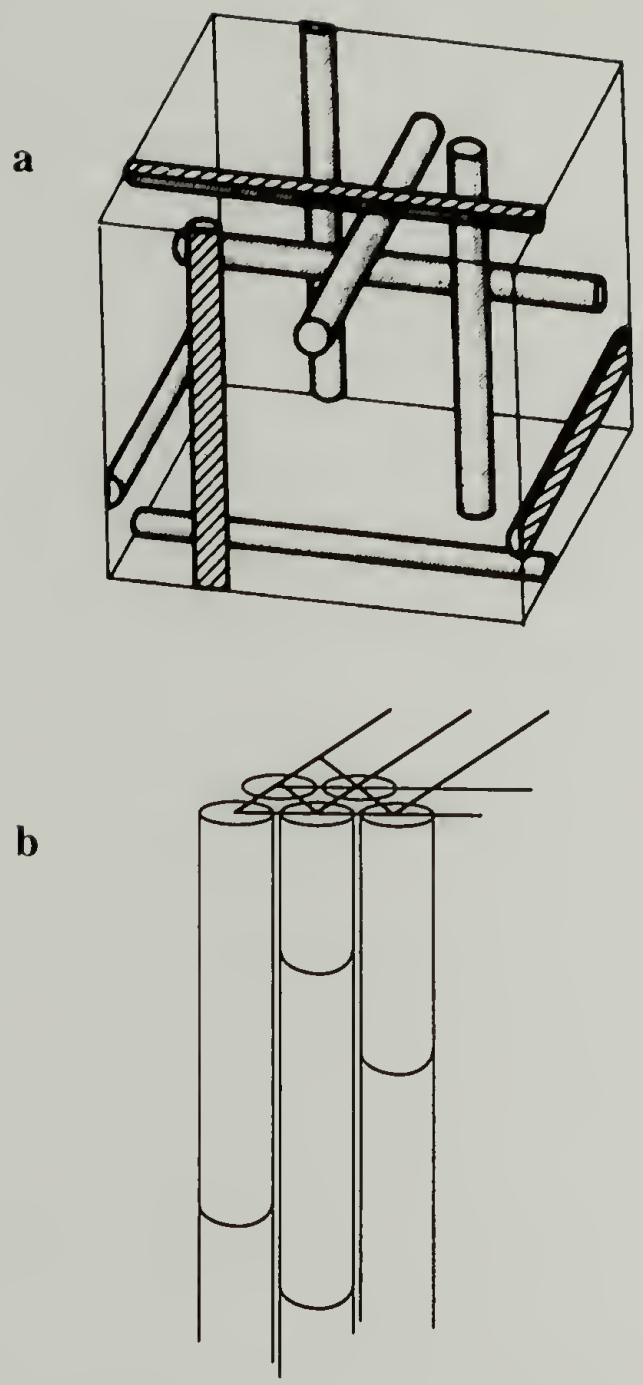

Figure 1.5 Schematic representations of a cubic phase (**a**) and a columnar phase (**b**). The cubic meshophase has a complicated interwoven network and the columnar phase is characterized by a set of X-ray reflections that can be indexed to a two dimensional hexagonal lattice. From Ref. 12

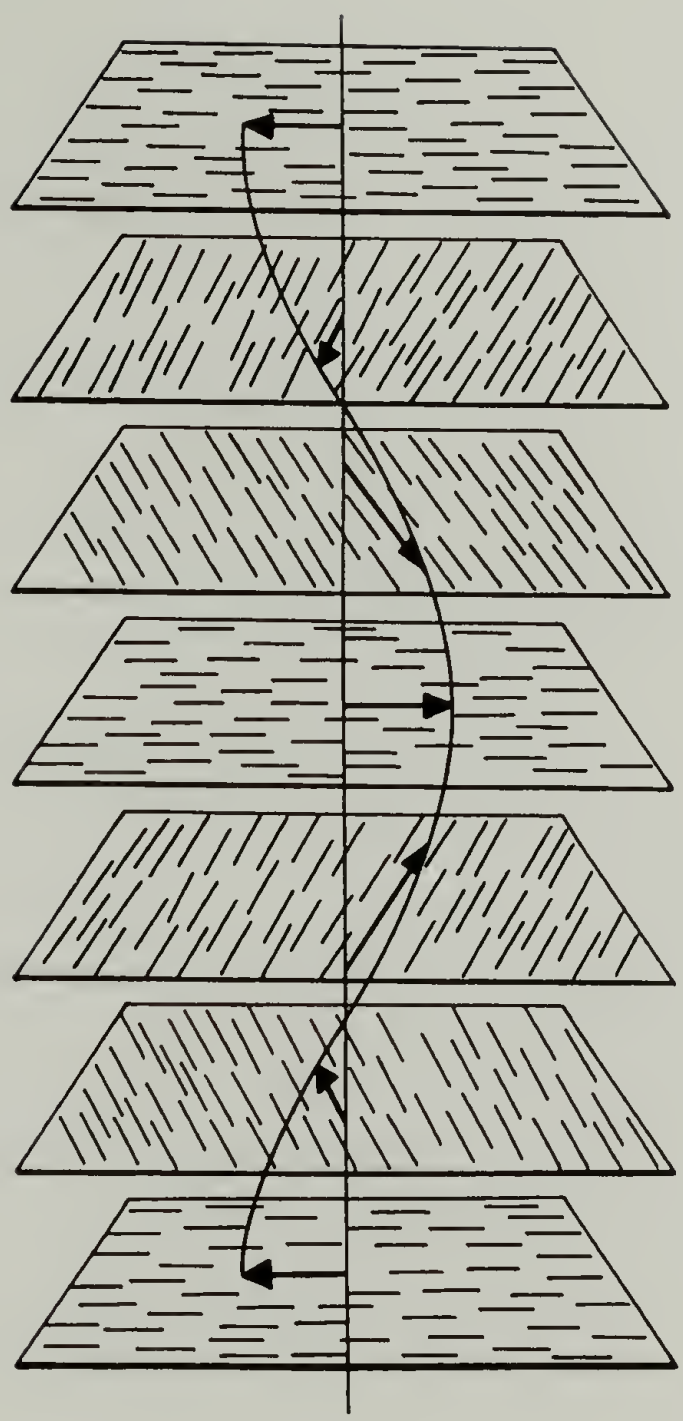

Figure 1.6 Schematic representation of cholesteric LC phase. The layers in the figure are for convenience. In reality, there is no discernible layering in cholesteric phase.

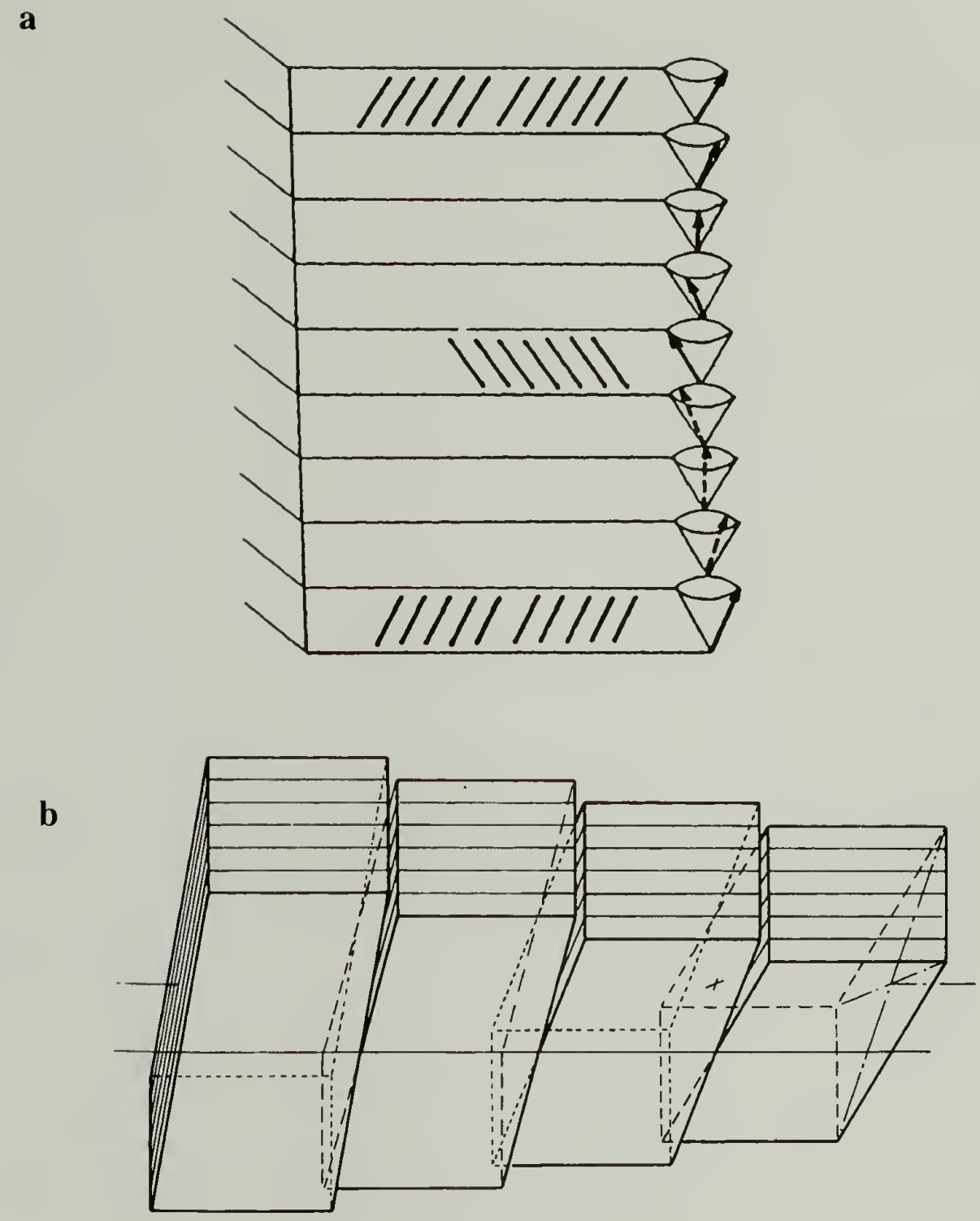

Figure 1.7 Schematic representations of chiral smectic LC phases. **a**, Smectic C* phase. **b**, Smectic A* (Twist grain boundary) phase. In the smectic C* phase, molecules are tilted in the layers as in smectic C ordering, however the projection of the tilt on the layer plane rotates from one layer to the next layer. Smectic A* phase consists of smectic A blocks separated by twist grain boundaries. From Ref. 22.

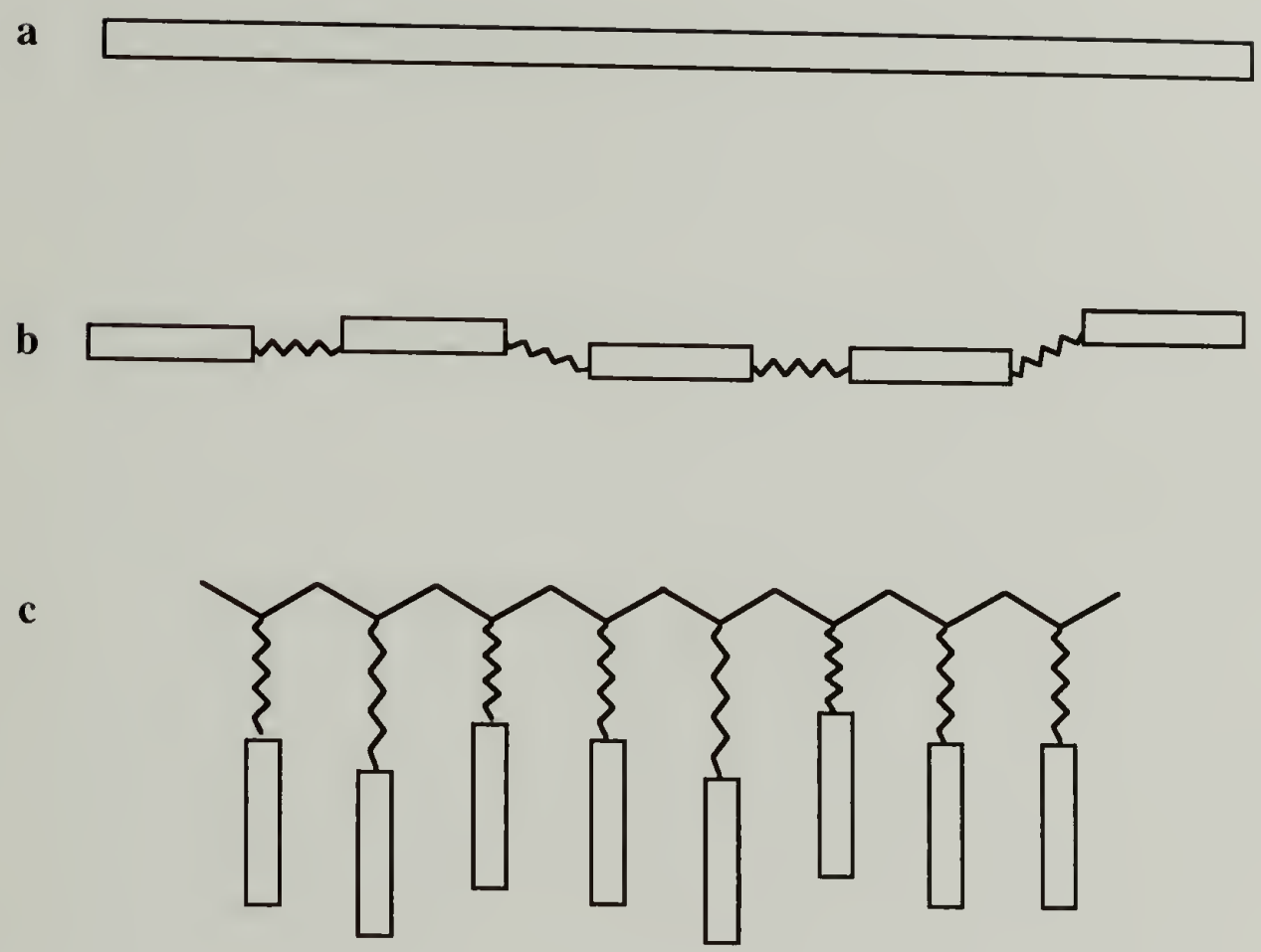

Figure 1.8 Schematic representations of LC polymers. **a**, rod-like main chain LC polymers. **b**, modified main chain LC polymers. **c,** side chain LC polymers.

a

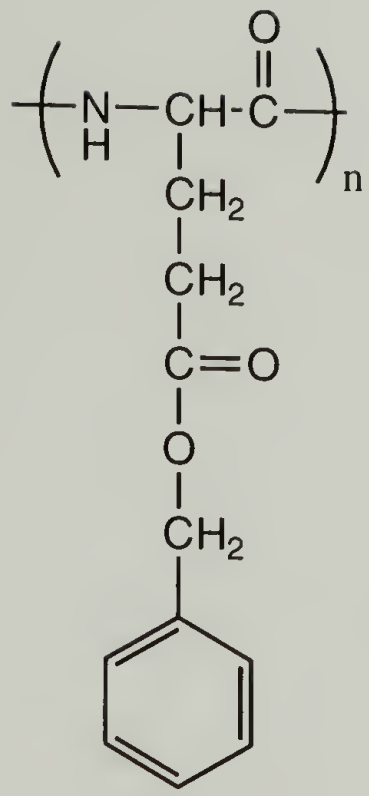

b

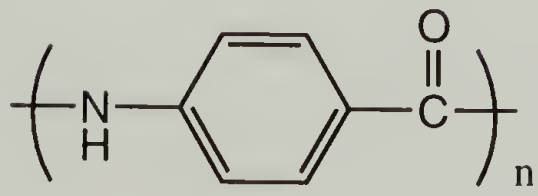

c

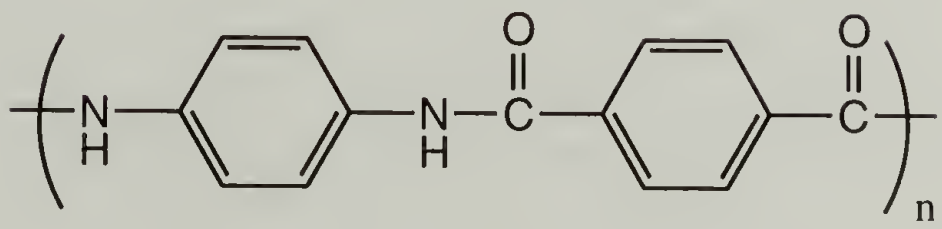

Figure 1.9 Examples of rod-like main chain LC polymers. Poly(γ-benzyl α,L-glutamate) (PBLG) (**a**), poly(p-benzamide) (PBA) (**b**) and poly(p-phenylene terephthalamide) (PPTA) (**c**).

1.8 References

1. Flory, P. J. *Principles of Polymer Chemistry*; Cornell University Press: New York, 1953.

2. Creighton, T. E. *Proteins*; W. H. Freeman and Company: New York, 1993.

3. Szwarc, M.; Van Beylen, M. *Ionic Polymerization and Living Polymers*; Chapman & Hall: New York, 1993.

4. Leninger, A. L. *Biochemistry*; Worth Publisher, Inc.: New York, 1970.

5. McGrath, K. P.; Tirrell, D. A.; Kawai, M.; Mason, T. L.; Fournier, M. J. *Biotechnol. Prog.* **1990**, 6, 188.

6. Cappello, J.; Crissman, J.; Dorman, M.; Mikolajczak, M.; Textor, G.; Marquet, M.; Ferrari, F. *Biotechnol. Prog.* **1990**, 6, 198.

7. Kricheldorf, H. R. *α-Aminoacid-N-Carboxy-Anhydrides and Related Heterocycles*; Springer: New York, 1987.

8. Deming, T. J. *Nature* **1997**, 390, 386.

9. Deming, T. J. *J. Am. Chem. Soc.* **1998**, 119, 2759.

10. Voet, D.; Voet, J. G. *Biochemstry*; John Wiley & Sons: New York, 1990.

11. Block, H. *Poly(γ-benzyl-L-glutamate) and Other Glutamic Acid Containing Polymers*; Gordon and Breach: New York, 1993.

12. Chandrasekhar, S. *Liquid Crystals*; Cambridge University Press: New York, 1977.

13. Beguin, A.; Billard, J.; Bonamy, F.; Buisine, J. M.; Cuvelier, P.; Dubois, J. C.; Le Barny, P. *Mol. Cryst. Liq. Cryst.* **1984**, 115, 9.

14. Gray, G. W.; Goodby, J. W. G. *Smectic Liquid Crystals*; Heyden & Son, Inc: Philadelphia, 1984.

15. Demus, D.; Richter, L. *Textures of Liquid Crystals*; Chemie: Weinheim, 1978.

16. Elliot, A. E.; Ambrose, E. J. *Discuss. Faraday Soc.* **1950**, 9, 246.

17. Robinson, C. *Trans Faraday Soc.* **1956**, 52, 571.

18. Flory, P. J. *Proc. Roy. Soc. (London)* **1956**, A234, 73.

19. Papkov, S. P.; Kulichikhin, V. G.; Kalmykova, V. D. *J. Polym. Sci., Polym. Phys. Ed.* **1974**, 12, 1753.

20. Ober, C. K.; Jin, J.-I.; Lenz, R. W. *Adv. Polym. Sci.* **1984**, 59, 103.

21. Mcardle, C. B. *Side Chain Liquid Crystal Polymers*; Blackie and Sons: Glasgow, 1989.

22. De Gennes, P. G.; Prost, J. *The Physics of Liquid Crystals*; Clarendon Press: Oxford, 1993.

23. Gibson, H. W. in *Liquid Crystals The Fourth State of Matter*; Saeva, F. D., Ed.; Macel Dekker, Inc: New York, 1979.

CHAPTER 2

SYNTHESIS OF GENETICALLY ENGINEERED MONODISPERSE DERIVATIVES OF POLY (α, L-GLUTAMIC ACID)

2.1 Introduction

Genetic engineering principles[1,2] were used to synthesize a series of monodisperse poly(α,L-glutamic acid) (PLGA) analogues (**PLGA-X**) of structure **1**. These polypeptides are of interest, at least from the standpoint of polymer materials science, for their properties as polyelectrolytes, characterized by well-defined helix-coil transitions.[3,4] In addition, the ester derivatives of **PLGA-X**, which may be prepared by chemical alkylation, should adopt persistent rod-like structures in solution, in analogy with the ester derivatives of PLGA. Rod-like polymers derived from **PLGA-X**, e.g. poly(γ-benzyl α,L-glutamate) (PBLG) derivatives (designated as PBLG-X in chapter 3) are highly monodisperse with respect to their rod lengths which are determined precisely by the number of repeating units multiplied by the axial rise per residue of 1.5 Å . PBLG forms liquid crystalline solutions and oriented solid films under a variety of conditions,[5] and has played a central role in elucidating the physical chemistry and materials science of rod-like macromolecules[6]. It is expected that the structural uniformity of **PLGA-X** and their derivatives will play a critical role in elucidating the true characteristics of rod-like polymers in their purest form and ultimately allow design and synthesis of complex macromolecular and supramolecular structures from the rod-like macromolecules. Reported herein are the details of the genetic design and DNA cloning strategy as well as the corresponding bacterial synthesis and characterization of **PLGA-X**s.

$GluAsp(Glu_{17}Asp)_XGluGlu$ (**PLGA-X**, X=3, 4, 5, and 6) **1**

2.1.1 Poly(α,L-glutamic acid) (PLGA)

The helix-coil transition of PLGA can be induced by a change in pH, temperature, and solvent. The transition is dependent on the molecular weight of the polymer and typically accompanied by changes of degree of ionization, specific rotation and intrinsic viscosity.[7,8] Experiments demonstrate that the helix-coil transition takes place through intermediate species containing both helical and coil states[24]. However the PLGA samples available to date are polydisperse samples which are prepared by ring-opening polymerization of N-carboxy-α-aminoacid anhydrides and ambiguity arises over this intermediate mechanism or an all-none mechanism.

2.1.2 pQE-15 Expression System

The synthesis and purification of the PLGA analogue **PLGA-4** as a protein fusion to glutathione-S-transferase (GST) has been described before.[10] A preliminary communication of the biosynthesis of this material reported low yields, though the product could be obtained in homogeneous form *via* affinity purification. In an effort to increase the expression yield to provide enough sample for materials characterization, Conticello and coworkers have tested the expression of **PLGA-4** in a variety of different expression systems.[15] Following their results, we have employed the pQE-15 (Qiagen) expression system[11] in which the target proteins are expressed as C terminal fusions to mouse dihydrofolate reductase (DHFR). In addition to the DHFR, the fusion protein also contains a $(His)_6$ tag at the N-terminus for metal affinity column purification.[12] The pQE-15 system employs a powerful T5 promotor which is recognized by *E. coli* RNA polymerase. This plasmid also contains a double *lac* operator sequence that serves to regulate the expression of the target gene. A low basal level of transcription is maintained by a separate multi-copy plasmid (pREP4) that encodes the *lac* repressor and the level of induction of the target

protein sequence can be directly regulated by control of the isopropyl-β-D-thiogalactopyranoside (IPTG) concentration.

2.2 Experimental Section

2.2.1 Materials

T4 DNA ligase, calf intestinal phosphatase (CIP) and all restriction enzymes were purchased from New England Biolabs. Ribonuclease A, Deoxyribonuclease I, Antifoam agent, Ampicillin, Kanamycin and cyanogen bromide were purchased from Sigma Chemical Co. *Escherichia coli* strain DH5αF' was purchased from Bethesda Research Laboratories. Plasmid pUC-18 and DEAE Sephadex anion-exchange resin were purchased from Pharmacia. Expression plasmid pQE-15, *E. coli* strain SG13009 (containing pREP4) and Ni-NTA resin were purchased from Qiagen Inc.

2.2.2 General Methods

Procedures for DNA manipulation, transformation of competent cells and bacterial growth were adopted from Sambrook, Fritsch and Maniatis or from instructions provided by manufacturers.[13] Cell density measurements were done on a Hitachi U2000 spectrophotometer in plastic cuvettes at λ=600 nm. A New Brunswick 80 L mobile pilot plant (MPP-80) was used for large scale fermentation and centrifugation was performed using a Cepa Z41 continuous centrifuge which was attached directly to the MPP-80 fermentor. Centrifugation for DNA manipulation and protein purification was done using either Eppendorf centrifuge 5402 (for volume less than 1.5 mL) or Beckman centrifuge J2-21. For column purification, Bio-rad Econo-Column chromatography columns were used and Pharmacia peristaltic pump P-1 was used for flow rate control.

2.2.3 Design and Synthesis of DNA

Design and synthesis of oligonucleotides of sequence **2** was reported earlier[10].

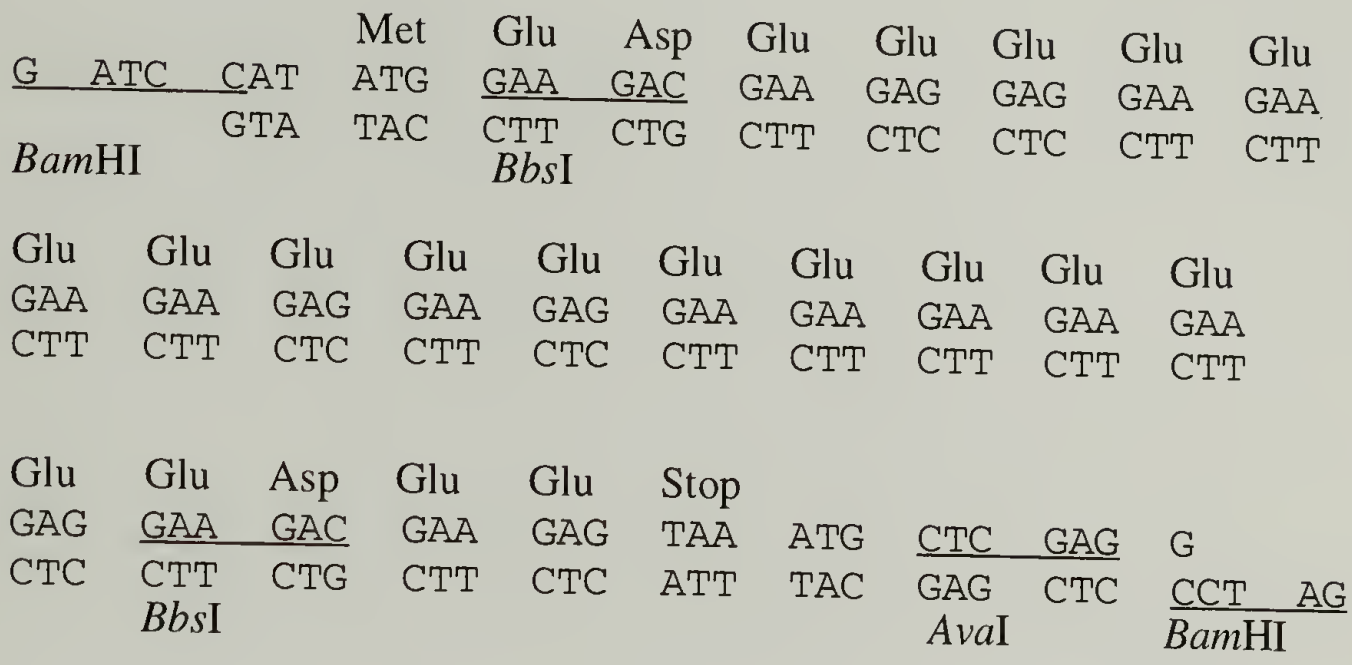

2

Oligonucleotides **2** were synthesized on a Milligen/Biosearch Model 8700 DNA synthesizer . The purified oligonucleotide duplex was ligated into *Bam*HI digested pUC18 and the recombinant DNA (designated as pUC18-89) was used to transform *E. coli* strain DH5αF'.

2.2.4 Preparation of DNA Monomer

A saturated culture (500 mL) in 2 x YT medium (containing 200 mg/ml ampicillin) was grown from a single colony of DH5αF' containing pUC18-89. Cells were harvested and plasmid was separated from the lysed cells following the Qiagen Maxi Plasmid Prep protocol. The pUC18-89 (50 µL, 1 µg/µL) was mixed with 50 µL of 10 X *Bbs*I buffer and 350 µL of doubly distilled(dd) H_20. *Bbs*I (50 µL, 250 U) was added and the reaction was incubated at 37 °C overnight. The digest was directly loaded on a 15% polyacrylamide gel. The monomer bands (3 bands, each from 20 µL loading) were cut out from the gel, finely chopped and soaked in 1.5 mL of elution buffer. After overnight

incubation at 37°C the slurry was passed through a microcentrifuge separation tube and washed twice with elution buffer. To the combined solution (2 mL) were added 40 μL of oyster glycogen solution and 5 mL of 100% ethanol. Following overnight incubation at -10°C, the monomeric DNA was pelleted by centrifugation, washed, dried and redissolved in 20 μL of ddH_2O. The linearized pUC18-89 without the 54 bp *Bbs*I fragment (designated as pUC803) was also isolated and dephosphorylated by CIP treatment (designated as pUC803-P).

2.2.5 Generation of Multimers

The monomer solution (3 μL, ≈10 ng/μL) was mixed with 1 μL of 10 X ligation buffer and 5.5 μL of ddH_2O. T4 DNA ligase (0.5 μL, 20 units/μL) was added and the reaction mixture was incubated at 14°C. After 24 hr, 4 μL of pUC803-P solution (≈2.5 ng/μL) was added and another 0.5 μL of T4 DNA ligase, 1 μL of 10 X ligation buffer, and 4.5 μL of ddH2O were added. After another 24 hr incubation at 14°C, the ligation mixture was directly used to transform *E. coli* strain DH5αF' competent cells which were then grown on a 2 x YT medium plate containing 200 mg/ml ampicillin. From the analysis of 66 colonies by *Bam*HI digestion of purified plasmids, transformants containing synthetic multimer DNA inserts, ranging in size from 1 to 10 repeats of the monomer segment were identified. Transformants containing 3, 4, 5, and 6 repeats of the DNA monomer segment were chosen for further analysis. The recombinant plasmid derived from pUC803 and a multimer is designated as pUC803-multimer.

2.2.6 Construction of Bacterial Expression Vectors

Plasmids containing various inserts (pUC803-3, 4, 5, and 6) were isolated from transformed cells grown to saturation in 5 mL, 2 x YT cultures by a modified alkaline lysis miniprep method. From 1.5 mL of saturated culture, 40 μL DNA solution was prepared.

To 30 μL of each plasmid solution were added 6 μL of 10 X *Bam*HI buffer, 0.6 μL of 100 X BSA buffer and 22 μL of ddH_2O. *Bam*HI (1.5 μL, 100 U/μL) was added and the reaction mixture was incubated at 37 °C overnight. Each of 30 μL of digestion mixtures was loaded on a 1.5% agarose gel and separated by electrophoresis. The bands corresponding to the artificial gene which were identified by ethidium bromide were cut and purified by Qiaex II gel extraction kit. Qiaex II support (15 μL) was used to prepare 35 μL of each DNA solutions. Each of the DNA solutions (2 μL, ≈6 ng/μL) was mixed with 1 μL of *Bgl*II digested, dephosphorylated pQE-15 (≈7 ng/μL) and ligated by T4 DNA ligase (0.5 μL, 10 units) in the presence of 1 μL of 10 X ligase buffer and 5.5 μL of dd H_2O. A portion of each ligation mixture was used to transform *E. coli* strain SG13009 containing pREP4. The presence and orientation of inserts in the recombinant plasmids were determined by digestion with *Ava*I, which yields restriction fragments of sizes dependent on the direction of insertion. The recombinant plasmids were designated as pQE-15-X, where X is the number of repeats of DNA monomer segment.

2.2.7 Protein Expression

A single colony of *E. coli* strain of SG13009 (pREP4) containing pQE-15-X was used to inoculate 5 mL of 2 x YT medium containing 200 μg/mL ampicillin and 30 μg/mL kanamycin and allowed to grow overnight at 37°C. This culture was used to inoculate 100 mL of the same medium and cells were grown at 37°C. When the culture reached OD_{600nm} of 1.2, expression of target protein was induced with β-isopropylthiogalactoside (IPTG) to a final concentration of 0.01 mM. Cells were isolated by centrifugation and the whole cell lysates were analyzed on a 12% SDS polyacrylamide gel and the protein was visualized by coomasie blue staining. For the western blot experiment, the protein was transferred to a nitrocellulose membrane for 30 min. at 100 V. Mouse anti-RGS-$(His)_4$ was bound to the target protein and anti-mouse Ig. horseradish peroxidase-linked whole antibody from sheep was used as a second antibody[23].

2.2.8 Large-Scale Protein Expression and Purification

A single colony of *E. coli* strain SG13009 (pREP) containing pQE-15-4 was used to inoculate 10 mL of 2 x YT medium containing Kanamycin and Ampicillin (same concentration as in 2.2.7). These cultures were grown to saturation and were used to inoculate 1L of 2 x YT medium containing the same antibiotics. An overnight culture was used to inoculate 60 L of YT medium containing Ampicillin (100 μg/mL) and Kanamycin (20 μg/mL). This culture was incubated at 37°C with aeration and with agitation rate of 250 rpm until the OD_{600nm} of 1.2 was reached. At that point, IPTG was added to a final concentration of 0.01 mM to induce target protein synthesis. After 3 hr, cells were isolated by continuous centrifugation, resuspended in 1 L of sterile ddH_2O and frozen at -80°C.

The cells were lysed by repeated processes of thawing and freezing. To the lysate were added 60 mL of 5 M NaCl and 15 mL of 1 M Tris-Cl pH 7.9 were added after addition of PMSF (50 mg) and egg white lysozyme (0.1 mg) and the mixture was incubated at 37°C for 2 hr. Subsequently, $MgCl_2$ (6 mmole), DNAseI (0.1 mg) and RNAseA (0.1 mg) were added and the lysate was incubated for another 3 hr. The mixture was centrifuged at 18,000xg at 4°C for 50 min. Supernatant was decanted and the pellet was dissolved in 1 L of binding buffer (6 M guanidine chloride (GuCl), 0.1M NaH_2PO_4, 0.01 mM Tris-HCl, pH 8.0) and stirred overnight after adjusting the pH to 8.0. The insoluble materials were removed by centrifugation at 39,200xg at 4°C for 50 min. The clear supernatant was mixed with 150 mL of Ni- NTA agarose resin (Qiagen) previously equilibrated with binding buffer and stirred overnight at room temperature. The resin was isolated by centrifugation (≈950xg) for 45 min, combined with 400 mL of binding buffer and stirred for 4 hr. The resin was isolated again by centrifugation and washed with 400 mL of wash buffer (8 M urea, 0.1 M NaH_2PO_4, 0.01 M Tris-HCl, pH 8.0) then with 700 mL of second wash buffer (8 M urea, 0.1 M NaH_2PO_4, 0.01 M Tris-HCl, pH 6.9) as

described before. The resin mixture was transferred to a column (5.5 x 20 cm) and sequentially washed with 400 mL of elution buffer (8 M urea, 0.1 M NaH_2PO_4, 0.01 M Tris-HCl, pH 5.4) and 200 mL of a second elution buffer (8 M urea, 0.1 M NaH_2PO_4, 0.01 M Tris-HCl, pH 4.5). All washes and the column flow-through were collected as separate fractions. The protein content of each fraction was analyzed by 12% SDS polyacrylamide gel electrophoresis after desalting. The fraction containing pure product (pH 5.4 elution) was transferred to dialysis tubing (molecular weight cut off (MWCO) = 12-14kD) and dialyzed for 4 days under running distilled water. The dialysate was lyophilized to afford the purified fusion protein PLGA-4 (600 mg). Similar expression and purification procedures were used to prepare fusion proteins of PLGA-3, 5, and 6.

The fusion protein (260 mg) was dissolved in 96% formic acid (190 mL) and H_2O was added to adjust the concentration to 70% formic acid. To this solution, 260 mg of cyanogen bromide was added and the clear mixture was purged with N_2 for 15 min. The reaction was protected from light and stirred for 48 hr at room temperature. Volatile compounds (water, formic acid and CNBr) were removed by rotary evaporation followed by evacuation under dynamic vacuum overnight. The residual solids were resuspended in 50 mM Tris-Cl pH 8.0 (150 mL) by vigorous stirring for 12 hr and the pH was adjusted to 8.0 with dilute aqueous NaOH. The soluble fraction was isolated by centrifugation and used to charge a column of 50 mL of DEAE-Sephadex A-25 previously equilibrated with 50 mM Tris-HCl pH 8.0. The charged column was sequentially washed with 250 mL volumes of solutions of 50 mM Tris-HCl pH 8.0 containing 100 mM, 500 mM, 2 M and 4 M NaCl respectively. Each of these washes was collected as a separate fraction and individual fractions were analyzed by electrophoresis on a non-denaturing 12% polyacylamide gel using 10 mM Na_2HPO_4 as a running buffer. Protein was visualized with 0.2% methylene blue. The cleaved product was located exclusively in the 2M NaCl fraction. This fraction was transferred to dialysis tubing (MWCO = 3-5kD) and dialyzed for 5 days under running distilled water. The dialysate was lyophilized affording pure

cleaved protein PLGA-4 (90 mg). Similar procedures were used to produce pure proteins PLGA-3, 5, and 6 with comparable yield.

2.3 Results and Discussion

2.3.1 Gene Construction

Design and synthesis of oligonucleotides of sequence **2** was reported earlier.[10] The Asp codons serve as unique recognition sites for *Bbs*I. Use of only Glu as repeating units requires long stretches of repetitive use of a single codon, a situation that might cause genetic instability,[14] and Zhang and coworkers have chosen Asp as a second repeating unit because of its structural similarity to Glu.

Starting from pUC-18-89, variants of pUC803 (pUC803 is equivalent to pUC-18-89 minus the 54 bp *Bbs*I fragment) containing multimers of DNA monomer segments were constructed by first cutting out the 54 bp monomeric DNA sequence from pUC-18-89 by *Bbs*I digestion, then multimerization of the monomeric DNA with T4 DNA ligase, followed by reinsertion of a multimeric DNA back into the pUC803 (designated as pUC803-X, X=number of repeats of monomeric DNA). Instead of isolating individual multimers after the multimerization step, a population of multimers was inserted into pUC803 and subsequently screened for the target lengths. From the analysis of 66 colonies by *Bam*HI digestions of purified plamids, transformants containing synthetic multimer DNA ranging in size from 1 to 10 repeats of monomer segment were identified. The *Bam*HI fragments of pUC803-3, 4, 5, and 6 were purified and inserted into *Bgl*II site of expression vector pQE-15 (designated as pQE-15-X). The presence and orientation of inserts in the final recombinant expression plasmids were determined by digestion with *Ava*I, which yields restriction fragments of sizes dependent on the direction of insertion. Figure 2.1 shows the comparative gel electrophoresis of DNA multimers generated by *AvaI* digestion of pQE-15-Xs. The expected numbers of base pairs are 913, 967, 1021 and 1075 for *Ava*I fragments of pQE-15-3, 4, 5, and 6 respectively. The positions of the bands

from Figure 2.1 agree with the expected numbers of base pairs and confirm the integrity of the final recombinant expression vectors.

2.3.2 Protein Expression

The proteins are produced from the pQE-15 expression system[11] in which the target protein is expressed as a C-terminal fusion to mouse dihydrofolate reductase (DHFR, 19 kD) that also contains a $(His)_6$ at the N-terminus for immobilized metal affinity chromatography.[12] Small scale expression was performed in 2 x YT media with ampicillin and kanamycin as antibiotics. Figure 2.2 shows the cell growth profiles of SG13009 (pREP4) strains containing pQE-15-3, 4, 5, and 6. Induction phase is prolonged and the slope of the log phase is decreased as the size of the multimeric inserts was increased from 3 to 6. The reduced growth rate as a result of longer multimeric insert was also evident when the cells were grown from a single colony on a culture plate. The size of the colony was smaller for the cells with longer multimeric inserts. This suggests that there is an inverse relationship between the growth rate and the number of Glu codons. The reduced growth rate is evident both before and after target protein induction. Cultures of cells with pQE-15-3 reached OD_{600nm} of 1.2 after 2 hr but cultures of pQE-15-6 containing cells took almost 6 hr to reach the same optical density. Work by Mawn and coworkers[26] showed that, in some cases, large amounts of PLGA-X protein can be accumulated in the bacterial cell. This suggests that the reduced growth rate may not be a result of toxicity of the expressed protein. It is also unlikely that the longer generation time is caused by slow replication time of repetitive DNA sequence since the target gene represents only a small portion of the DNA present in the bacterial cell. The difference in growth rate in relation to the number of Glu codons was not observed for pUC-18, a cloning vector but only in the expression vetor (pQE-15). Therefore, it is reasonable to assume that the variation in growth rate is caused at the RNA level.

Polyacrylamide gel (12%) electrophoresis (SDS-PAGE) and western blot analyses of the whole cell lysates containing fusion proteins of different multimers are shown in Figure 2.3. New bands with apparent molecular weights of 33,400, 35,700, 38,000 and 40,300 can be detected in lanes 2, 3, 4 and 5 respectively after coomassie brilliant blue staining. These bands were absent before induction with IPTG (lane 1) but were present 3 hr after fusion protein synthesis had been initiated. Expression of DHFR alone without multimer insert is shown in lane 6. The intensity of the fusion protein bands is significantly weaker than that of the pure DHFR suggesting less efficient expression of the fusion protein compared to DHFR alone. In addition, there is a continuous decrease in the intensity of protein bands as the length of target protein is increased. (Lanes 3-5). This is more apparent in the corresponding western blot (Figure 2.3 (b)). This suggests that the yield of recombinant protein depends on the number of repeats appended to the fusion partner, decreasing as the number of repeats increases. The reason for the relatively low accumulation of the fusion protein and the decrease in protein expression with respect to longer chain length is not readily apparent; however the preliminary results from Conticello and coworkers suggest that plasmid instability, toxicity and degradation of expressed protein, and inefficient transcription of the target gene sequence are not responsible for the low expression yield.[15] Interestingly, their results on the expression level of **PLGA-4** in response to different induction levels indicate greater yield of protein at lower induction level. In the pQE-15 system, transcription of the target sequence is driven by a powerful T5 promoter that is recognized by *E. coli* RNA polymerase. This plasmid also contains a double *lac* operator sequence downstream of the promoter that regulates transcription of the target gene. A low basal level of transcription is maintained by a separate multi-copy plasmid that encodes for *lac* repressor. Under normal conditions of protein expression, increasing the IPTG concentration would cause a corresponding increase in the accumulation of the target sequence, or at least its rate of synthesis, until full induction is reached. Increasing the number of repeats leads to an increase in [Glu_{17}Asp] mRNA

dosage at a fixed level of induction, creating an effect similar to that observed upon increasing the induction. All of these results strongly suggest that protein expression is limited at the translational stage.

Glutamic acid-rich polypeptides have been expressed in *E. coli* as protein fusions to β–galactosidase by incorporation of small, in-frame inserts late in the *lac* Z coding sequence[20]. These fusions were used to evaluate the absolute rate of *in vivo* translation of the individual Glu codons GAA and GAG. The coding sequence for each fusion was composed of sixty codons, 48 of which corresponded to one of the Glu codons, which were present in stretches of eight contiguous condons. Both translation rate and protein accumulation depended on the identity of the Glu codon in the sequence. The common codon GAA was found to be translated at a rate approximately three times that of the less common codon GAG and the corresponding protein fusion accumulated to a higher level (50% higher) for fusions containing the more common codon. This protein was reported to accumulate to a level of approximately 13% of total cellular protein. The difference in expression levels between the constitutionally identical fusion proteins was ascribed to formation of ribosome queues at the less rapidly translated GAG sequences. It was also found that the rates of protein synthesis did not change when glutamic acid was supplemented to the medium at a concentration of 50 μg/mL.

In bacteria, proteins with long stretches of glutamate residues have not been found although segments of tandem Glu residues have been reported in higher organisms. Sugimoto et. al. found a glutamic acid-rich protein from bovine retina, where 68 of 109 amino acids are glutamic acid and the longest run of Glu is 4.[16] Ambler listed some unusual sequences including Glu_{30} as the C-terminal domain of *Drosophila* troponin-T, Glu_{30} in a *Plasmodium* glutamic acid-rich protein, and runs of Glu at the C-termius of several vertebrate developmental proteins.[17] Some evidence has been presented for the dramatic decrease in yield of oligopeptide concatamers fused to neutral carrier protein beyond a certain number of repeats e.g. in expression of fusion proteins containing six

repeats of the 14 residue yeast α-mating factor.[18] However the causes of the observed low levels expression of **PLGA-X** remain to be elucidated.

Currently, there are continuing investigations in Tirrell's research group to understand and optimize the translation processes of **PLGA-X** expression. For example, Mawn is studying the level of protein accumulation in response to over expression of the glutamyl-tRNA ($tRNA^{Glu}$) and corresponding aminoacyl-tRNA synthetase in order to test the hypothesis that the low expression yield of PLGA-X gene is due to the depletion of aminoacylated-$tRNA^{Glu}$ in cells where the vast majority of ribosomes are recruited to translate a coding sequence composed of long stretches of consecutive Glu codons. If this is the case, the ribosome will stall on Glu codons. One way to overcome the aminoacylated-$tRNA^{Glu}$ depletion is to over produce the aminoacylated-$tRNA^{Glu}$. This can be achieved by over expressing the $tRNA^{Glu}$ and also over expressing glutamyl-tRNA synthetase which is needed for charging $tRNA^{Glu}$. The coding sequence of these genes can be assembled using chemically synthesized oligonucleotides[21] or using PCR amplification of purified *E. coli* genomic DNA . Over-expression of the gene can be accomplished by placing the gene under the control of constitutive promoter[25].

Another hypothesis for explaining the variation of growth rate and protein expression in relation to the number of Glu codons stems from the toxicity of the transcribed mRNA. For example, there is a similarity between the gene sequence (**2**) and the Shine-Dalgarno sequence[29], a sequence involved with initiation of protein synthesis in procaryotes. Virtually all of the known *E. coli* mRNA initiation sites include a oligonucleotide sequence or a part of the sequence **3**. This polypurine stretch known as the Shine-Dalgarno sequence usually lies 4-7 base pairs before the start (AUG) codon and is believed to pair with its complement located close to the 3' end of 16S rRNA (Figure.2.4).

5'------A G G A G G------3' **3**

If the rRNA should recognize part of sequence **2** as the Shine-Dalgarno sequence, small ribosomal subunits can be held up by this gene and eventually affect expression of this gene and also, if the ribosome pool becomes depleted by this process, affect the expression of other proteins vital to cell growth.

Bula and coworkers[22] have reported an inverse relationship between the level of protein expression and a number of serine codons when expressing a serine-rich part of Herpes simplex virus protein in *E. coli.* They proposed a model in which the serine-rich domain induces premature termination of translation and concluded that this effect is not due to any specific secondary structure in the mRNA or lack of sufficient seryl-tRNA synthetase.

2.3.3 Large-Scale Protein Expression and Purification

Protein expression of PLGA-X was scaled up to 60 L with the use of a New Brunswick 80 L mobile pilot plant (MPP-80). All experimental conditions were the same as in the small scale experiment. Target protein synthesis was induced at $OD_{600nm} = 1.2$ and continued for 3 hr. After 3 hr of induction time, the culture reached an OD_{600nm} of 3.8 and 100 g of wet cells were isolated by continuous centrifugation. Purification of the DHFR fusion proteins was accomplished under denaturing conditions by immobilized metal affinity chromatography. Batch processing proved to be effective for the charging and washing steps of the purification procedure. Figure 2.5 shows the purification of the **PLGA-4** fusion protein. The target protein is present in essentially pure form in pH 5.4 elution (lane 6). Lyophilization after dialysis of this fraction yielded approximately 600 mg of **PLGA-4** fusion protein. Yields of the **PLGA-X** fusion proteins are shown in Table 2.1.

PLGA-X was released from the fusion protein by cyanogen bromide cleavage. The cleavage reaction was typically performed in 70% formic acid solution at room temperature for 2 days. However, even after 5 days the cleavage reaction was not complete

and although in small quantity, protein with fragment of the DHFR still attached was present (Fig. 2.6, band 1). However anion-exchange chromatography purification removed most of the higher molecular weight impurities (Fig. 2.8) When the reaction mixture was analyzed after a long period of CNBr reaction time or from the reaction conducted at higher temperature (60°C), a number of discrete protein bands were present in 12% polyacrylamide gel electrophoresis which ran lower than the target protein (Fig. 2.6). The lower bands were found to be the degraded product of the target protein and the degradation seemed to have occurred specifically at the aspartic acid residue. A possible degradation process is proposed in Figure 2.7 which is very similar to the degradation process for the CNBr reaction at methionine site. The acid lability of the peptide bond between aspartic acid residue and proline residue has been reported before[27, 30] and preferential cleavage and release of aspartic acid at high temperature (100°C) in dilute acid was studied by Tsung and coworkers[28]. By running the cleavage reaction at room temperature for short period of time (less than 2 days), the complication of degradation were circumvented and relatively pure proteins of **PLGA-X**s were isolated after anion exchange chromatography purification. Figure 2.8 compares the distribution of relative molecular mass of PLGA-Xs (lanes 1-4)with that of conventional PLGA of polydispersity index 1.2 (lane 5); the difference in uniformity is striking. Yields and amino acid analyses of the final **PLGA-X**s are shown in Table 2.1 and 2.2 respectively. The discrepancies between the theoretical values and the experimental values are possibly caused by a presence of partially cleaved proteins, the protein containing part of the DHFR.

2.4 Conclusions and Future Perspective

A series of monodisperse derivatives of poly(α,L-glutamate) were produced in *E. coli* by recombinant DNA biosynthesis techniques. The proteins were expressed as fusions to DHFR in the pQE-15 expression system. The desired polypeptide was cleaved from DHFR with cyanogen bromide and purified to homogeneity. The uniformity of molecular

size of the biosynthetically derived PLGA analogues is demonstrated in an electrophoresis experiment as narrow bands with step differences in band positions, in comparison to the continuous and broad band of conventional polydisperse PLGA.

A routine procedure of preparing pure $GluAsp(Glu_{17}Asp)_XGluGlu$ (**PLGA-X**, X=3, 4, 5, and 6) in the amount of 50 to 80 mg was developed. However, the current expression yields are still too low for materials characterization purpose. Ideally, multigram samples are needed for the full characterization of liquid crystal properties. The reason for relatively low accumulation of fusion protein is not readily apparent and more carefully designed experiments are needed to explain this problem. Three interesting observations were made from the expression of PLGA-Xs in bacterial host (SG13009), the inverse relationship between the cell growth rate and number of Glu codons, the inverse relationship between the expression yield and the number of Glu codons at constant IPTG concentration and the inverse relationship between the expression yield and the IPTG concentration at constant number of Glu codons[15]. It will be of great interest for both molecular biologists and polymer chemists to elucidate this peculiar behavior.

Table 2.1 Yields of Purified Proteins (PLGA-Xs) from 60 L Expression[a]

	Fusion Protein[b]	Cleaved Protein[c]
PLGA-3	560 mg (9.3 mg/L)	75 mg (1.2 mg/L)
PLGA-4	600 mg (10 mg/L)	80 mg (1.3 mg/L)
PLGA-5	430 mg (7.2 mg/L)	57 mg (0.95 mg/L)
PLGA-6	300 mg (5.0 mg/L)	55 mg (0.92 mg/L)

a 60 L expression was conducted using New Brunswick 80 L mobile pilot plant fermentor. The OD_{600} at harvest was 1.8 which corresponded to about 100 g of wet cells.

b After immobilized metal affinity chromatography.

c After CNBr cleavage reaction and anion exchange chromatography.

Table 2.2 Amino Acid Analyses of **PLGA-X**s (mole%)

	PLGA-3		**PLGA-4**	
	theor.	expl.	theor.	expl.
Asp	6.89	8.58	6.58	19.43
Glu	93.1	80.79	93.42	74.04
Gly	-	2.76	-	1.18
Tyr	-	1.17	-	-
Val	-	1.77	-	0.79
Leu	-	2.38	-	-
Met	-	-	-	0.75
Ile	-	-	-	1.25
Lys	-	2.54	-	2.56

	PLGA-5		**PLGA-6**	
	theor.	expl.	theor.	expl.
Asp	6.38	8.66	6.25	5.93
Glu	93.62	69.74	93.75	72.17

Figure 2.1 Comparative gel (1.2% agarose gel) electrophoresis of *AvaI* digests of recombinant expression vectors pQE-15-Xs. Lanes 1, 2, 3, and 4 are *AvaI* digests of pQE-15-X with X=3, 4, 5, and 6 respectively; Lane 5, 100 bp DNA ladder.

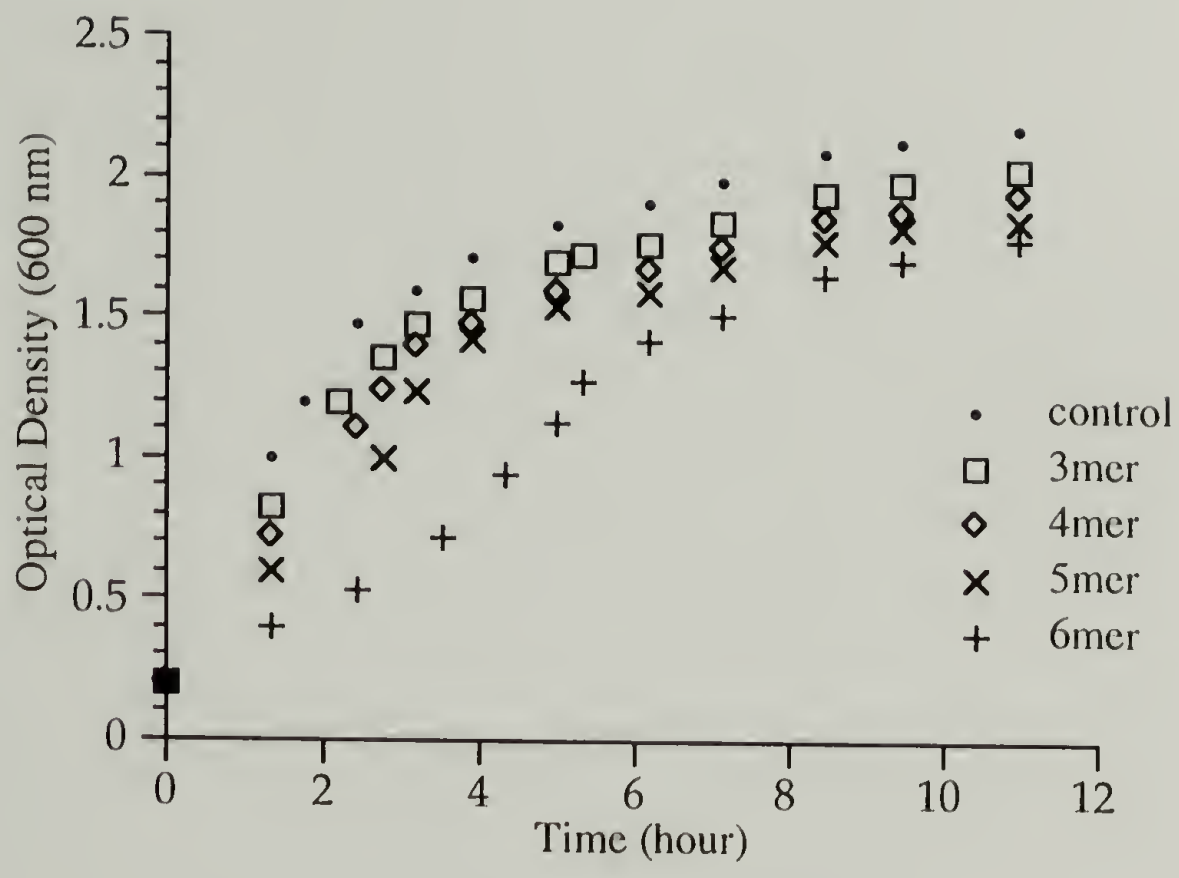

Figure 2.2 Cell growth profiles in protein expression of cells transformed with pQE-15-X. (X= 0 (◦) , 3 (□), 4(◇), 5(×), and 6(+)). IPTG was added at OD_{600}=1.2.

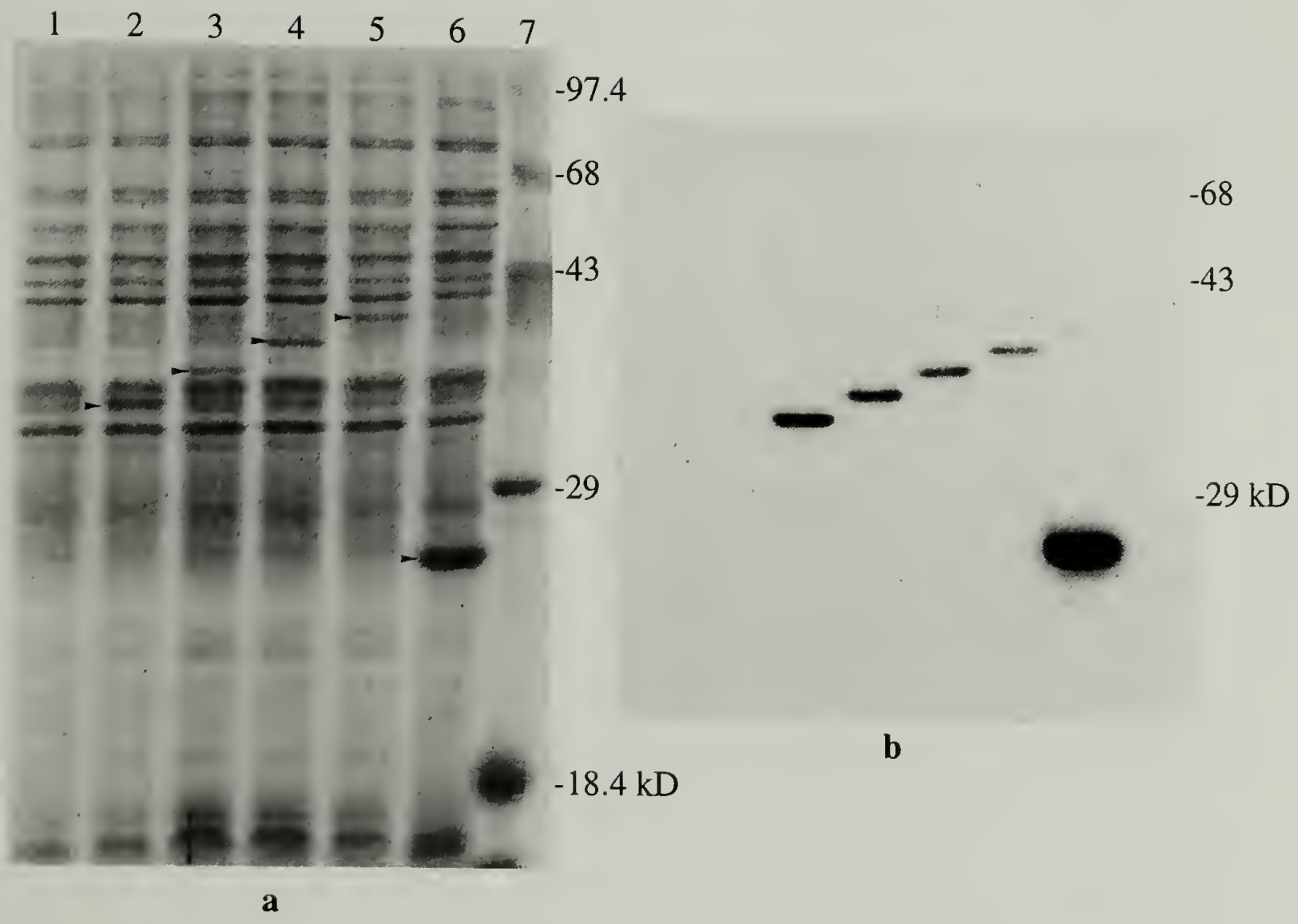

Figure 2.3 SDS-PAGE (12%) (**a**) and western blot (**b**) of proteins in whole cell lysates. Lane 1 contains the nascent polypeptides derived from cell transformed with pQE-15-3 before the target protein induction. Lanes 2-6 contain the nascent polypeptides derived from the cells transformed with pQE-15-X with X=3, 4, 5, 6, and 0 respectively, 3 hr after the target protein induction. Lane 7 contains molecular weight marker. Target protein bands are marked with arrow heads.

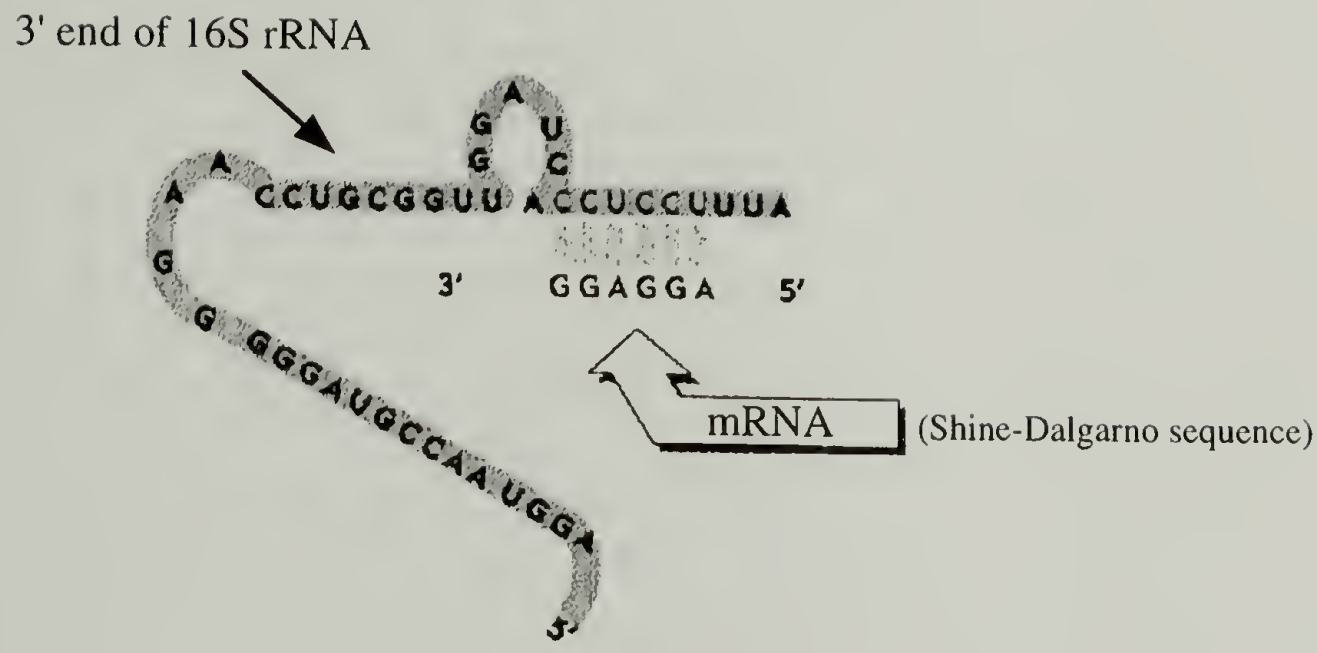

Figure 2.4 Base pairing between rRNA and mRNA at initiation. From Ref. 29.

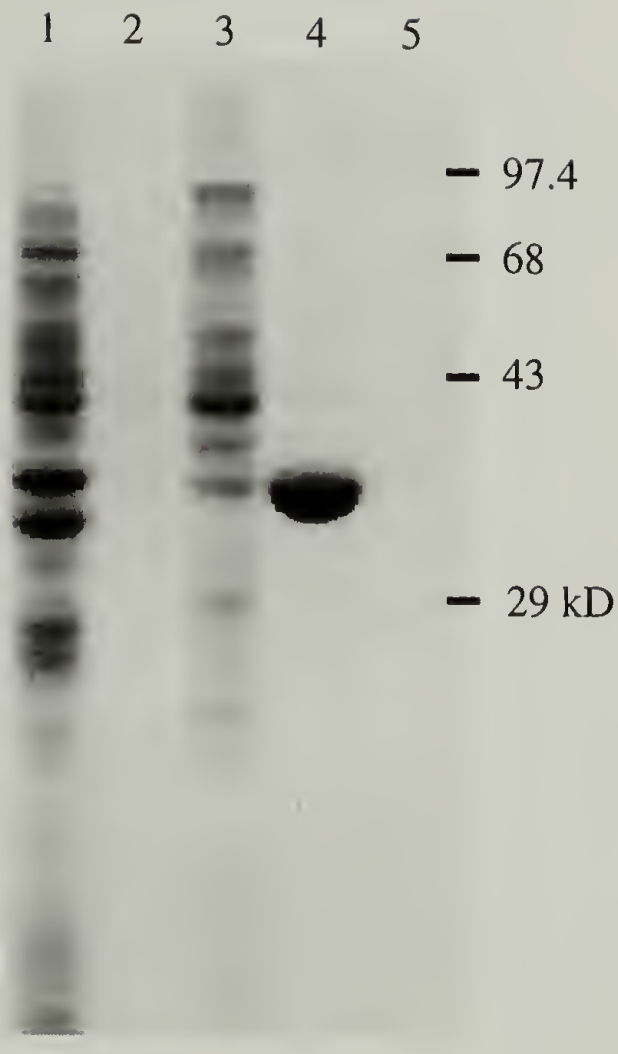

Figure 2.5 Protein purification of PLGA-4 fusion using immobilized metal affinity chromatography. Lane 1 contains crude cell lysate after induction. Lanes 2-5 contain wash buffers of pH=8.0, 6.9, 5.4 and 4.5 respectively. The target protein is present essentially at the pH 5.4 fraction.

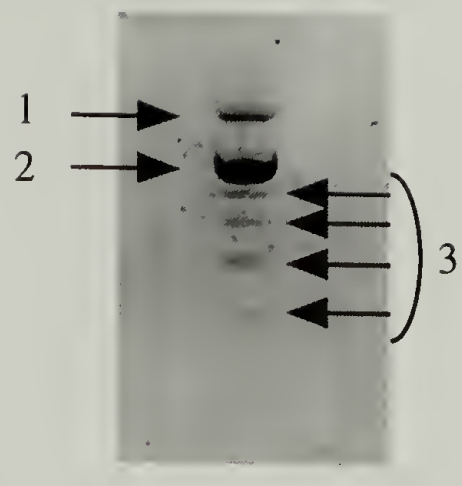

Figure 2.6 Degradation of PLGA-6 during CNBr cleavage reaction. The cleavage reaction was run for 4 days at 60°C and the crude reaction product was analyzed by 12% polyacrylamide gel. 1 is a partially cleaved protein band which contains part of fusion protein sequence. Band 2 is a target protein (PLGA-6) and discrete bands (3) running below the target protein band are the degraded product. Protein bands are visualized with 0.1 methylene blue.

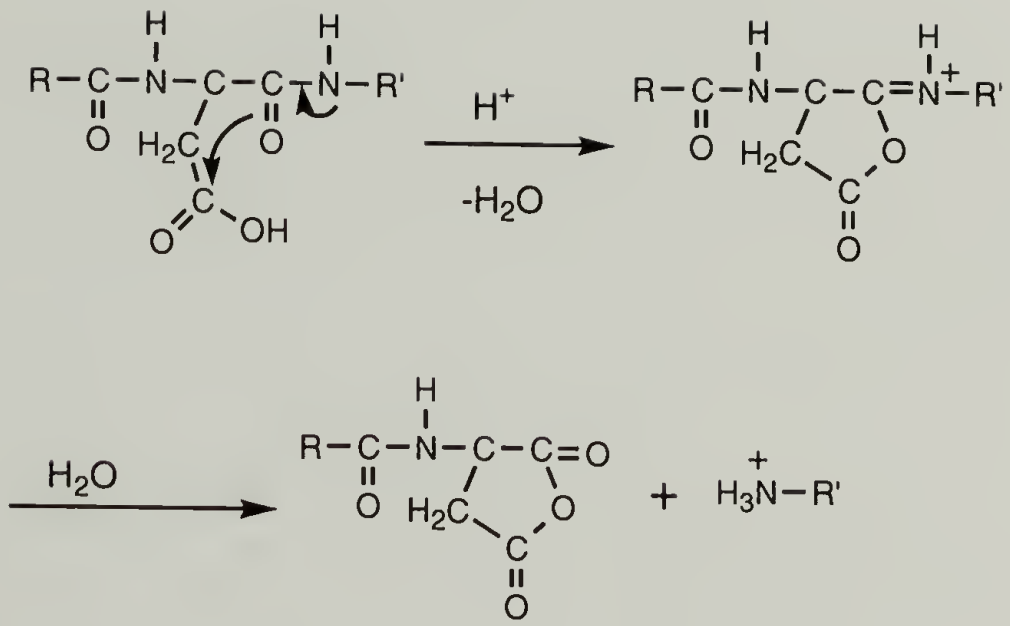

Figure 2.7 Possible degradation process at aspartic acid residue.

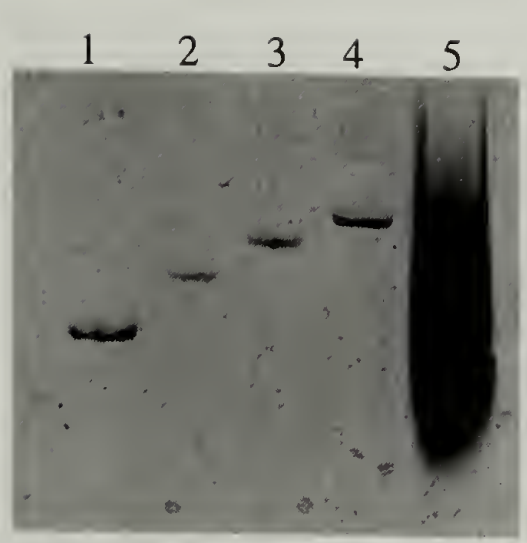

Figure 2.8 Comparative gel electrophoresis of PLGAs. Lanes 1-4 contain purified PLGA-X with X=3, 4, 5, and 6, respectively. Lane 5 contains conventional polydisperse PLGA (DP=98, PDI=1.2). Protein bands are visualized with 0.1% methylene blue.

2.5 References

1. McGrath, K. P.; Tirrell, D. A.; Kawai, M.; Mason, T. L.; Fournier, M. J. *Biotechnol. Prog.* **1990**, 6, 188.

2. McGrath, K. P.; Fournier, M. J.; Mason, T. L.; Tirrell, D. A. *J. Am. Chem. Soc.* **1992**, 114, 728.

3. Poland, D.; Scherga, H. A. *Theory of Helix-coil Transitions in Biopolymers*; Academic Press: New York, 1970.

4. Holtzer, A. *J. Am. Chem. Soc.* **1994**, 116, 10837.

5. McMaster, T. C.; Carr, H. J.; Miles, M. J.; Carins, P.; Morris, V. J. *Macromolecules* **1991**, 24, 1428.

6. Du Pre, D. B.; Samulski, E. T. in *Liquid Crystals The Fourth State of Matter*; Saeva F. D., Ed.; Dekker: New York, 1979; pp 203.

7. Doty, P.; Wada, A.; Yang, J. T.; Bout, E. R. *J. Polym. Sci.* **1957**, 23, 851.

8. Burlatsky, S.; Deutch, J. *Science* **1993**, 260, 1782.

9. Nakano, K.; Fujita, Y.; Maeda, M.; Takagi, M. *Polymer* **1992**, 33, 3997.

10. Zhang, G.; Fournier, M. J.; Mason, T. L.; Tirrell, D. A. *Macromolecules* **1992**, 35, 3601.

11. Bujard, H.; Gentz, R.; Lanzer, M.; Stueber, D.; Mueller, M.; Ibrahimi, I.; Haeuptle, M.-T.; Dobberstein, B. *Meth. Enzymol.* **1987**, 155, 416.

12. Le Grice, S. F. J.; Gruninger-Leitch, F. *Eur. J. Biochem.* **1990**, 187, 307.

13. Sambrook, J.; Fritsch, E. F.; Maniatis, T. *Molecular Cloning: A Laboratory Manual*, 2nd ed.; Spring Harbor Laboratory Press: New York, 1989.

14. Mahajan, S. K. In *Genetic Recombination*; Kucherlapati, R.; Smith, G. R., Eds.; American Society for Microbiology: Washington, DC, 1998; Ch. 3.

15. Conticello, V. P.; Zhang, G.; Fournier, M. J.; Mason, T. L.; Tirrell, D. A. manuscript in preparation.

16. Sugimoto, Y.; Yatsunami, K.; Tsujimoto, M.; Khorana, H. G. *Proc. Natl. Acad. Sci. USA* **1991**, 88, 3116.

17. Ambler, R. P. *Biochem. Soc. Trans.* **1991**, 19, 517.

18. Kuliopulos, A.; Walsh, C. T. *J. Am. Chem. Soc.* **1994**, 116, 4599.

19. Makrides, S. C. *Microbiol. Rev.* **1996**, 60, 512.

20. Sorenson, M. A.; Pedersen, S. *J. Mol. Biol.* **1991**, 222, 265.

21. Normanly, J.; Masson, J.-M.; Kleina, L. G.; Abelson, J.; Miller, J. H. *Proc. Natl. Acad. Sci.* **1986**, 83, 6548.

22. Bula, C.; Wilcox, K. W. *Protein Expression Purif.* **1996**, 7, 92.

23. Rosewell, D. F.; White, E. H. *Meth. Enzymol.* **1978**, 57, 409.

24. Schwartz, G. *Biopolymers* **1968**, 6, 873.

25. Kleina, L. G.; Masson, J.-M.; Normanly, J.; Abelson, J.; Miller, J. H. *J. Mol. Biol.* **1990**, 213, 705.

26. Mawn, M. V.; Tirrell, D. A.; Mason, T. L. manuscript in preparation.

27. Inglis, A. S. *Meth. Enzymol.* **1983**, 91, 324.

28. Tsung, C. M.; Fraenkel-Conrat, H. *Biochemistry* **1965**, 4, 793.

29. Lewin, B. *Genes V*; Oxford University Press: Oxord, 1994.

30. Piszkiewics, D.; Landon, M.; Smith, E. L. *Biochem. Biophys. Res. Commun.* **1970**, 40, 1173.

CHAPTER 3

SMECTIC ORDERING IN SOLUTIONS AND FILMS OF MONODISPERSE DERIVATIVES OF POLY(γ-BENZYL α,L-GLUTAMATE)

3.1 Introduction

Solutions and melts of stiff ("rod-like") macromolecules often exhibit nematic liquid crystalline phases characterized by orientational - but not positional - molecular order[1, 2]. Smectic phases, in which macromolecular rods are organized into layers roughly perpendicular to the molecular director, are rare, owing at least in part to the polydisperse nature of macromolecular systems prepared by conventional polymerization processes. Here we report the synthesis of a series of monodisperse derivatives of poly(γ-benzyl α,L-glutamate) (PBLG), and evidence for smectic ordering in PBLG solutions and films.

PBLG is a typical model of a helical polymer with rigid rod structure. Because of its ready availability and good solubility combined with stable rod like structure, PBLG probably has been the most extensively studied synthetic polypeptide in a variety of subjects such as structural determination of the α-helix, helix-coil transition, dielectric properties, hydrodynamic and liquid crystalline properties[3]. In addition, the behavior of self assembled PBLG and its side chain derivatives at interfaces has drawn much attention recently because of opportunities for engineering surface arrays for potential new applications[4, 5]. Unfortunately, interpretation of the physical properties and preparation of highly ordered supramolecular architectures from PBLG are complicated by the inherent polydispersity of PBLG which is traditionally prepared by ring-opening polymerization of the N-carboxy-α-amino acid anhydride[6]. For example, PBLG is known to form lyotropic cholesteric or nematic liquid crystalline (LC) phases[7], however the effect of polydispersity on the formation of such mesophases is unclear.

Since their discovery by Robinson the lyotropic liquid crystalline phases (cholesteric and nematic), exhibited by PBLG have fascinated scientists for many years and PBLG is still considered to be the model system for rod-ordering LC theories[8]. Phase diagrams of PBLG solutions were determined experimentally[9, 10] and found to be in general agreement with the phase diagram proposed by Flory[11]. However, a critical comparison of these theories and experiments has been complicated by the polydisperse nature of the PBLG system[12]. In addition, a different type of LC phase may exist in a more homogeneous system because the polydispersity would favor nematic ordering. Tobacco mosaic virus[13], a monodisperse rod-like polymer, was reported to form smectic phases in colloidal solutions. Smectic like ordering of either rod polymers or rod-coil block copolymers from lyotropic solution has been reported recently,[14,15] however there has been no direct evidence for smectic arrangement of PBLG chains. On the other hand, PBLG chains have a strong tendency to aggregate in concentrated solutions and such attractive forces may promote formation of smectic mesophases[16,17]. It was also shown by computer simulation that the smectic phase can be induced by the rod-like shape itself through an excluded volume effect.[18]

The objective of the work presented in this chapter is to prepare a series of monodisperse derivatives of poly(γ-benzyl α,L-glutamate) from biosynthesized poly(α,L-glutamate) derivatives and to identify and characterize the smectic ordering of these monodisperse rod-like polymers in solution and in the solid state.

3.1.1 Solution Properties of PBLG

PBLG is soluble in a wide variety of solvents and most of these solvents are helicogenic. They include partially halogenated hydrocarbons such as chloroform, dichloroethane, and dichloromethane, and also other common organic solvents such as benzene, dioxane and m-cresol. However, the highly anisotropic PBLG has a strong tendency to aggregate in many of these solvents which is in part due to the large dipole

moment brought about by the directionally aligned hydrogen bonds of the rod-like polypeptide backbone[19]. It was reported that even in dilute, isotropic solution, PBLG often exists in a form of multimeric aggregates, however the aggregation in DMF was shown to be rather minor compared to that occuring in other solvents[20]. Small quantities of acids, such as dichloroacetic acid (DCA) and trifluoroacetic acid (TFA), when added to the PBLG solutions, were shown to be effective in disrupting the aggregation and provided solutions of non-interacting helices[21]. However at higher concentration of acids, PBLG denatures, forming a random-coil structure.

The conformational transitions between α-helix and random coil can be induced by the addition of denaturants or by changing the temperature[22]. The basic thermodynamic constants for such transitions are well documented in the literature[3]. The mechanism of the DCA or TFA-induced transition has been a subject of controversy. One possible explanation is that the acid associates, through competitive hydrogen bonding with NH groups in the backbone, and C=O groups in the side chain[23, 24]. However, when the acid is present at a concentration less than 10% of the solution, the helical stability is not affected[21]. The helical conformation of PBLG in DCA solution can be induced by a so-called, "inverted thermal transition"[25, 26]. When the temperature of the solution is high, a demixing between polymer and DCA occurs, and the PBLG which was a random coil at low temperature is converted to a helical conformation as the temperature is raised. As a consequence, PBLG has isotropic phases in two separate temperature regions. The peculiar low temperature isotropic phase is often referred to as a reentrant isotropic phase[27 28].

The rod-like rigidity in solution has made PBLG a typical model polymer for the investigation of viscosity and visco-elastic behavior. The rheological property unique to LC solutions - the negative normal stress differences at medium shear rate - was first discovered by Kiss and Porter, in the PBLG-m-cresol system[29].

The combination of the rigidity and long persistence length of PBLG together with the presence of the dipole moment of the amide bond results in a macromolecule possessing a very large dipole moment. This was first reported by Wada[30] and has been the subject of considerable interest since. Each residue of PBLG contributes a dipole moment (3.5 Debye/residue) derived from amide and ester groups whose resolved components along the helix axis are additive provided no disruption or bending of the helix occurs. Under such conditions, the total dipole moment of an individual PBLG molecule is directly proportional to molecular weight. The divergence from such proportionality has been related to the flexibility of the polymer and was used to calculate the persistence length of PBLG[31].

3.1.2 Liquid Crystalline Properties of PBLG

PBLG liquid crystals are prepared simply by dissolving the polymer in a solvent that supports the α-helical conformation. The solution becomes liquid crystalline spontaneously when the polymer solution exceeds a certain limiting concentration. The homogenous liquid crystalline phase is preceded by a biphasic regime in which isotropic solution is in equilibrium with liquid crystalline solution. The liquid crystalline phase can be readily recognized; it is highly birefringent and exhibits the optical characteristics of the cholesteric structure[32]. The polymer concentrations which define the three regimes, the isotropic state, biphasic state and liquid crystal state are fairly independent of solvent but depend strongly on the aspect ratio (L/D) and temperature of the system. These qualitative observations suggest that the rod-like shape of the polypeptide molecule, and not specific polymer-solvent interaction, are responsible for the formation of the liquid crystalline phase. Molecular descriptions of the transition from an isotropic to the liquid crystalline order of rod-like polymers carried out by Onsager, Isihara, and Flory focus on the change in entropy of the system[33]. By applying a lattice model to a system composed of noninteracting, impenetrable, rod-like particles and inert spherical solvent molecules, Flory produced a phase diagram of a rod-like polymer solution which was in general agreement

with experimentally determined phase-diagram (Figure 3.1)[9, 10, 11]. However, critical comparison of theory and experiment has been complicated by the polydisperse nature of the PBLGs available to date. For example, the two coexisting liquid crystalline phases observed by Horton and coworkers may have been a result of phase separation of different chain length of polydisperse PBLG rods[10].

3.1.3 Smectic Ordering of Rod-Like Polymers

Smectic ordering is characterized by the positional molecular order in addition to orientational order with molecules arranged in a layer-like structure with layers roughly perpendicular to the direction of the molecules. Smectic phases are formed by a wide variety of compounds (including main and side chain polymers) containing low molecular weight mesogens[34], however, such ordering is rare in stiff ('rod-like') macromolecules[1]. McMillan proposed a model for smectic ordering, which was in part an extension of the Maier-Saupe model for the nematic phase, in which smectic order is derived from attractive forces between neighboring molecules[17]. However, it was unclear if such ordering can be induced by pure entropic forces with non-interacting rods. More recently, Stroobants, Lekkerkerker and Frenkel reported discovery of smectic A ordering from computer simulation of a system of non-interacting hard spherocylinders (SLF model) (Figure 3.2)[18]. Then, Meyer and coworkers reported definitive experimental observation of smectic A ordering in tobacco mosaic virus (TMV), a monodisperse rod-like particle, under conditions where TMV behaves as hard cylinders[13]. PBLG has been a typical model of non-interacting rod for Flory and Onsanger's rod ordering theory for nematic liquid crystalline phases[33]. Currently there has not been any experimental evidence that conclusively shows the existence of smectic ordering of PBLG molecules.

3.1.4 Solid State Properties of PBLG

Attempts to retain specific mesomorphic structure in the solid state date from the late 1930s when it was shown that some thermotropic liquid crystal phases could be quenched to low temperatures to form a metastable state in which the liquid crystalline ordering is retained[35]. In the case of lyotropic liquid crystals, similar results could be obtained in principle by freeze-drying or slow evaporation of the solvent. Solid homogeneous films can be prepared by evaporating solutions of PBLG in volatile solvents such as chloroform and dichloromethane. In a majority of cases, the polypeptide assumes an α-helical conformation, unless it is of low molecular weight, in which case both α-helix and β-sheet are observed. Solvent nature and casting conditions can both influence the morphology of PBLG films. Tobolsky and coworkers have investigated the supramolecular structure of PBLG in the solid films and concluded that the PBLG helices lie in the plane of the film and that the direction of the helical axes is randomly oriented in the film plane[36]. The anisotropic swelling characteristics of the film and the observation of iridescent colors reflected from the film surfaces promoted the suggestion that the solid films partially retain the cholesteric structure of the liquid crystalline phase[37]. This was further proven by the observation of retardation lines characteristic of cholesteric phases in plasticized PBLG films. X-ray studies on plasticized films show that the spacing between the planes of hexagonally packed helices changes as the polymer/plasticizer ratio is changed[38].

When solutions of PBLG are slowly evaporated in a strong magnetic field, highly oriented films are obtained. The orientation occurs while the evaporating solutions pass through the concentration range in which they are liquid crystalline and becomes permanently locked in when the PBLG becomes solid. X-ray diffraction of the magnetically oriented PBLG film is similar to the fiber diffraction patterns obtained from mechanically oriented PBLG[39]. The typical diffraction pattern of oriented films is that of the 18/5 helix, however depending on the solvent and drying condition, films with 7/2

helix can also be obtained[40]. Although NMR studies of PBLG liquid crystal solutions indicate formation of oriented nematic phases in magnetic fields for most helicogenic solvents, the macroscopic orientation is not always present in the solid films. Apparently, the strong interaction between the polymer chains, especially at high concentration, which is dictated by the solvent type, concentration and temperature of the system, seems to affect the macroscopic ordering during the drying process.

Analyzing a fractured surface of solid PBLG is another way of characterizing the molecular order of PBLG rods in the solid state. Samulski and Tobolsky reported scanning electron micrographs of PBLG in both unoriented and oriented states. Sheath-like structures reminiscence of cholesteric supramolecular order were observed in unoriented samples. In the case of oriented samples, fibrillar morphology was apparent in which the fibril axes were parallel to the magnetic field direction.

Microcrystals in the form of semihexagonal and ribbon-like structures of PBLG aggregates can be obtained by crystallizing PBLG from hexafluoroisopropanol[41]. Even though the crystal had well defined hexagonal symmetry no electron diffraction pattern was obtained. The thickness of the crystal was approximately a third of the length expected for unfolded PBLG chain and many crystals were subdivided into sectors. From these observations, the authors were led to the conclusion that the PBLG chains are in a folded state in the crystals. Thin films of ordered PBLG can be prepared by epitaxial growth of polymer on the surface of inorganic and organic single crystals e.g. NaCl[42].

Electron diffraction of PBLG film was first reported by Parsons and Martius[43]. These workers obtained electron diffraction patterns nearly identical to the X-ray diffraction pattern of mechanically drawn PBLG fiber and demonstrated the fidelity of the electron diffraction experiment in elucidating the helical structure of synthetic peptides.

3.1.5 Surface and Interfacial Chemistry of PBLG

Interfacial order of PBLG at an air-water interface was investigated by Malcom[44]. Infrared spectroscopy and electron diffraction of a collapsed film which was transferred to a solid surface were found to be consistent with a structure composed of condensed, ordered arrays of α-helices with their long axes parallel to the air-water interface[45]. The Π (surface pressure)-Å^2 (area/molecule) isotherm was reported and compression of PBLG film at the air-water films resulted in bilayer formation of PBLG rods[46]. In order to reduce the brittleness of the film to facilitate the transfer to a solid substrate, Wegner et al synthesized long alkyl derivatives of PLGA and studied their interfacial and ordering behavior during the transfer process[5].

Another and more recent interest in PBLG monolayers involves tethering the end of PBLG on a solid substrate with controlled orientation and molecular conformation. The resulting highly polar film has potential applications in non-linear optical devices and piezoelectric materials. In addition, this well-defined substrate may serve as a template for more complex supramolecular architectures, or by incorporation of desired functional groups, find application in liquid crystal displays and biosensors[47, 48]. Samulski and coworkers first reported an investigation on the adsorption behavior of PBLG on gold surfaces[4]. PBLG (MW=20,000) was prepared by ring-opening NCA polymerization and the N-terminus of the peptide was reacted with lipoic acid to introduce a disulfide group. In contrast to the physisorbed and Langmuir Blodgett (LB) deposited films, the PBLG with disulfide end group showed non planar distribution of helix axes suggesting preferential binding of peptides to gold surface by disulfide end group. Frank and Chang applied both *grafting from* and *grafting to* approaches to study the assembly behavior of PBLG on silicon (100) native surface. Recently, Wegner and coworkers prepared a PBLG monolayer film showing piezoelectric properties. However, most of the surfaces prepared to date were shown to have significant variation in film thickness and the average orientation of helical rods deviated significantly from the surface normal. Such difficulties

in preparing well-organized monolayer films may have been partly due to the polydisperse nature of the sample that was prepared by conventional polymerization methods. Therefore, the monodisperse PBLG not only has direct bearing on many fundamental aspects of physical chemistry but also has wide implications for use such as chemical sensors, optical switches and piezoelectric or ferroelectric devices.

3.2 Experimental Section

3.2.1 Materials

Benzaldehyde tosylhydrazone, benzyltriethylammonium chloride, trifluoroacetic acid and dimethylsulfoxide (HPLC grade) were purchased from Aldrich. HPLC grade benzene and polydisperse PBLG (DP≈98, PDI=1.2) were purchased from Sigma and chloroform, methylene chloride, dioxane and pentane were purchased from Fisher Scientific. All reagents were used without further purification.

3.2.2 Synthesis of Phenyldiazomethane

To a suspension of benzaldehyde tosylhydrazone (0.75 g, 2.7 mmol) in benzene (40 ml), 14% (w/w) aq. NaOH solution (75 ml) containing 7 mg (0.03 mmol) of benzyltriethylammonium chloride was added. The reaction mixture was protected from light and refluxed at 70°C for 5 hr. The benzene phase containing phenyldiazomethane was separated, washed with water, dried over Na_2SO_4, and used directly in the benzylation step.

3.2.3 Synthesis of PBLG Derivatives (**PBLG-3**, **4**, **5**, and **6**)

The following procedure is representative of the method used for benzylation of monodisperse derivatives of poly(α,L-glutamic acid). **PLGA-4** (sodium salt, 100 mg, 0.6 mmol repeating units) was dissolved in 15 ml of water and acidified with dilute aq.

HCl (final pH=1.3). The precipitated polymer was purified by ultrafiltration (Amicon, molecular weight cut-off = 3000 Da) to remove residual NaCl and dried under vacuum overnight. The polymer was dissolved in 40 ml of dimethylsulfoxide and 20 ml of the phenyldiazomethane (1.3 mmol) solution was added. The reaction mixture was stirred at room temperature for 48 hr in the dark and concentrated to dryness by vacuum distillation. The remaining solid was dissolved in dichloromethane, precipitated by addition to pentane, redissolved in tetrahydrofuran and reprecipitated by addition to water. Similar procedures were used for the preparation of **PBLG-3**, **5**, and **6**. The yield was 70%: ^{1}H NMR ($CDCl_3$/TFA) δ 2.0-2.1 (2H, β-CH_2), 2.4 (2H, γ-CH_2), 2.9 (aspartic acid, β-CH_2), 4.6 (1H, α-CH), 4.9 (aspartic acid, α-CH), 5.1 (2H, benzylic CH_2), 7.3 (5H, Ar-H).

3.2.4 Polarized Light Optical Microscopy

Solutions of known concentration were prepared in 1 mm diameter capillary tubes and equilibrated for 4-5 days at room temperature. Capillaries were immersed in a shallow water bath for direct observation; in some cases, a syringe was used to transfer a small portion of the solution to a glass slide. An Olympus BX microscope was used for observation with polarizer and analyzer in cross (90°) position.

3.2.5 X-ray Diffraction

Concentrated solutions of PBLG in $CHCl_3$ (97%) / TFA (3%) were prepared in small vials. Solutions were transferred to a Teflon plate and annealed for 4 days at room temperature with the same solvent vapor by allowing the sample to sit at an elevated position in a closed vessel containing the solvent. The solvent was slowly evaporated and the residual solvent was removed under vacuum for 2 days (Figure 3.3). For the oriented sample, the film that was previously cast from $CHCl_3$/TFA solution was annealed with dioxane vapor in 1.98 Tesla magnetic field by the same procedure.

X-ray diffraction patterns were recorded in either evacuated flat-plate Rigaku small-angle X-ray camera or flat-plate Statton camera with pin-hole collimation and Ni-filtered Cu Kα radiation. The beam direction was normal to the film surfaces.

3.2.6 Transmission Electron Microscopy (TEM)

For TEM observation, a PBLG-4 film cast from $CHCl_3$/TFA solution was ultramicrotomed using a diamond knife at room temperature, producing sections 500 Å thick. TEM imaging and electron diffraction were performed at 200 kV; a cryogenic sample holder was used to reduce beam damage.

3.2.7 Atomic Force Microscopy (AFM)

NanoScope IIIa scanning probe microscope from Digital Instruments was used for AFM experiments. The AFM image was acquired in tapping mode at room temperature.

3.3 Results and Discussion

3.3.1 Synthesis of Monodisperse Derivatives of Poly(γ-benzyl α,L-glutamate) (**PBLG-X**)

Benzylation of PLGA-X was achieved by treating the acid form of the polymer with phenyldiazomethane. Phenyldiazomethane was synthesized by treatment of benzaldehyde tosylhydrazone with sodium hydroxide in a two phase reaction, in conjunction with benzyltriethylammonium chloride as phase transfer catalyst[51]. After the reaction, the red-orange benzene solution containing phenyldiazomethane was washed with water, dried with Na_2SO_4 and used for the benzylation reaction without further purification. The solution showed a strong absorption band at λmax=490 nm. Phenyldiazomethane was stable in benzene solution and remained active for more than a month at room temperature.

$GluAsp(Glu_{17}Asp)_XGluGlu$ (X=3, 4, 5, and 6) **PLGA-X**

$Glu(OBzl)Asp(OBzl)\{[(Glu(OBzl)]_{17}Asp(OBzl)\}_XGlu(OBzl)Glu(OBzl)$

(X=3, 4, 5, and 6) **PBLG-X**

Preparation of the acid form of PLGA-X was found to be the crucial step for the successful synthesis of PBLG-X. During the acidification procedure, proteins precipitated at around pH 3 then re-dissolved as the pH was reduced to 1.4. In pH 1.4 solution, protein eventually precipitated after overnight storage at 4°C or during the ultrafitration process. When proteins were isolated from the pH 3 solution, the final yields of the side chain substitution were low (≈40%). However proteins from pH 1.4 solution gave more than 95% benzylation of the side chains. When the pH of the solution was reduced to 1.3, the protein remained soluble in the solution which may have facilitated the protonation of the side chains.

After the acidification step, it was found that removing the residual salt from the protein was essential for achieving high substitution yield of the side chains of PLGA-X. NaCl is a side product from the acidification reaction and Cl^- ion can act as a nucleophile to react with the active form of phenyldiazomethane. Ultrafiltration was performed on the acidified sample to remove residual salt and this procedure increased the side chain substitution yield from 65% to more than 95%.

The purified PLGA-X was reacted with phenyldiazomethane solution in DMSO for 2 days and the reaction mixture was concentrated to dryness by vacuum distillation. The remaining phenyldiazomethane co-distilled with DMSO. The remaining solid was dissolved in dichloromethane and preciptated by addition to pentane. The remaining solid was not soluble in dichloromethane when the yield of benzylation reaction was low. The proton NMR spectra of PBLG-3, 4, 5 and 6 are shown in Figure 3.4-3.7. The spectra are

virtually identical to that of conventional PBLG (Figure 3.5 lower trace) with the exception of two weak aspartic acid resonances at 2.9 ppm and 4.9 ppm. Integrations of the spectra indicate 94%, 98%, 95% and 97% benzylation of the side chains of PLGA-3, 4, 5, and 6, respectively.

In order to gain information about polydispersity, the PBLG samples were analyzed with gel permeation chromatography. To prevent aggregation of the polymer, DMF containing 0.1 M of LiBr was used as a carrier solvent. DMF was reported to be a non-associating solvent for PBLG, and LiBr was added to further ensure non-associating conditions[20]. The polydispersity index (PDI) of PBLG-Xs were typically about 1.05 in contrast to 1.3 of the polydisperse PBLG. Although smaller than that of polydisperse counterpart, the PDI of PBLG-X did indicate a value above the theoretical value 1.00. It is speculated that the breadth of GPC trace in the monodisperse PBLG-Xs is a result of limitations inherent to the GPC experiment. Natural broadening of the band is typical of all chromatographic analyses as a result of diffusion of the compound during the analysis time period.

We have also conducted matrix assisted laser desorption ionization (MALDI) mass spectroscopy experiments in a variety of experimental conditions. However, aggregation of the polymer has prevented observation of any meaningful signal from the MALDI-TOF (time of flight) mass spectrometer. We are currently in the process of optimizing the desorption ionization condition for the PBLG.

3.3.2 Smectic Ordering in Solutions and Films of Monodisperse Derivatives of PBLG

The liquid crystalline phases of PBLG are formed in a number of solvents, including benzene, nitrobenzene, chloroform, DMF, pyridine, dioxane, dichloromethane, and m-cresol[67]. It has been shown that, in all circumstances, the liquid crystalline phases are induced by the rod-like structure of PBLG which is brought about by extended helical molecular conformation.

The properties of PBLG-4 were initially investigated in dioxane solution. A concentrated solution of PBLG-4 (approximately 45%) in dioxane was highly birefringent when examined with the polarized light optical microscope. Films of PBLG-4 and polydisperse PBLG (DP≈98, PDI=1.2) were cast on a Teflon plate. A concentrated solution of PBLG in dioxane was placed on a Teflon plate surface and annealed by allowing the swollen film to sit in the solvent vapor for 4 days. After slowly evaporating the solvents, the film was dried in vacuum for 2 days. Figure 3.8 shows the wide angle X-ray diffraction patterns of these films. Both polydisperse (a) and monodisperse (b) samples show reflections at around 13 Å (very strong), 7.5 Å (strong) and 6.5 Å (strong). The 13 Å spacing is close to the reported values of interchain distances of PBLG rods and the relative ratio of these spacings suggests hexagonal packing of the rods. The 13 Å , 7.5 Å, and 6.5 Å reflections can be assigned to the spacings of (10), (11), and (20) lattice planes, respectively, of a 2 dimensional hexagonal lattice[52]. No diffraction pattern was obtained from small angle X-ray diffraction experiments. These results suggests that when films are cast from dioxane solution, the ordering behavior of the polydisperse and monodisperse PBLGs in solid films is almost identical. PBLG rods are packed in hexagonal lattice with no longitudinal molecular order. The liquid crystalline state exists because of the asymmetric shape and liquid like mobility of the molecule, in solutions or in melts. It has been reported that PBLG molecules have a tendency to aggregate in dioxane solution[16]. Even in dilute solution, the PBLG rods were reported to exist as a multimeric aggregates. Such aggregation can inhibit the free movement of individual rods and affect the liquid crystalline ordering of the PBLG solutions.

The formation of the liquid crystalline phase has been shown to proceed in stages as the concentration of polymer is increased[67]. When the polypeptide exceeds a certain limiting concentration, the solution separates into two liquid crystalline phases. The polypeptide-rich phase is birefringent and departs from the more dilute and isotropic medium in the form of spherical liquid droplets. If the two-phase solution is cooled or the

PBLG concentration is further increased, the droplets grow in size and coalesce forming a continuous birefringent fluid.

These reported results were reproducible when different concentrations of polydisperse PBLG (DP≈98, PDI=1.2) were investigated in mixtures of $CHCl_3$ (97%) and trifluoroacetic acid (TFA, 3%). Addition of TFA has been reported to inhibit aggregation of PBLG in concentrated solutions while maintaining the rod-like rigidity of the main chain[21]. Figure 3.9 shows the phase separated birefringent droplets which were present in a solution approximately 22 % of this polydisperse polymer. At higher concentration, a typical finger print texture of PBLG's cholesteric LC phase was observed (data not shown). However, when solutions of monodisperse sample PBLG-4 were analyzed, the phase separated birefringent droplets were not observed. The transition from the isotropic phase to the liquid crystalline phase seems to occur homogeneously throughout the sample. Figure 3.10 (a) shows a polarized light optical micrograph of isotropic (approximately 25%) solution of PBLG-4 in $CHCl_3$/TFA. When the concentration of PBLG-4 solution was increased to 30%, the texture became partially birefringent, (Figure 3.10 (b)) and the birefringence became stronger homogeneously throughout the sample as the concentration of solution was further increased.

Polarized light optical micrographs of concentrated solutions (approximately 35-40%) of PBLG-Xs are shown in Figure 3.11 and Figure 3.12. The PBLG-4, 5 and 6 solutions are highly birefringent and iridescent, however, PBLG-3 appears dark. The aspect ratios of these polymers are listed in Table 3.1. According to Flory's rod-ordering theory, the critical aspect ratio for the existence of liquid crystalline phase is 7. The aspect ratio of 6.9 of the PBLG-3 seems to be too small to allow formation of a stable liquid crystalline phase. Films of PBLG-Xs were prepared by slow evaporation of this solution on a Teflon surfaces as described before. The mesomorphic textures were retained even after complete removal of the solvent. Solution-cast films of PBLG have been reported to maintain their liquid crystalline order after solvent evaporation, with the molecular chains

oriented parallel to the film surface[37]. Figure 3.13 compares the X-ray diffraction patterns of polydisperse PBLG (DP≈98, PDI=1.2) and monodisperse PBLG-4, both cast from $CHCl_3$/TFA solutions. Both patterns are characterized by a broad wide-angle reflection with spacing of 13 Å which is the interchain distance of PBLG rods. The additional reflections present in the dioxane-cast films cannot be seen. This suggests that in $CHCl_3$/TFA cast films, the PBLG rods are not hexagonally packed but are packed with lateral disorder. In the case of PBLG-4, in the small angle region of the diffraction pattern, additional reflections with Bragg spacings of 57 Å and 38 Å can be seen. The small angle X-ray diffraction pattern (inset) indicates a well defined reflection at spacing of 114.5 ± 1.4 Å as well as the corresponding second-order reflection at 57 ± 0.3 Å. A spacing of 114.5 Å is nearly identical to the expected length of the PBLG-4 helix, given the axial rise per residue of 1.5 Å of the α-helix and the degree of polymerization of 76[53]. The coincidence of the helix length and the observed layer spacing strongly suggests smectic-like ordering in the $CHCl_3$/TFA cast solid film. Films of PBLG-5 and 6 were also cast from $CHCl_3$/TFA solution for X-ray diffraction analysis. Figure 3.14 shows the densitometer scans of the small-angle X-ray diffraction patterns of the PBLG-X films. PBLG-5 shows a well defined maximum at a spacing of 140 Å as well as the corresponding second order at 70 Å, the spacing which is again commensurate with the length of the PBLG-5 helix (141Å). However PBLG-6 did not show any small angle diffraction. A solid film of polydisperse PBLG of comparable molecular weight yielded no small-angle reflections in a similar diffraction experiment. Comparison of this curve with curves of PBLG-4 and 5 provides compelling evidence for the role of chain-length monodispersity in inducing smectic order and controlling the smectic layer spacings in films of rod-like polymers. It is not clear at this point as to why the expected smectic ordering is not seen with PBLG-6. One possible explanation is that the low mobility due to the longer chain length may have slowed down the ordering process.

Films of PBLG-Xs were found to retain smectic order when swollen in dioxane. An oriented sample of PBLG-4 was prepared by placing the dioxane-swollen smectic film in a magnetic field (1.98 tesla, 3 days) and evaporating the solvent. The anisotropy of the magnetic susceptibility causes macroscopic orientation of the rod-like PBLG chains along the magnetic field direction. Polarized light optical micrographs of the dioxane-swollen films after orientation show typical smectic texture with oriented elliptical disclination lines (Figure 3.15). The X-ray diffraction pattern of the oriented PBLG-4 film (dried to remove solvent) is shown in Figure 3.16. The diffraction arcs on the meridian are the second, third, fourth and fifth orders of the 114.5 Å spacing, whereas the broad equatorial reflection corresponds to the interchain distance of 12.5 ± 0.2 Å. This diffraction pattern is consistent with the supramolecular structure illustrated in Figure 3.17, with helical rods arranged in layers of thickness 114.5 Å. The breadth of the equatorial reflection, and the absence of additional wide-angle signals characteristic of the hexagonal structure of PBLG, indicate that the helical rods pack with substantial lateral disorder.

3.3.3 A Helical Smectic Phase in Solid Films of a Monodisperse Derivative of Poly(γ-benzyl α,L-glutamate)

PBLG forms a cholesteric mesophase in a variety of organic solvents. In a cholesteric LC phase, intermolecular forces favor alignment between molecules at a slight angle to one another and the director rotates throughout the sample. The cholesteric twist of PBLG is dictated by the optically active helical conformation of the macromolecules and the dielectric properties of the medium. When cast from the cholesteric LC phase, solid films of PBLG retain cholesteric order[37].

Small angle X-ray diffraction from films cast from monodisperse derivatives of PBLG yielded well-defined reflections with Bragg spacings nearly identical to the expected length of the PBLG helix suggesting smectic-like ordering in the cast solid film. The supramolecular structure of a sample oriented in magnetic field was shown to be smectic A

like. In an effort to characterize the supramolecular structure of an unoriented sample in detail, the unoriented PBLG-4 film, previously shown to form smectic-like order, was analyzed with transmission electron microscopy (TEM).

For TEM observation, the solid sample of PBLG-4 cast from $CHCl_3$/TFA solution was ultramicrotomed using a diamond knife at room temperature, producing sections 500 Å thick. The polymer was sensitive to the electron beam and the TEM imaging and electron diffraction were performed at 200 kV with a cryogenic sample holder.

Figure 3.18 (a) shows a typical bright-field image of the PBLG-4 film. A banded texture with repeat distance of about 100 nm to 130 nm and disclinations of strength s = +1/2 and -1/2 are observed. The length scale of this banding is, by an order of magnitude, too large to be associated with the smectic layer spacing. There is , however, ample precedent for the TEM observation of banded textures in ultramicrotomed sections of glassy materials with liquid crystalline order when the director field is twisting, as in a cholesteric[54, 55]. Cholesteric compounds when quenched and sectioned with a diamond knife exhibit banding due to thickness variations. When the knife passes approximately parallel to the helical axis, a sinusodial surface topography is produced due to preferential crack propagation following the twist of the director field. The thin microtomed sections are bounded by two sinusoidal fracture surfaces and the phase relationship between these periodic topographies results in thickness variations which are maximized when the two surfaces are 180° out of phase. This sinusoidal fracture surface topography in PBLG-4 was imaged by atomic force microscopy (AFM), on the microtomed block face after the thin sections had been cut. Figure 3.18 (b) shows the AFM topography image of a PBLG-4 microtomed surface in which the banding period is confirmed to be about 100-110 nm and the peak to valley distance (double the amplitude) of the banding is found to be about 30 nm.

To correlate the chain orientation with morphology, coupled electron diffraction and imaging experiments were conducted. Figure 3.19 (b) shows a typical electron diffraction

pattern of PBLG-4 film. The equatorial spots at a spaeing of 12.6 Å eorrepond elosely to the spacing of the 100 refleetion from the hexagonal paeking of heliees previously reported for diffraction experiments on semicrystalline PBLG samples[43, 57]. The horizontal streaks in the electron diffraction pattern also correspond to the diffractions typically observed as the first layer line of an α-helix[57]. This electron diffraction pattern provides a clear indication of the orientation of the PBLG-4 rods which can be mapped to the defocused image of the banded morphology shown in Figure 3.19 (a). This image shows only the material contributing to the diffraction and preserves the rotational orientation between the pattern and image. Electron diffraetion eoupled with imaging establishes that the ehain axes of the PBLG-4 rods lie parallel to the 120 nm banding pattern. These bands neeessitate a twisting director perpendicular to the rod direction, as in cholesterie order. The X-ray diffraetion data simultaneously necessitates layering with 114.5 Å repeat, and a chain axis normal to these smectic layers i.e. smeetic A. These geometrieal requirements can only be satisfied by the smectic A* structure[58,59], which is illustrated in Figure 3.20. The geometrical requirements are inconsistent with other twisted liquid erystal struetures sueh as smectic C*.

The smectic A* strueture was first predieted by Renn and Lubensky between cholesteric and smeetic A phases. Their *twist-grain-boundary (TGB)* model [60,61] proposed that grain boundaries of screw discloeations account for rotation of blocks of smeetic A layers, as drawn in our Figure 3.17. Experimental observation of the smeetie A* strueture was first reported by Goodby et. al.[62] and subsequently by other investigators[63, 64, 65]. To date, this structure has been found in several chiral thermotropic liquid erystals in different sequences such as isotropic-smectic A*-smectic C*[62], cholesteric-smectic A*-smectic A[63], and cholesteric-smectic A*-smectic C*[64]. To our knowledge the present study of PBLG-4 is the first report of a smectic A* strueture in a lyotropic liquid crystal.

Although there is some suggestion of finer scale structure, the detail revealed by TEM images of the present study is not sufficient to allow assessment of whether the

helical rotation of the smectic layers actually occurs in the blocky manner postulated by theory or whether the deformation is more continuous.

Polarized light optical micrographs of PBLG-4 showed fan-like textures (Figure 3.8 (b) which does allow for the the possibility of a twisting director, as in cholesteric or a smectic A*. When the sample was macroscopically aligned in a magnetic field, focal-conic texture was observed (Figure 3.12) and a smectic A like ordering was revealed by X-ray diffraction of the solid film. The magnetic alignment of PBLG-4 must have untwisted the material and produced smectic A ordering. In the absence of the aligning field, the helical chirality of the rods produces a twisted smectic A i.e. the smectic A* ordering. The smectic A* symmetry observed in genetically synthesized, monodisperse PBLG derivative results from the superposition of the cholesteric twist observed in conventional polydisperse PBLG (as a result of chirality of the helical rod) and a drive to form a layered structure brought about by the monodispersity in chain length.

3.4 Conclusions and Future Perspective

A rod-like polymer, a derivative of poly(γ-benzyl α,L-glutamate) was prepared in a set of uniform chain lengths by benzylation of side chains of monodisperse poly(α,L-glutamate) derivatives. These polymers showed unique smectic ordering in solutions and films due to monodispersity in chain length and the layer spacings of the smectic phase were nearly identical to the length of the PBLG helix[68]. An oriented PBLG film was produced by magnetic alignment of PBLG molecules and X-ray diffraction showed smectic A like ordering of the PBLG helix. In the absence of aligning field, helical chirality of the rods produced a twist in the smectic sample and smectic A* ordering was observed in the solid film. These results suggest that bacterial synthesis of the monodisperse PLGA precursors provides a powerful strategy for inducing smectic ordering in solutions and films of PBLG and controlling the layer spacings of smectic ordering on length scales of tens of nanometers.

Construction of ordered architectures at the nanometer scale has been an active scientific area because of potential creation of nanoscale devices. Current approaches, "engineering down" methods, employed largely by computer chip industry, are practically limited to about 1 μm, and the possibility of "engineering up" from molecules to functional devices has become increasingly attractive. The result presented in this chapter clearly shows the importance of controlling the molecular architecture of polymers for achieving well defined self-assembly. Exploitation of such smectic order to produce two-dimensional polymers, novel diffraction gratings, and membranes of controlled thickness and permeability, may be readily imagined. It was explained in the introduction section of this chapter that there have been many attempts to prepare a well-ordered monolayers of PBLGs. The vertically (with respect to the surface) ordered monolayer can be applied to NLO and piezoelectric materials and laterally ordered monolayer (LB film) may be used prepare patterned arrays for potential sensor technology. However, monolayers with well defined supramolecular architecture have not yet been achieved and the practical utilization has been lagging behind. These optical and electrical applications require long range order and uniform chain length. The bacterial methods for polypeptide synthesis, in which artificial genes encoding the polymer are expressed in bacterial vectors, offer the opportunity to make macromolecules with very well defined chain length. The monodisperse PBLG derivatives prepared in this way are expected not only to help understand fundamental physics of rod-like polymers but also to have substantial impact in the utilization of rod-like polymers for future applications.

Table 3.1 Comparison of LC Related Properties of PBLG-Xs

	PBLG3	PBLG4	PBLG5	PBLG6
Number of Repeating Units	58	76	94	112
Rod Length (1.5 Å/repeat)	87 Å	114 Å	141 Å	168 Å
Aspect Ratio (L/D)[a]	6.9	9.1	11.3	13.4
% Substitution of Side Chains	94.4%	98.0%	94.6%	97.4%
Order in Concentrated Solution	Isotropic	Smectic	Smectic	Unknown
Observed Layer Spacing	-	114 Å	140 Å	-

a, D=12.5 Å (From Ref. 68)

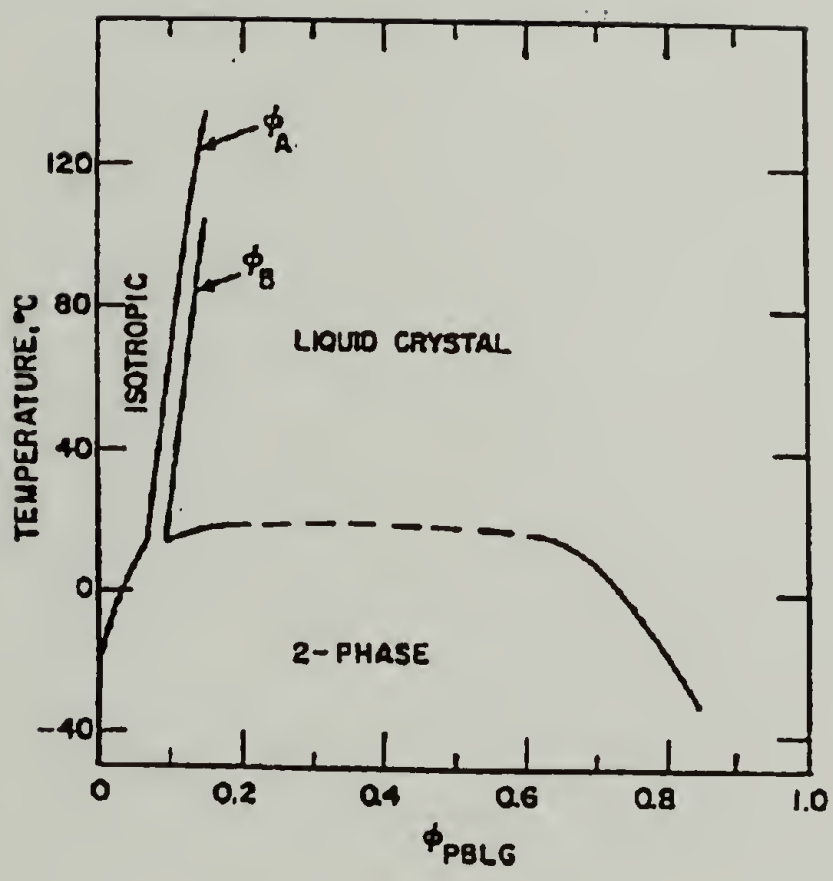

Figure 3.1 Phase diagram for PBLG-DMF system. From Ref. 66.

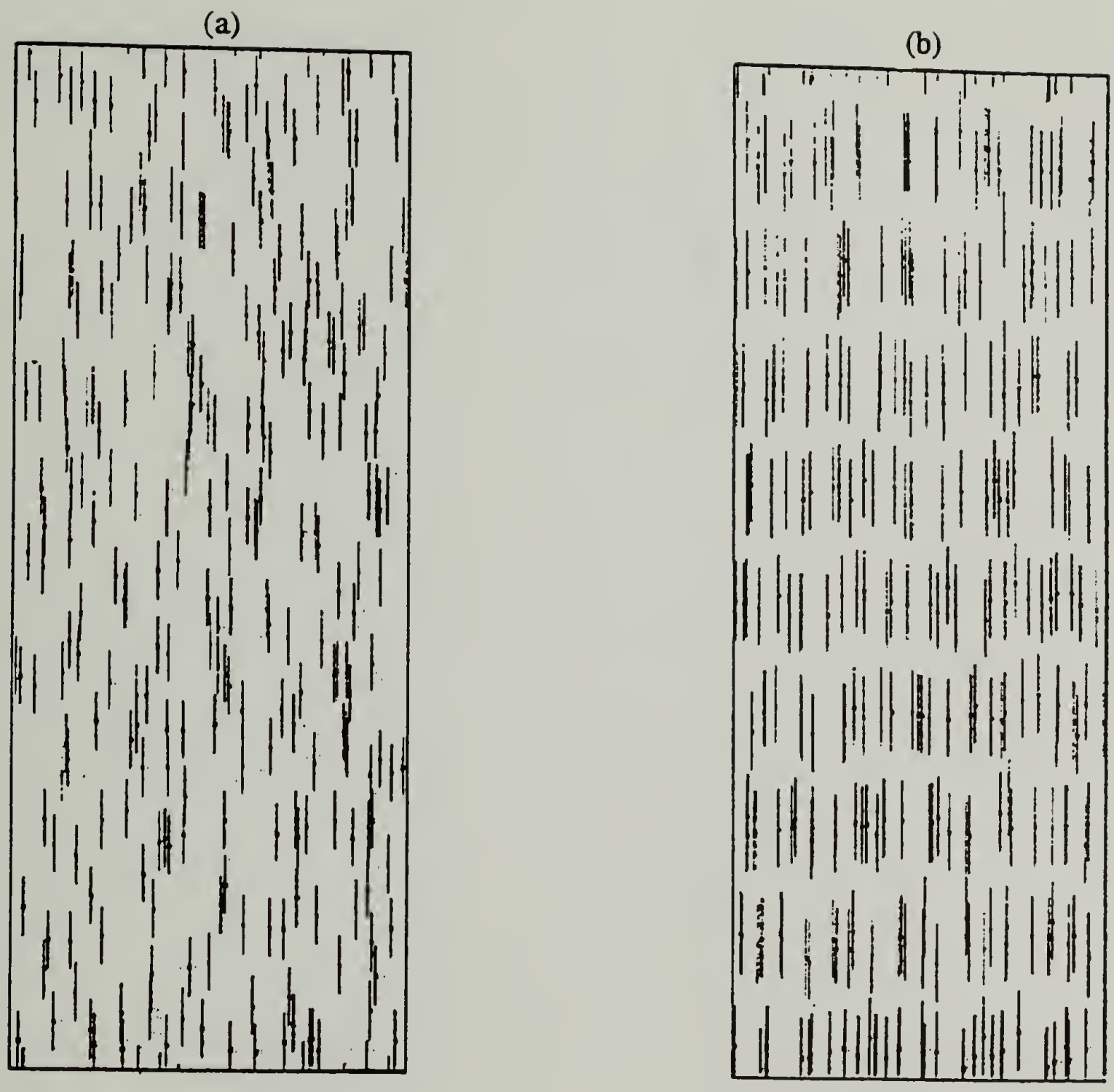

Figure 3.2 Snapshots of typical molecular configuration during simulation of system of 270 spherocylinders with aspect ratio (L/D) = 5. (a) Nematic phase, relative density 0.24. (b) Smectic phase, relative density 0.62. From Ref. 18.

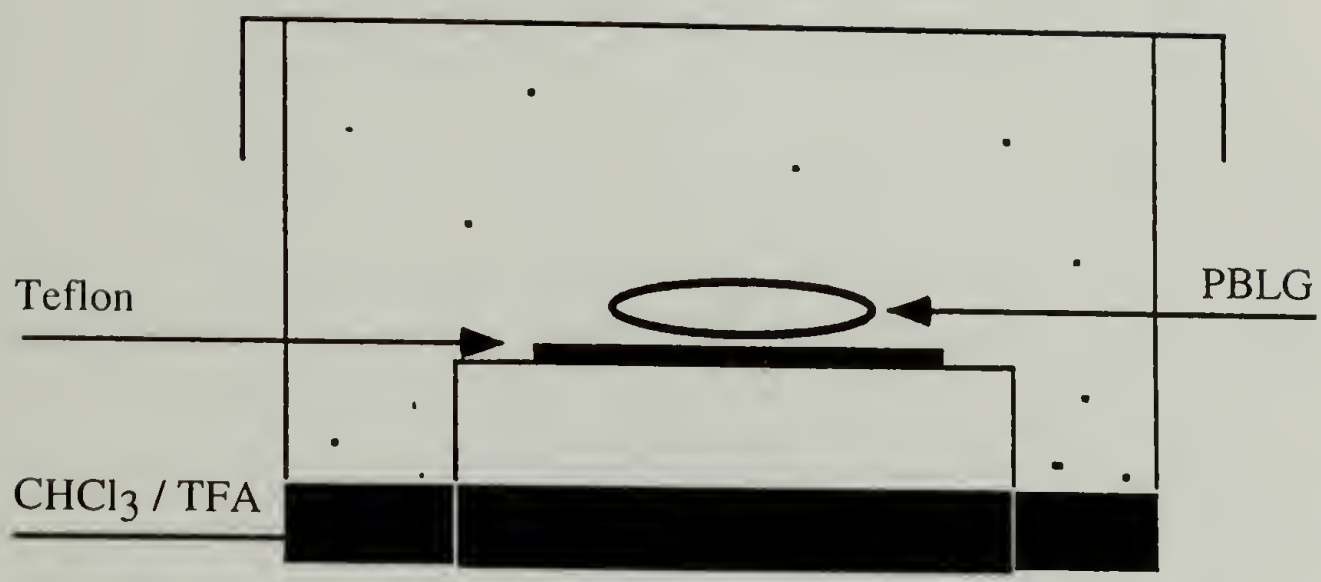

Figure 3.3 Schematic representation of a vessel used to anneal PBLG films.

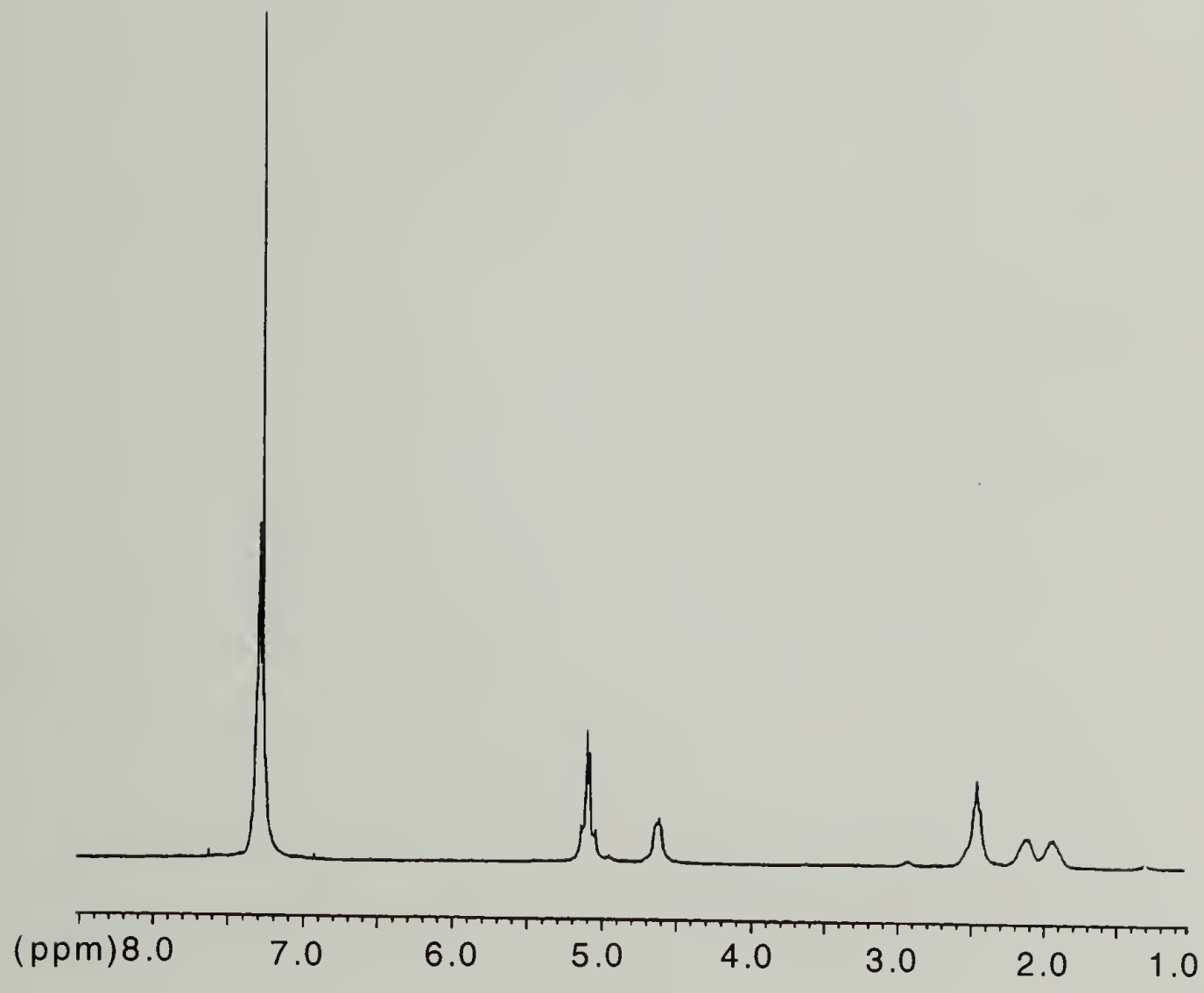

Figure 3.4 ^{1}H NMR spectrum (300 MHz) of PBLG-3 in $CDCl_3$/TFA.

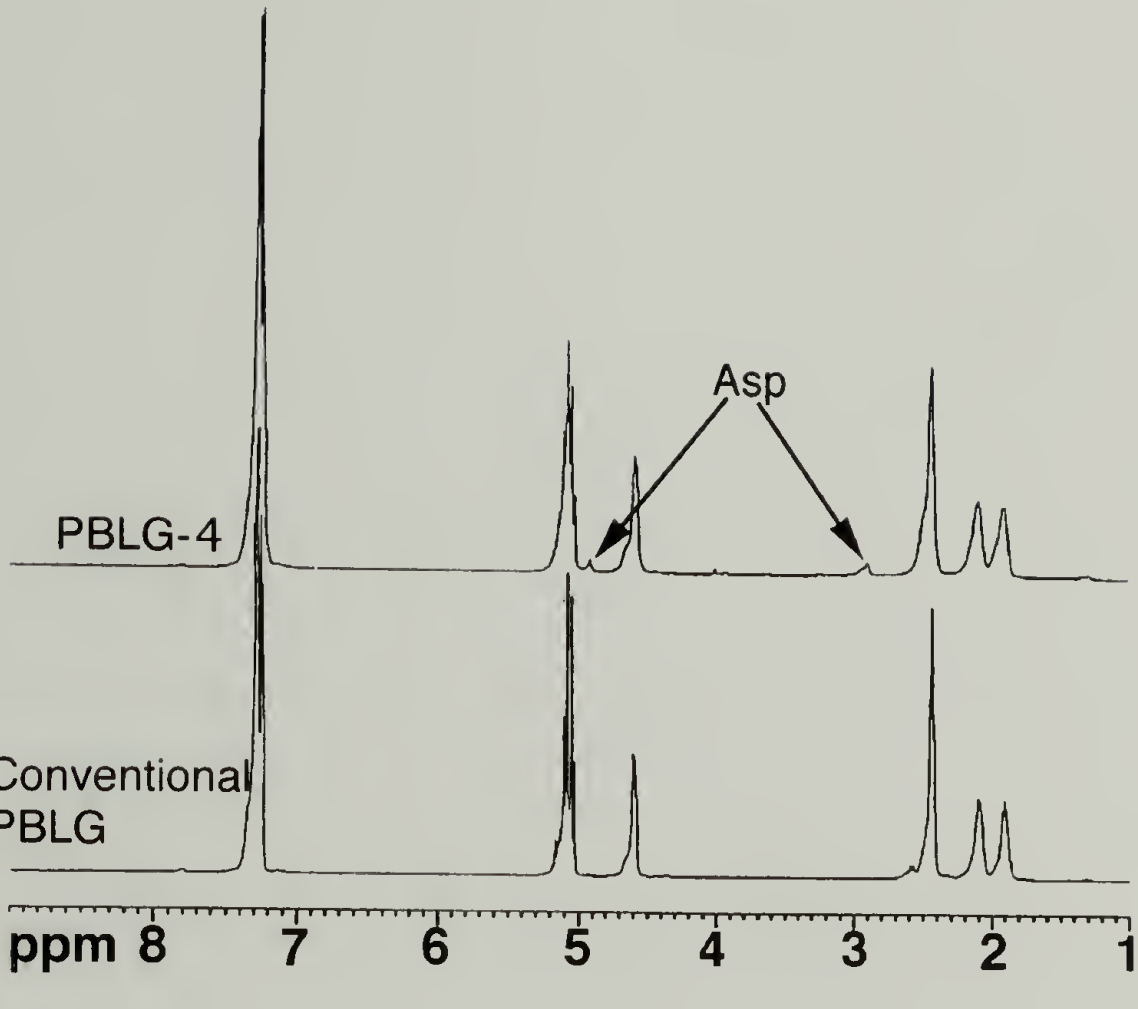

Figure 3.5 ^{1}H NMR spectra (500 MHz) of PBLG-4 (top trace) and conventional PBLG (Mw 20,100, polydispersity index PDI=1.2, Sigma Chemical Co.; bottom trace) in $CDCl_3$/TFA.

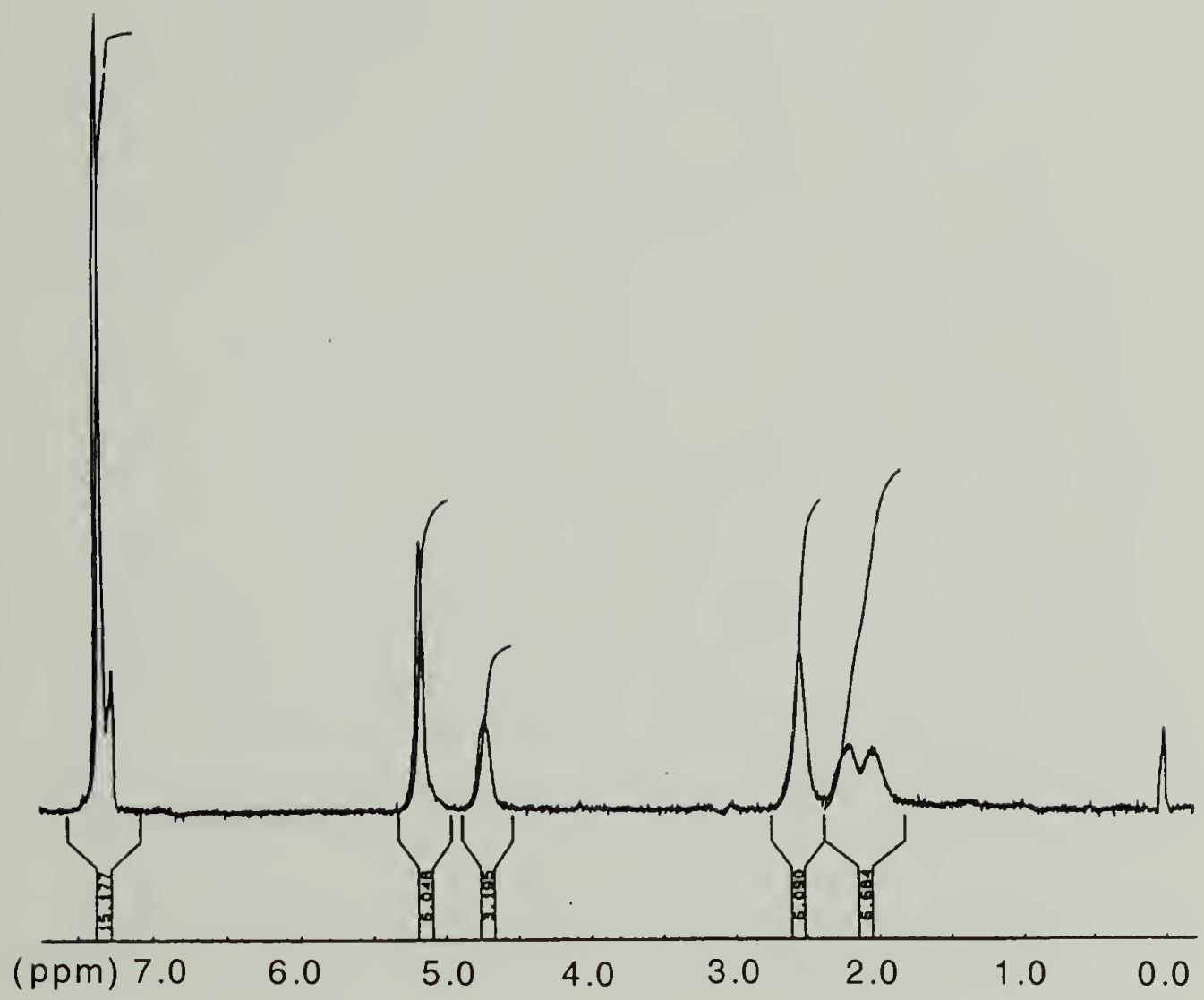

Figure. 3.6 ^{1}H NMR spectrum (200 MHz) of PBLG-5 in $CDCl_3$/TFA.

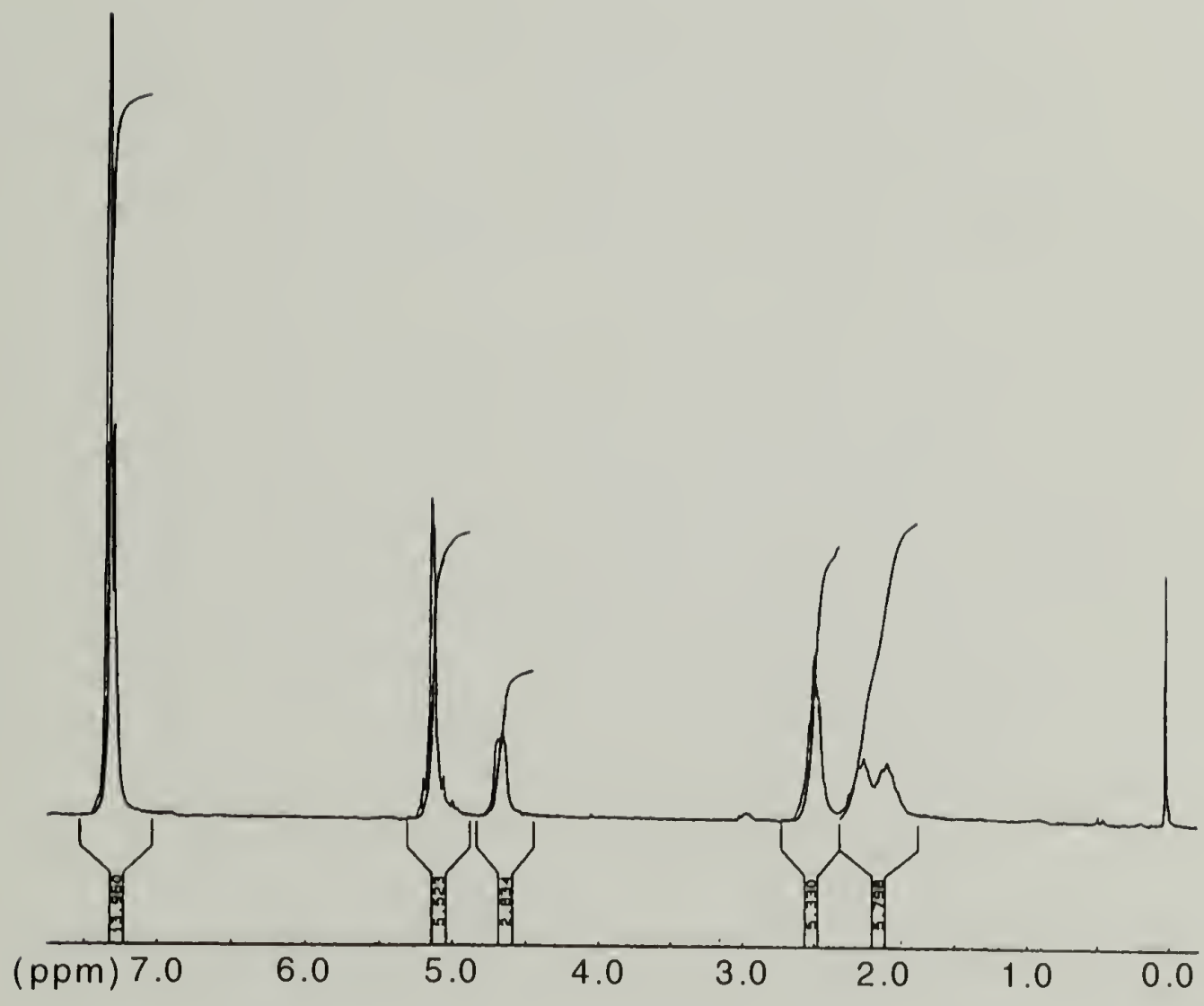

Figure 3.7 ^{1}H NMR spectrum (200 MHz) of PBLG-6 in $CDCl_3$/TFA.

a

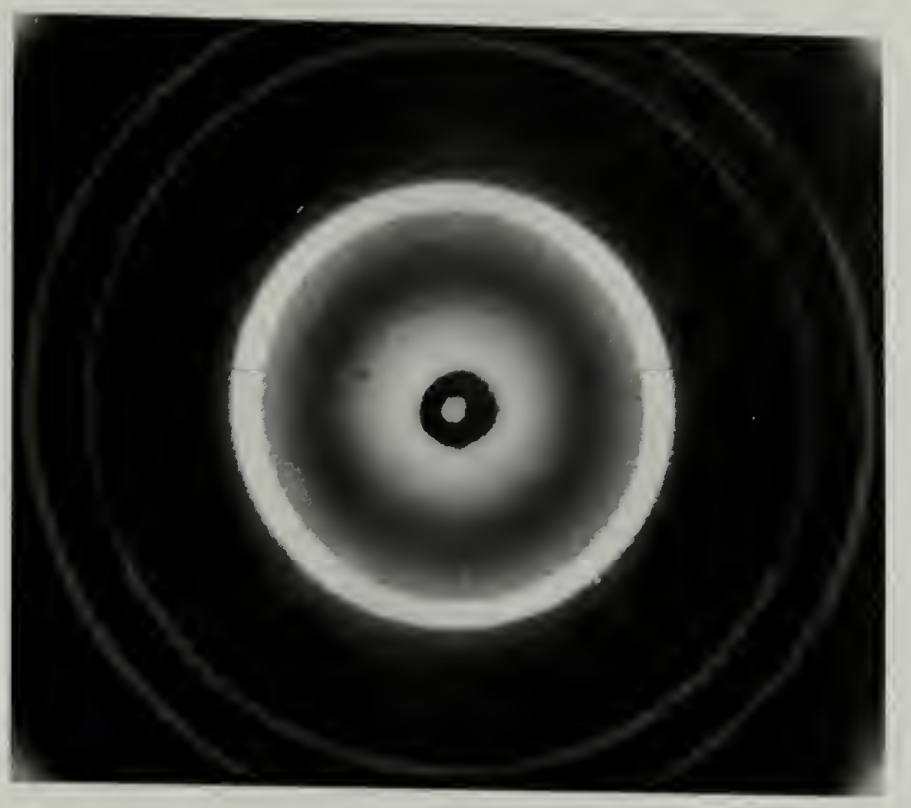

b

Figure 3.8 X-ray diffraction patterns of conventional PBLG (Mw 20,100, PDI=1.2) (a) and PBLG-4 (b) films cast from dioxane.

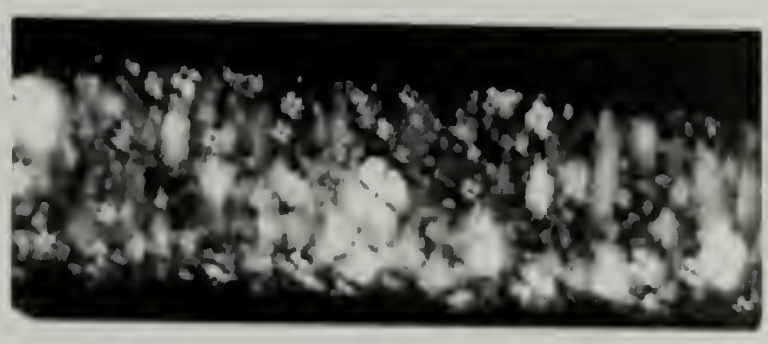

Figure 3.9 Polarized light optical micrograph (magnification x20) of polydisperse PBLG (DP=98, PDI=1.2) in solution (22%) of $CHCl_3$ (97%) / TFA (3%). Micrograph shows the phase separation of birefringent liquid crystalline phase from isotropic phase in a form of spherical droplets.

a

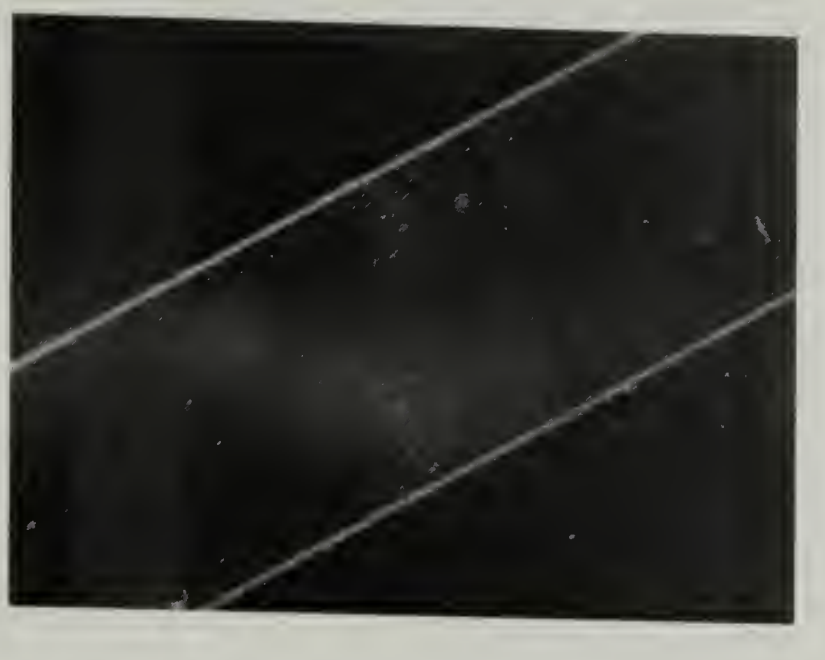

b

Figure 3.10 Polarized light optical micrographs (Mag. x40) of PBLG-4 in $CHCl_3$ (97%) / TFA (3%) solution. a, Isotropic, 25% (weight/volume) solution. b, Partially birefringent (33%) solution.

a

b

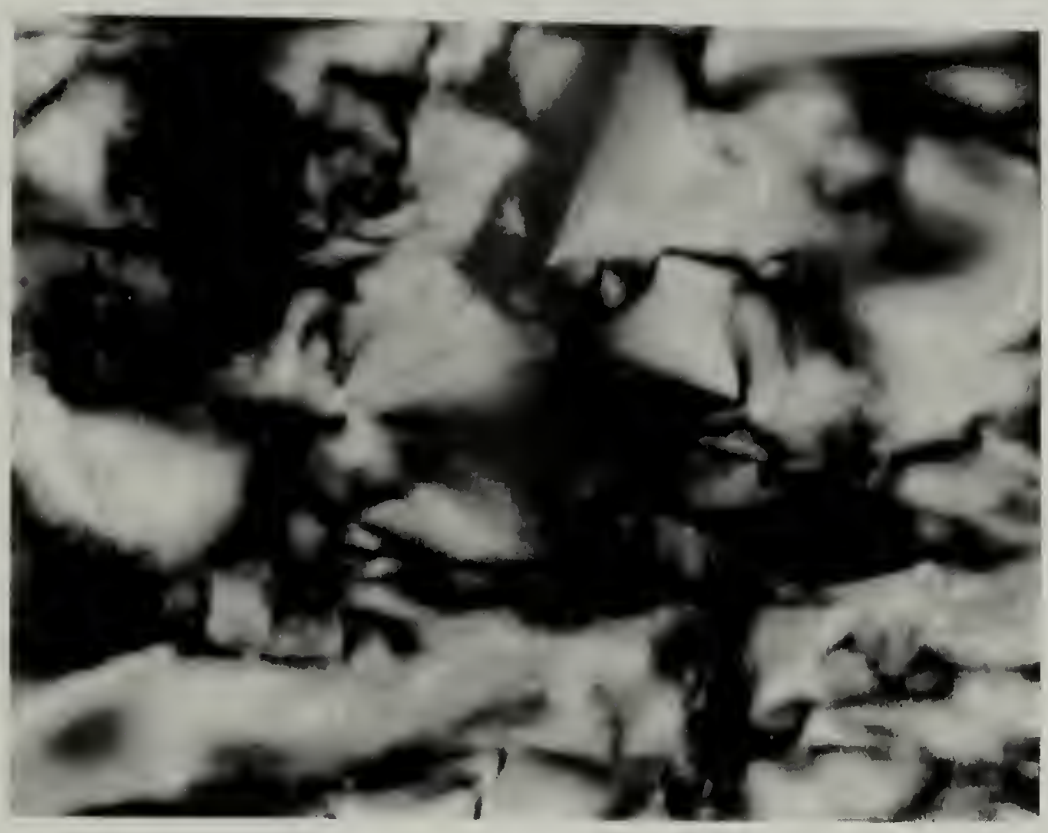

Figure 3.11 Polarized light optical micrographs of PBLG-3 (a) and PBLG-4 (b) in solutions of approximately 40% (w/v) $CHCl_3$(97%) / TFA(3%).

(Mag. x200)

a

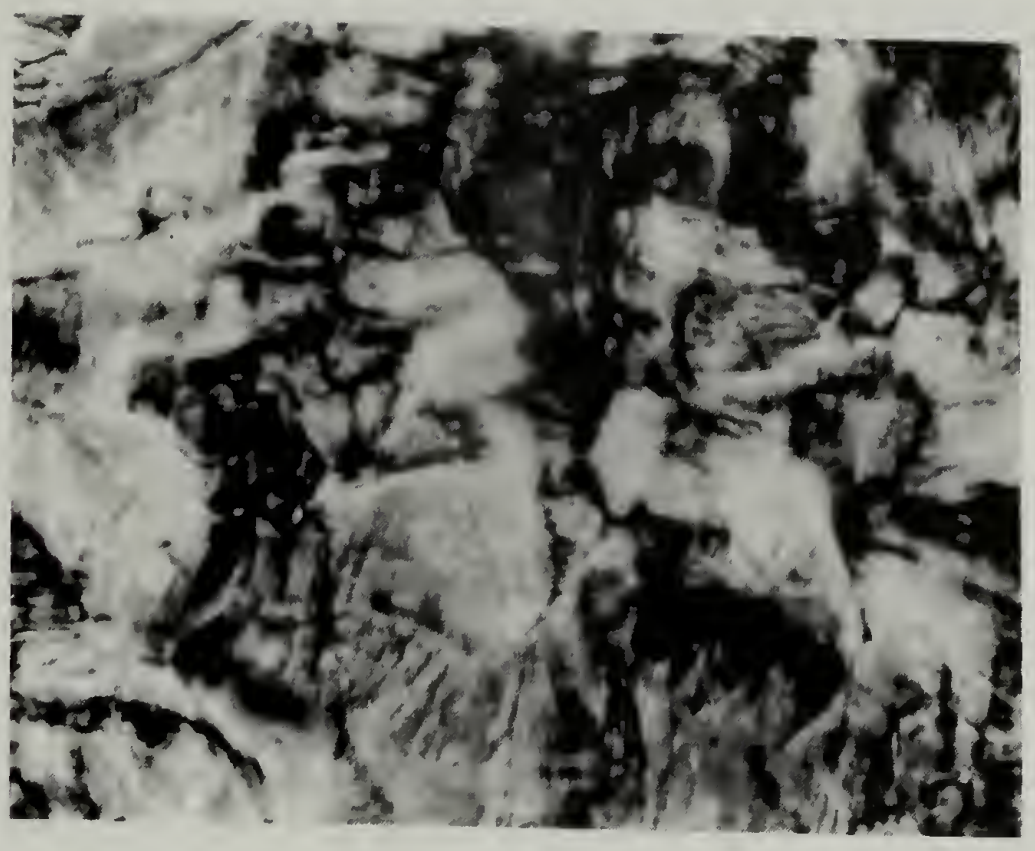

b

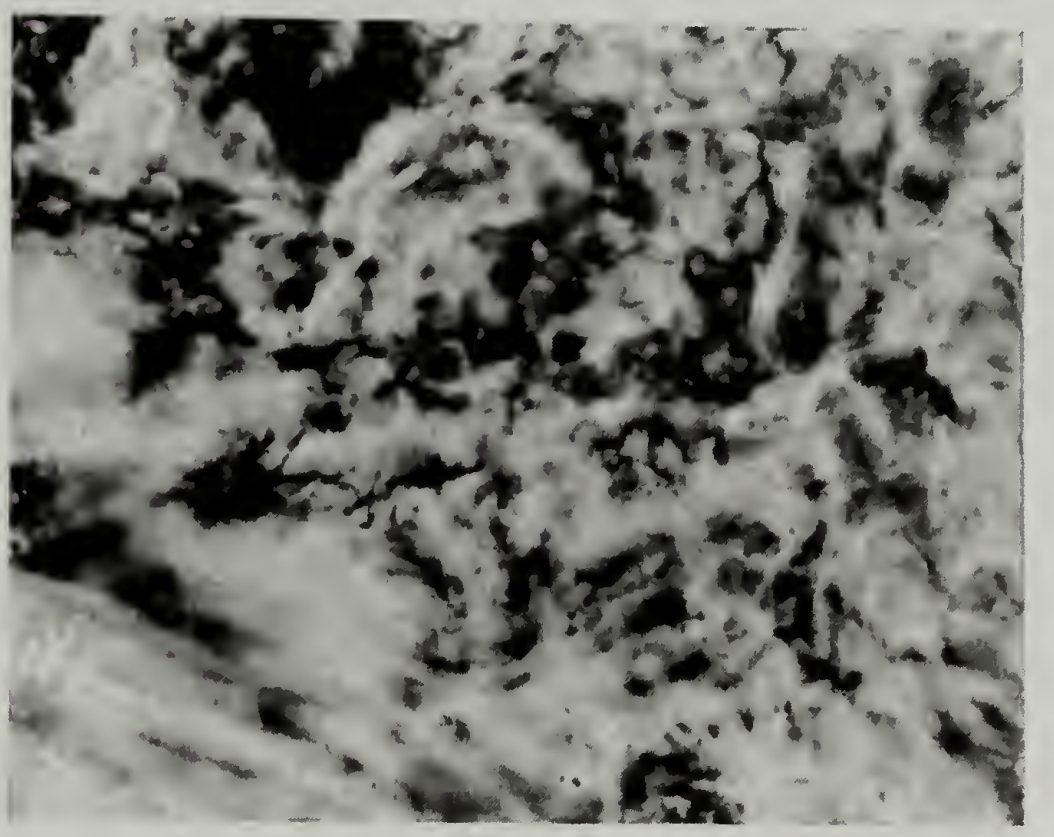

Figure 3.12 Polarized light optical micrographs of PBLG-5 (a) and PBLG-6 (b) in solutions of approximately 40% (w/v) $CHCl_3$ (97%) / TFA (3%). (Mag. x200).

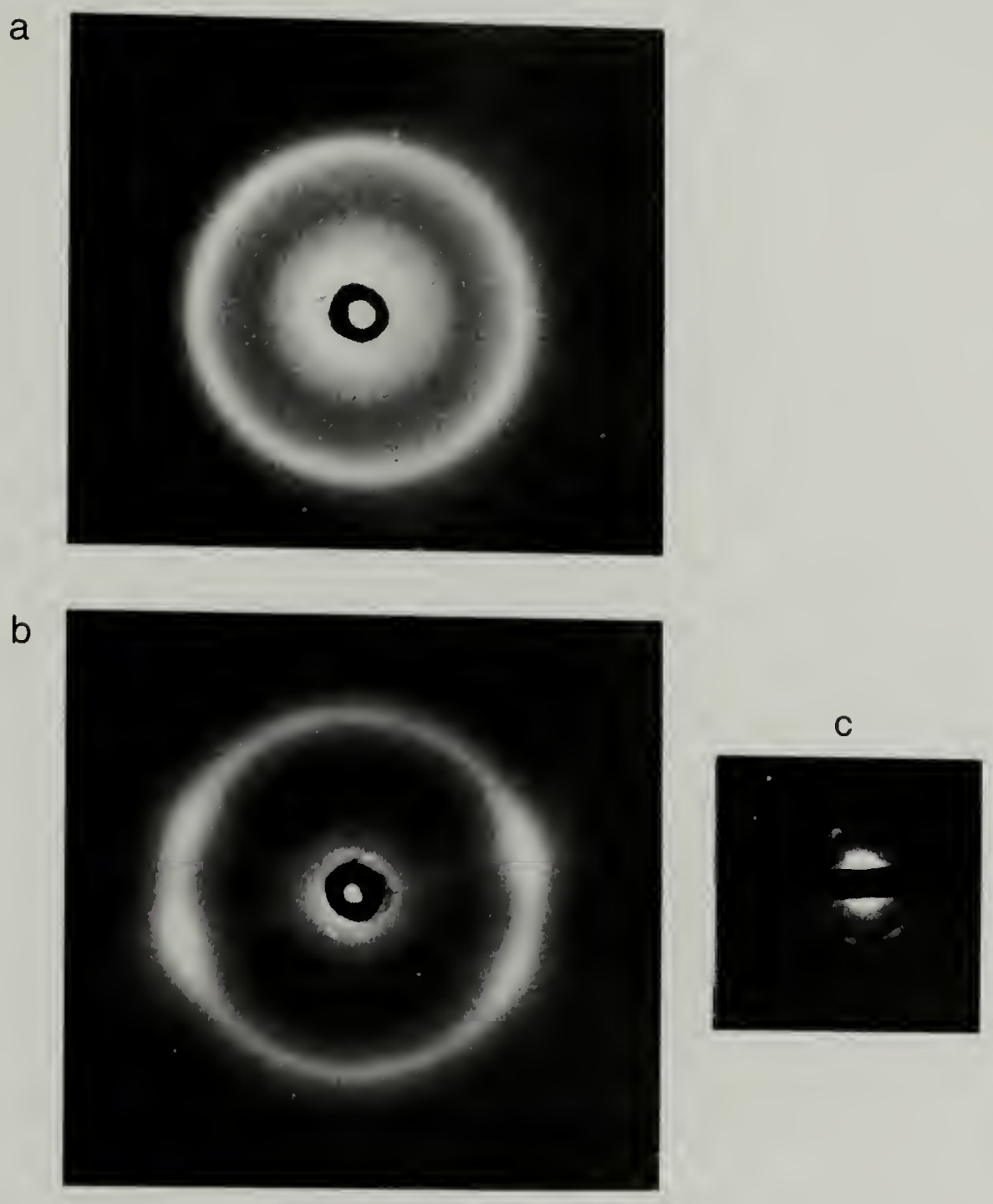

Figure 3.13 X-ray diffraction patterns of PBLG films cast from $CHCl_3$/TFA. a, Polydisperse PBLG (DP=98, PDI=1.2). b and c, PBLG-4. a and b are obtained from Statton wide angle X-ray camera, and c from Rigaku small angle X-ray camera.

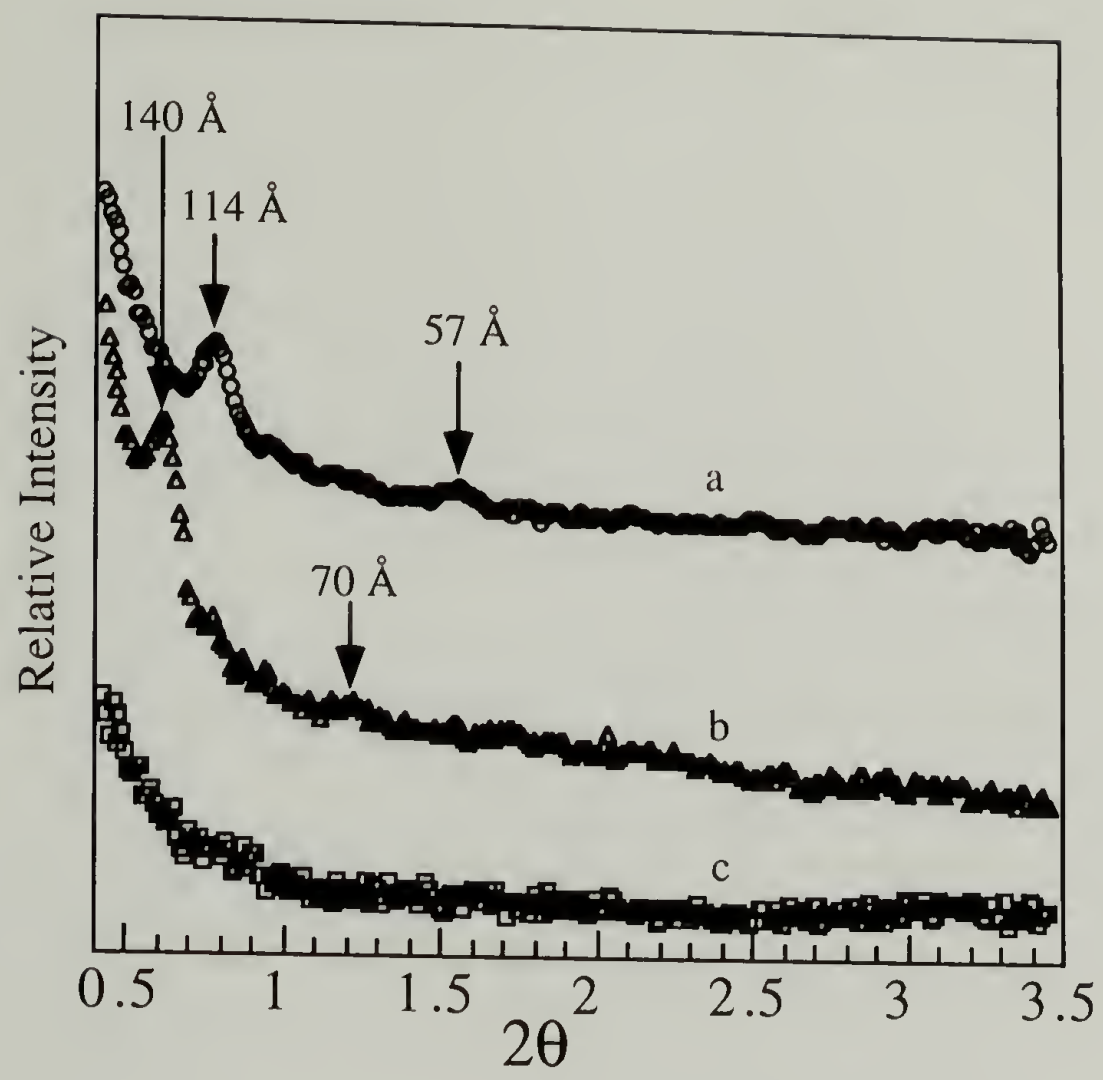

Figure 3.14 Densitometer scans of the small-angle X-ray diffraction patterns of films prepared from solutions of PBLG-4 (curve a), PBLG-5 (curve b) and polydisperse PBLG (DP=98, PDI=1.2; curve c). X-ray diffraction patterns were recorded in an evacuated flat-plate Rigaku small-angle X-ray camera with pin-hole collimation and Ni-filtered Cu Kα radiation with the beam direction normal to the film surface.

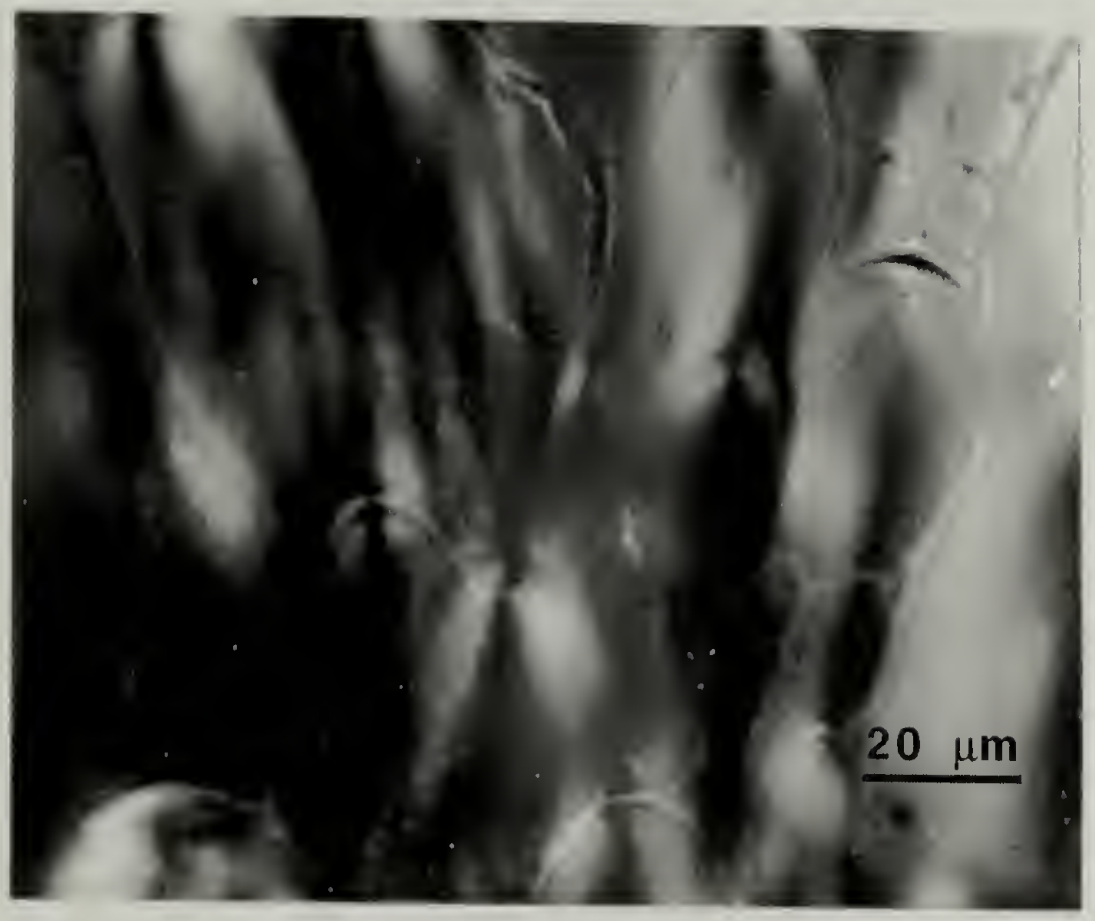

Figure 3.15 Polarized light optical micrograph of swollen film of PBLG-4 in dioxane (approximately 35% polymer) oriented at 50°C in a 1.98 Tesla magnetic field. The micrograph shows typical smectic focal-conic texture.

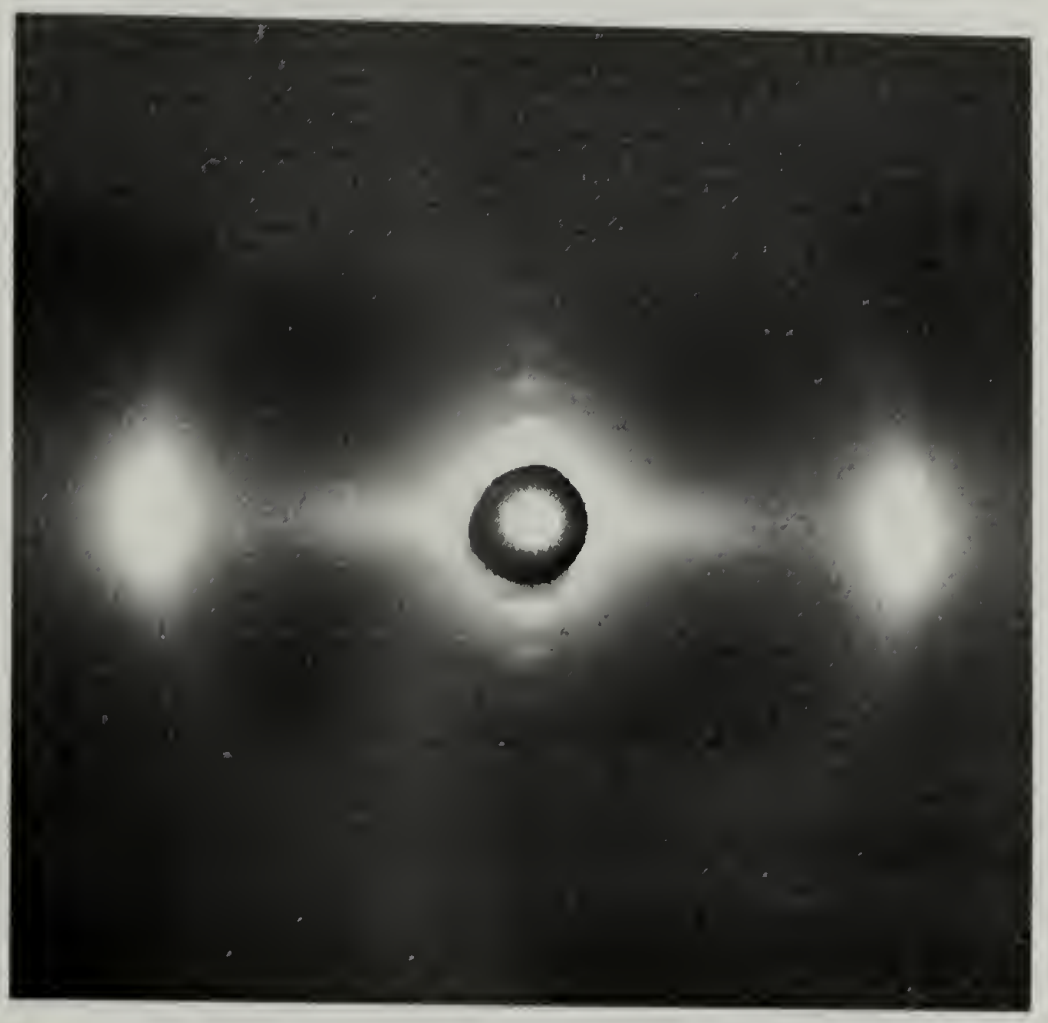

Figure 3.16 X-ray diffraction pattern of a dried, oriented PBLG-4 film prepared from the dioxane-swollen polymer. The meridional reflections are successive orders of a 114.5 Å spacing which is commensurate with the helix length of PBLG-4. The equatorial reflection corresponds to the interchain distance of 12.5 Å.

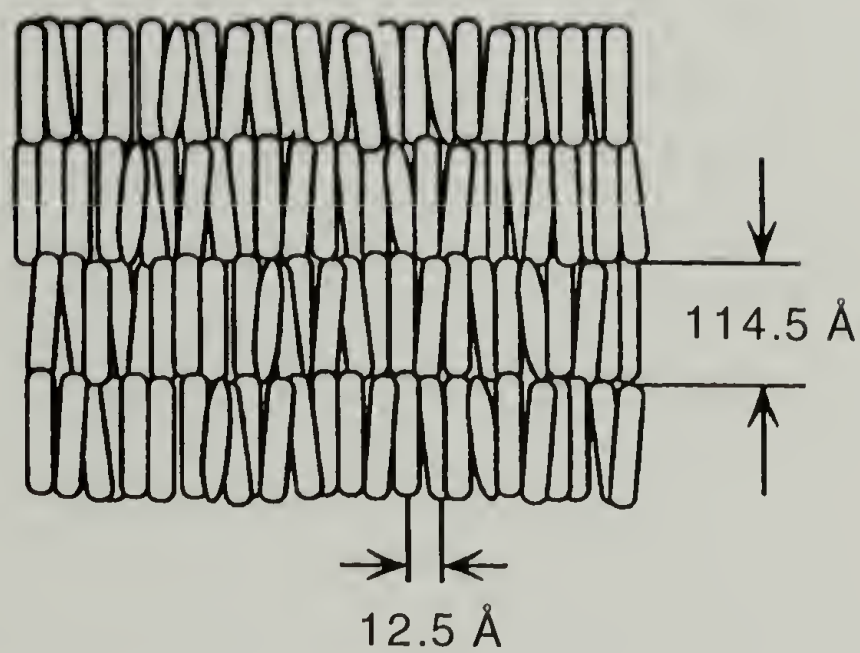

Figure 3.17 Schematic diagram of the smectic-like structure of PBLG-4, showing the origin of 12.5 Å and 114.5 Å reflections.

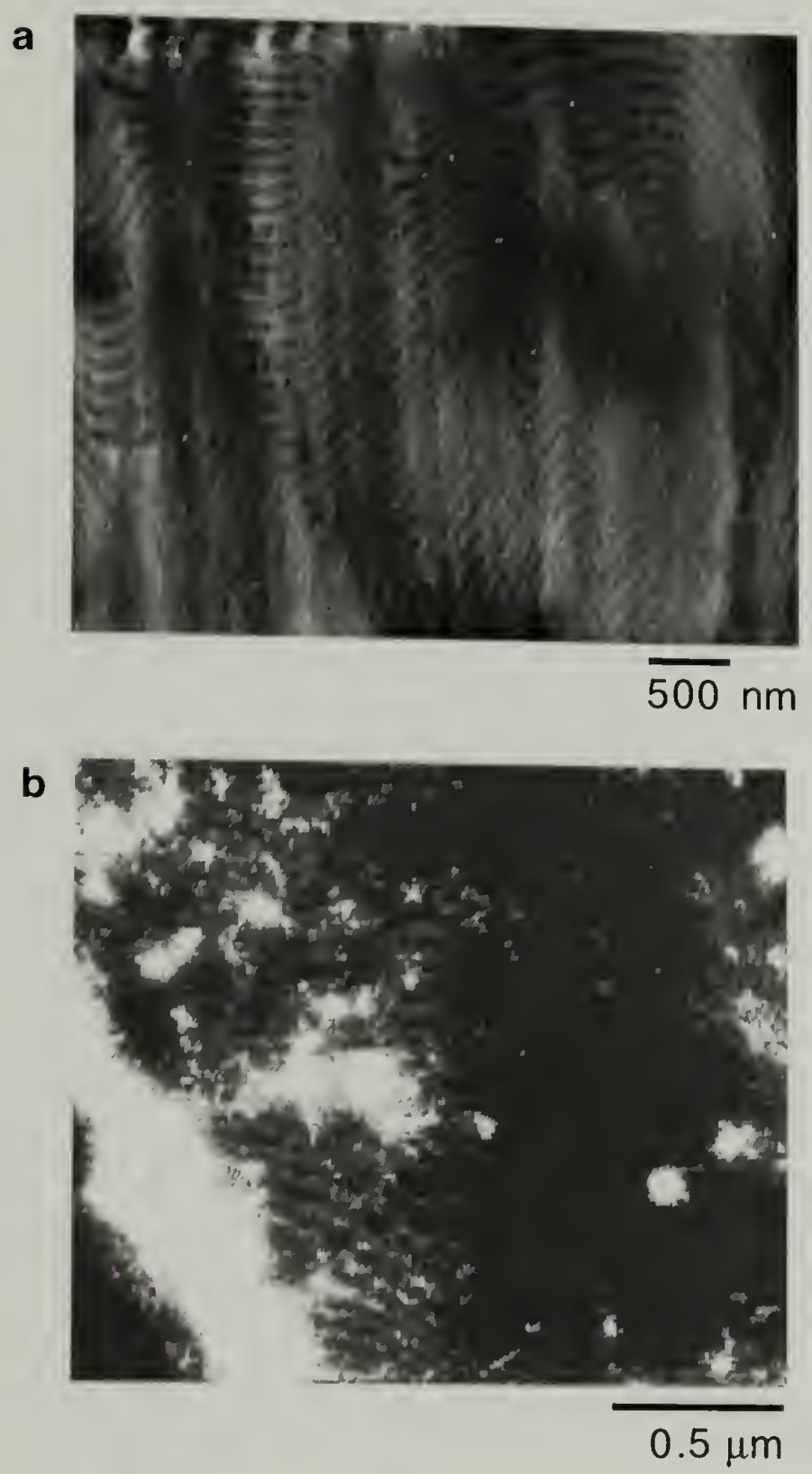

Figure 3.18 Electron micrograph and atomic force micrograph of PBLG-4 film cast from $CHCl_3$/TFA.

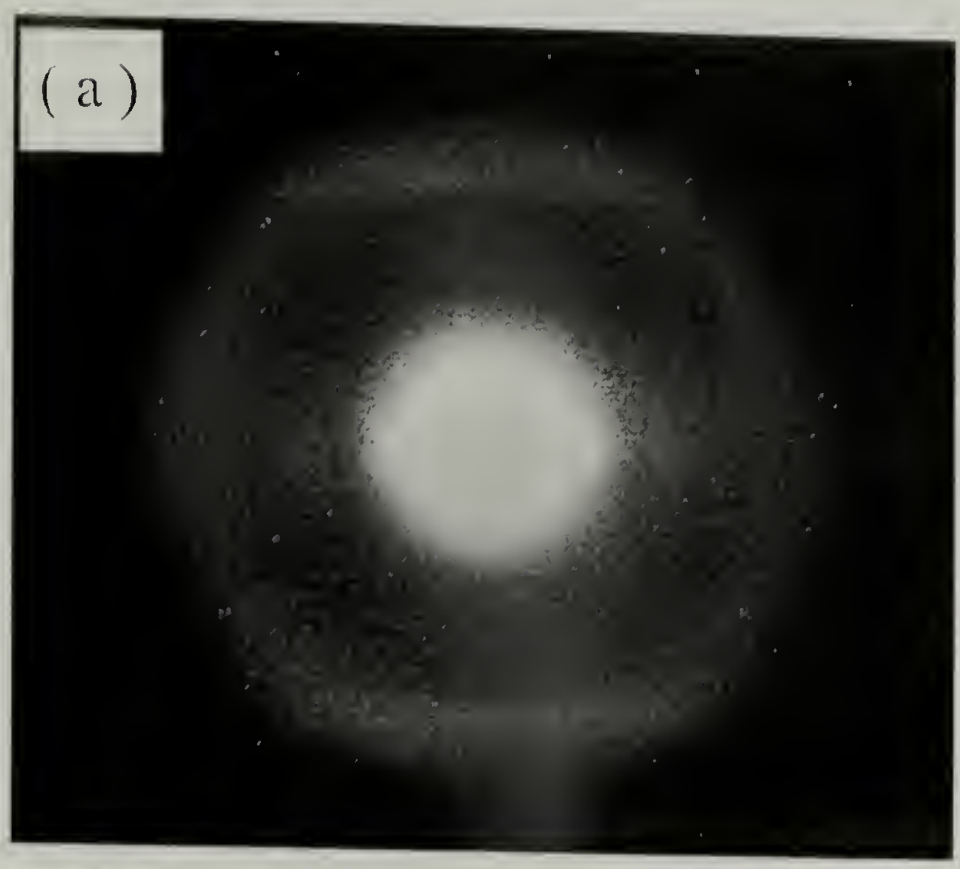

Figure 3.19 Electron diffraction pattern (a) and defocused image (b) of PBLG-4 film.

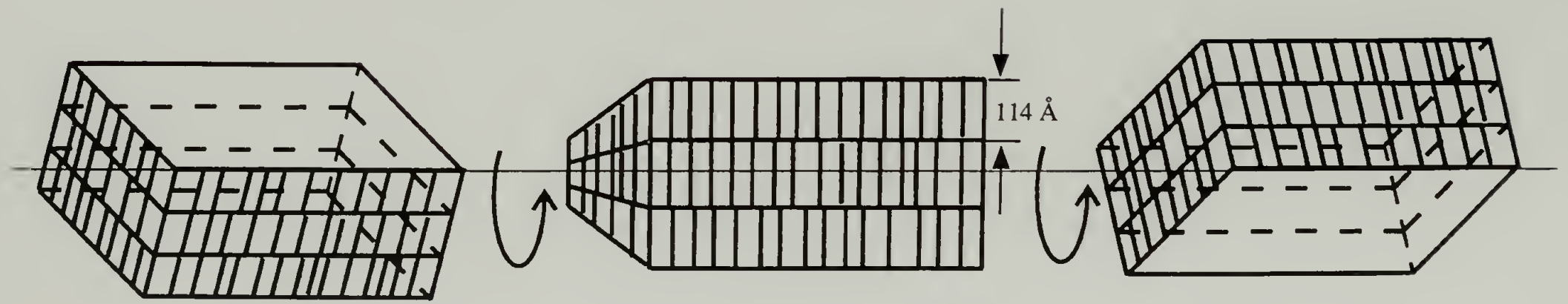

Figure 3.20 Schematic representation of Smectic A*-like supramolecular order in PBLG-4 film.

3.5 References

1. Papkov, S. P. *Advances in Polymer Science* **1984**, 59, 75.

2. Preston, J. In *Liquid Crystalline Order in Polymers* ; Blumstein, A., Ed.; Academic Press: New York, 1978; pp 141.

3. Block, H. *Poly(γ-benzyl-L-glutamate) and Other Glutamic Acid Containing Polymers* ; Gordon and Breach: New York, 1993.

4. Enriquez, E. P.; Gray, K. H.; Guarisco, V. F.; Linton, R. W.; Mar, K. D.; Samulski, E. T. *J. Vac. Sci. Technol. A*, **1992**, 10, 2775.

5. Mathauer, K.; Schmidt, A.; Knoll, W.; Wegner, G. *Macromolecules* **1995**, 28, 1214.

6. Kricheldorf, H. R. *α-Aminoacid-N-Carboxy-Anhydrides and Related Heterocycles*; Springer: New York, 1987.

7. Robinson, C.; Ward, J. C. *Nature* **1957**, 180, 1183.

8. Straley, J. P. *Mol. Cryst. Liq. Cryst.* **1973**, 22, 333.

9. Wee, E. L.; Miller, W. G. *J. Phys. Chem.* **1970**, 75, 1446.

10. Horton, J. C.; Donald, A. M.; Hill, A. *Nature* **1990**, 346, 44.

11. Flory, P. J. *Proc. Roy. Soc. Lond.* **1956**, A234, 73.

12. Peterson, H. T.; Matire, D. E. *J. Chem. Phys.* **1974**, 61, 3547.

13. Wen, X.; Meyer, R. B.; Caspar, D. L. D. *Phys. Rev. Lett.* **1989**, 63, 2760.

14. Albrecht, C.; Lieser, G.; Wegner, G. *Prog. Colloid Polym. Sci.* **1993**, 92, 111.

15. Chen, J. T.; Thomas, E. L.; Ober, C. K.; Mao, G.-p. *Science* **1996**, 273, 343.

16. Powers, J. C. Jr.; Peticolas, W. L. *Advances in Chemistry* #63; American Chemical Society: Washington D.C., 1967.

17. McMillan, W. L. *Phys. Rev.* **1971**, A4, 1238.

18. Stroobants, A.; Lekkerkerker, H. N. W. *Phys. Rev.* **1987**, A36, 2929.

19. Powers, J. C. Jr.; Peticolas, W. L. *Biopolymers* **1970**, 9, 195.

20. Doty, P.; Bradbury, J. H.; Holtzer, A. M. *J. Am. Chem. Soc.* **1956**, 78, 947.

21. Duke, R. W.; Du Pre, D. B.; Hines, W. A.; Samulski, E. T. *J. Am. Chem. Soc.* **1976**, 98, 3094.

22. Markley, J. L.; Meadows, D. H.; Jardetzky, O. *J. Mol. Biol.* **1967**, 27, 25.

23. Kresheck, G. C.; Kierleber, D.; Albers, R. J. *J. Am. Chem. Soc.* **1972**, 94, 8889.

24. Stephens, R. M.; Bradbury, E. M. *Polymer* **1976**, 17, 563.

25. Cabani, S.; Paci, A.; Rizzo, V. *Biopolymer* **1976**, 15, 113.

26. Karasz, F. E.; Gajinos, G. E. *Biopolymers* **1974**, 13, 725.

27. Rajan, V. T.; Woo, C.-W. *Phys. Rev. A* **1980**, 21, 990.

28. Subramanian, R. J.; Wittebort, R. J.; DuPre, D. B. *Mol. Cryst. Liq. Cryst* **1982**, 97, 325.

29. Kiss, G.; Porter, R. S.; *Mol. Cryst. Liq. Cryst.* **1980**, 60, 267.

30. Wada, A. *J. Chem. Phys.* **1959**, 30, 328.

31. Nakamura, H.; Husimi, G.; Jones, P.; Wada, A. *J. Chem. Soc. Faraday II* **1977**, 73, 1178.

32. Samulski, E. T.; Tobolsky, A. V. in *Liquid Crystals & Plastic Crystals*; Gray, G. W.; Winsor, P. A., Eds.; John Wiley & Sons Inc.: New York, 1974; pp 175.

33. Straley, J. P. *Mol. Cryst. Liq. Cryst.* **1973**, 22, 333.

34. Gray, G. W.; Goodby, J. W. G. *Smectic Liquid Crystals*; Heyden & Son: Philadelphia, 1984.

35. Vorlander, E. *Trans. Faraday Soc.* **1933**, 29, 907.

36. Mckinnon, A. J.; Tobolsky, A. V. *J. Phys. Chem.* **1966**, 70, 1453.

37. Samulski, E. T.; Tobolsky, A. V. *Nature* **1967**, 216, 997.

38. Samulski, E. T.; Tobolsky, A. V. *Mol. Cryst. Liq. Cryst.* **1969**, 7, 433.

39. Samulski, E. T.; Tobolsky, A. V. *Biopolymers* **1971**, 10, 1013.

40. Samulski, E. T.; Tobolsky, A. V. in *Liquid Crystalline and Ordered Fluids*; Johnson, J. F.; Porter, R. S., Eds.; Plenum Press: New York, 1970; pp 111.

41. Price, C.; Harris, P. A.; Holton, T. J.; Stubbersfield, R. B. *Polymer* **1975**, 16, 69.

42. Rybnikar, F.; Geil, P. H. *Makromol. Chem.* **1972**, 158, 39.

43. Parsons, D. F.; Martius, U. *J. Mol. Biol.* **1964**, 10, 530.

44. Malcolm, B. R. *Proc. Roy. Soc. Ser. A* **1968**, 21, 449.

45. Loeb, G. I. *J. Colloid. Interface. Sci.* **1968**, 21, 236.

46. Jones, R.; Tredgold, R. H. *J. Phys. D.* **1988**, 21, 449.

47. Machidas, S.; Urano, T. I.; Sano, K.; Kawata, Y.; Sunohara, K.; Sasaki, H.; Yoshiki, M.; Mori, Y. *Langmuir* **1995**, 11, 4838.

48. Urano, T. K.; Machida, S.; Sano, K. *Chem. Phys. Lett.* **1995**, 242, 471.

49. Chang, Y.-C.; Frank, C. W. *Langmuir* **1996**, 12, 5824.

50. Jaworek, T.; Neher, D.; Wegner, G.; Wieringa, R. H.; Schouten, A. J. *Science* **1998**, 279, 57.

51. Wulfman, D. S.; Yousefian, S.; White, J. M. *Synth. Commun.* **1988**, 18, 2349.

52. Robinson, C.; Ward, J. C.; Beever, R. B. *Discuss. Faraday Soc.* **1958**, 25, 29.

53. Fasman, G. D. *Poly(α-amino acid)*; Marcel and Dekker: New York, 1967.

54. Berreman, D. W.; Meiboom, S.; Zasadzinski, J. A.; Sammon, M. J. *Phys. Rev. Lett.* **1986**, 57, 1737.

55. Willcox, P. J.; Gido, S. P.; Muller, W.; Kaplan, D. L. *Macromolecules* **1996**, 29, 5106.

56. Bunning, T. J. *Liq. Cryst.* **1994**, 16, 769.

57. Bamford, C. H.; Elliott, A.; Hanby, W. E. *Synthetic Polypeptides*; Academic Press: New York, 1956.

58. Kelman, M. in *Liquid Crystals, Magnetic Systems and Various Ordered Media*; John Wiley & Sons Ltd.: New York, 1983.

59. Goodby, J. W.; Waugh, M. A.; Stein, S. M.; Chin, E.; Pindak, R.; Patel, J. S. *J. Am. Chem. Soc.* **1989**, 111, 8119.

60. Renn, S. R.; Lubensky, T. C. *Phys. Rev. A* **1988**, 38, 2132.

61. Lubensky, T. C.; *Renn, S. R. Phys. Rev. A* **1990**, 41, 4392.

62. Goodby, J. W.; Waugh, M. A.; Stein, S. M.; Chin, E.; Pindak, R.; Patel, J. S. *Nature* **1989**, 337, 449.

63. Lavrentovich, O. D.; Nastishin, Y. A.; Kulishov, V. I.; Narkevich, Y. S.; Tolochko, A. S.; Shiyanovski, S. V. *Europhys. Lett.* **1990**, 13, 313.

64. Nguyen, H. T.; Bouchta, A.; Navailles, L.; Barois, P.; Isaert, N.; Twieg, R. J.; Maaroufi, A.; Destrade, C. *J. Phys. II* **1992**, 2, 1889.

65. Anakkar, A.; Daoudi, A.; Buisine, J.-M.; Isaert, N.; Bougrioua, F.; Nguyen, H. T. *Liq. Cryst.* **1996**, 20, 411.

66. Miller, W. *Liquid Crystals and Ordered Fluids*; Plenum: New York, 1993.

67. Dupre, D. B.; Samulski, E. T. in *Liquid Crystals The Fourth State of Matter*; Saeva, F. D., Ed.; Marcel Dekker, Inc.: New York, 1979.

68. Yu, S. M.; Conticello, V. P.; Zhang, G.; Kayser, C.; Fournier, M. J.; Mason, T. L.; Tirrell, D. A. *Nature* **1997**, 389, 167.

CHAPTER 4

SYNTHESIS AND CHARACTERIZATION OF MONODISPERSE DERIVATIVES OF POLY(γ-4-(HEXADECYLOXY)BENZYL α,L-GLUTAMATE)

4.1 Introduction

Long alkyl chain derivatives of poly(α,L-glutamate)- for example, poly(γ-alkyl α,L-glutamate) (PALG) and poly(γ-4-alkoxybenzyl α,L-glutamate)- are typical models of "hairy (fuzzy) rod" polymers[1]. These compounds show both lyotropic and thermotropic liquid crystalline behavior since the long alkyl chains can act as a solvent at a temperature above their melting transitions[1,2]. These polymers are soluble in hydrocarbons and can be useful models for membrane proteins[3]. They are also of interest because of potential applications in photonics, electronics and chemical sensors[4,5]. The melting temperatures of these polymers depend on the length and composition of the side chains and their liquid crystalline properties have been shown to be similar to those of conventional PBLG. Most rod ordering theories are applicable to lyotropic systems and thermotropic systems have received less attention from the theoretical physics community. However, thermotropic systems provide advantages over lyotropic systems in terms of both characterization and application. First, the different liquid crystalline phases and their phase transition behavior are easy to characterize when the liquid crystal phase is induced by heat. Often times, lyotropic systems are difficult to study because of difficulties in preparing solutions of exact concentration especially when the amount of sample is limited. In thermotropic LCs, phase transitions can be investigated relatively easily by differential scanning calorimetry (DSC) and polarized light optical microscopy (POM) without concern for solvent evaporation. Secondly, self-assembly of hairy rod polymers at the air-water interface is expected to produce 2-dimensional liquid crystalline phases which can be transferred to solid substrates for engineering controlled surface arrays for potential sensor application[8].

Watanabe and coworkers have reported the preparation and characterization of a series of poly(γ-alkyl α,L-glutamate)s carrying different side chain alkyl groups[6]. In these polymers, the side chains were long enough to form crystalline phases composed of paraffin-like crystallites, and crystallization forced the α-helices to pack into a characteristic layer structure. The first melting temperatures of the polymers were 15°C, 41°C, 54°C and 62°C for the dodecyl, tetradecyl, hexadecyl and octadecyl side chains respectively. At the first melting transition, the side chain crystallites disappeared and the layer-like packing of α-helices was transformed into hexagonal packing. Transformation to the liquid crystalline phase took place as a first-order transition at a temperature typically about 20°C higher than that of the first melting transition. The typical LC phase was cholesteric and the cholesteric pitch was found to be a few microns at around 100°C for the dodecyl derivatives. When fractionated poly(γ-octadecyl α,L-glutamate) (PDI not reported) was studied, an interesting LC phase was observed at temperatures below the cholesteric LC phase which showed an optical texture, acquired from polarized light optical microscopy, resembling that of smectic A phases[7]. However, X-ray diffraction yielded no small-angle reflections and the exact nature of this intermediate LC phase is still unknown.

Wegner's group[8] has shown considerable interest in using poly(γ-alkyl α,L-glutamate)s as LB multilayer films. In the case of poly-[(γ-methyl α,L-glutamate)-co-(γ-n-octadecyl α,L-glutamate)] with 70% methyl and 30% octadecyl side chains, the flexible side chains provided a liquid-like matrix for the rods and improved the transferability of the polymeric LB films. Interestingly, the multilayers prepared by sequential dipping of the silicon wafer substrates (Y-type) showed bilayer structures. Even after annealing the multilayer films at temperature above the side chain melting temperature, there was no transition of the bilayer structure to the hexagonal structure.

Ponomarenko and coworkers[9,10] have prepared and characterized the solution and solid state properties of stoichiometric complexes of poly(α, L- glutamate) and alkyltrimethylammonium cations with alkyl chain lengths of twelve to eighteen carbon

atoms. In the polypeptide chains complexed with the short alkyl chains, consisting of twelve and sixteen carbon atoms, the surfactant alkyl side chains were disordered in the solid state, while the alkyl chains of complexes with longer surfactant chains (eighteen carbon atoms) crystallized on a hexagonal lattice. The octadecyltrimethylammonium complex underwent a side chain melting transition at 48°C; however unlike the PALG with crystalline side chains, the complex did not flow upon heating before decomposition and no ordered melt was observed.

Another type of hairy rod polypeptide was prepared by Iizuka and coworkers[11,12]. They have synthesized a series of poly(γ-4-alkyloxybenzyl α,L-glutamate)s by ring-opening polymerization of the corresponding N-carboxy α-amino acid anhydrides (NCAs) and characterized their liquid crystalline properties. The LC properties of these polymers were similar to those of the poly(γ-alkyl α,L-glutamate)s. Concentrated solutions of these polymers formed cholesteric mesophases. When heated, these polymers underwent "crystal to liquid crystal" transitions as a result of alkyl side chain melting at -6°C, 42°C, and 69°C for the dodecyl (C12), hexadecyl (C16) and dococyl (C22) derivatives respectively. Polymers of degree of polymerization (DP) less than 50 seem to transform directly from the crystalline state to a cholesteric mesophase at the first transition and those with a DP of 91 and higher showed a second transition above 100 °C. Circular dichroism and X-ray diffraction were performed on these samples, however the exact nature of the different liquid crystalline states and the origin of the thermal transitions are still unknown. Although the authors claim that the first melting transforms the samples from the solid to the liquid crystalline state, no direct evidence was reported such as disappearance of wide angle X-ray diffraction or a viscosity measurement that shows the liquid-like nature of the polymers after the first melting. It is speculated that such complications in the interpretation of thermal properties of these polymers are in part due to the polydisperse nature of the samples, which were prepared by conventional NCA ring-opening polymerization[13].

The solution properties of poly(γ-n-dodecyl α,L-glutamate) were studied by circular dichroism spectroscopy[3]. The stability of the helix in hexane solution with variation in the trifluoroacetic acid (TFA) composition was investigated and was found to be much less than that of PBLG. The helix to random coil transition of poly(γ-n-dodecyl α,L-glutamate) was almost complete when the TFA content was 5%, in contrast to 25% for PBLG. The reduced stability of the helical form of alkyl-derivatized PLGA was also observed in ionic complexes of PLGA and oppositely charged long alkyl chain surfactants[14, 15]. The helix to random coil transition for the stoichiometric complex of poly(L-lysine) cation and dodecyl sulfate anions occurred at a TFA content of 4-6 vol %. This polypeptide chain can adopt either α-helical or β-sheet conformations in the solid state, depending on the content of TFA in the solutions used for film casting. In general the helix stability lies in the order benzyl ⟩⟩ ethyl ⟩ methyl with PBLG significantly more stable. This has been ascribed to the shielding effect of the bulkier benzyl group which hinders the penetration of helix destabilizing molecules[16, 17].

One of the long-term goals of this work is to study smectic ordering of thermotropic polypeptides with uniform molecular rod length. In our previous work with poly(γ-benzyl α,L-glutamate), smectic ordering was observed only when TFA was added to the PBLG solution. Although the effect of TFA is unclear at this point, it is speculated that the addition of TFA could be a prerequisite for creating the lyotropic smectic ordering of long alkyl chain derivatives of PLGAs, a situation that may disrupt the rod-like structure of the more unstable poly(γ-alkyl α,L-glutamate). The stability of the poly(γ-(4-alkoxy)benzyl α,L-glutamate) helix in organic solvents upon titration with TFA has not been reported. However, we expected that the benzyl group of this polymer will stabilize the helix as in the case of PBLG and focused our attention on the synthesis and characterization of poly(γ-(4-hexadecyloxy)benzyl α,L-glutamate).

The objectives of this work are to prepare monodisperse derivatives of poly(γ-(4-hexadecyloxy)benzyl α,L-glutamate) from the biosynthesized poly(α,L-glutamate)

derivatives and characterize their thermal and structural properties. Polydisperse samples of this polymer were also prepared by the same synthetic method from commercially available polydisperse PLGA, and their physical properties were compared with those of monodisperse samples.

4.2 Experimental Section

4.2.1 Materials

Hexadecyl iodide, 4-hydroxybenzaldehyde, cesium carbonate, hydrazine and mercuric oxide (yellow) were purchased from Aldrich. Methanol, benzene and anhydrous diethyl ether were purchased from EM Science and DMSO from Sigma. Dioxane and dichlormethane were purchased from Fisher Scientific. All reagents were used without further purification.

4.2.2 Synthesis of 4-(Hexadecyloxy)benzaldehyde

A mixture of 7.5 g (61.4 mmol) of 4-hydroxybenzaldehyde and 10 g (30.7 mmol) of cesium carbonate in anhydrous methanol (300 mL) was refluxed for 1 hr. After removal of the solvent by rotary evaporation, the dry cesium salt was dissolved in DMF (200 mL), hexadecyl iodide (21.6 g, 91.4 mmol) was added and the mixture stirred for 48 hr at 80 °C. Then the solvent was removed by vacuum distillation and the remaining residue was dissolved in chloroform and filtered. The solvent was removed by rotary evaporation and the crude product was recrystallized from anhydrous acetone. The yield was 11 g, 50%: mp 45 °C; ^{1}H NMR ($CDCl_3$) δ 0.9 (t, 3H,-CH_3), 1.4 (m, 26H, -CH_2-), 1.8 (m, 2H, β-CH_2), 4.0 (t, 2H, α-CH_2), 6.9 (d, 2H Ar-H), 7.8 (d, 2H, Ar-H), 9.9 (s, 1H, aldehyde-H); IR (chloroform cast film) cm^{-1} 2919 (aliphatic C-H stretch), 1689 (carbonyl strech).

4.2.3 Synthesis of 4-(Hexadecyloxy)benzaldehyde Hydrazone

4-(hexadecyloxy)benzaldehyde (6.5 g, 18 mmol) was dissolved in 100 mL of anhydrous diethyl ether and the solution was slowly dropped into 150 mL of anhydrous diethyl ether containing 1.5 mL (47 mmol) of hydrazine at 4°C. In 3-5 min, a white precipitate appeared in the solution and the reaction was stirred at 4°C for 4 hr. The white preciptate was filtered and washed with cold anhydrous diethyl ether. The yield was 5.2 g, 65%: ^{1}H NMR ($CDCl_3$) δ 0.9 (t, 3H,-CH_3), 1.4 (m, 26H, -CH_2-), 1.8 (m, 2H, β-CH_2), 4.0 (t, 2H, α-CH_2), 6.9 (d, 2H Ar-H), 7.5 (d, 2H, Ar-H), 7.7 (s, 1H, imine-H); IR (KBr film) cm^{-1} 3354 (amine N-H), 2919 (aliphatic C-H).

4.2.4 Synthesis of 4-(Hexadecyloxy)phenyldiazomethane

4-(Hexadecyloxy)benzaldehyde hydrazone (1g, 2.25 mmol) was added to 50 mL of benzene and stirred at 40 °C until dissolution. HgO (1.3 g, 6 mmol) and 200 μL of saturated KOH/EtOH solution were added and the mixture was stirred at room temperature for 20 min. The reaction mixture was filtered twice and the red-purple benzene solution containing the diazo compound was washed with 100 mL of water 4 times. This solution showed a strong absorption band at λmax=500 nm and was used directly for the reaction with PLGAs. Titration with benzoic acid in benzene solution gave approximately 35% reaction yield.

4.2.5 Synthesis of Monodisperse Derivatives of Poly(γ-4-(hexadecyloxy)benzyl α,L-glutamate) (C16O-PBLGs)

PLGA-4 (sodium salt, 70 mg, 0.4 mmol repeating units) was dissolved in 15 mL of water and acidified to pH 1.4 with dilute aqueous HCl. The precipitated polymer was purified by ultrafiltration (Amicon, MWCO = 3000) and dried under vacuum overnight. The polymer was dissolved in 80 mL of DMSO and 50 mL of 4-(n-hexadecyloxy)phenyl

diazomethane (approximately 0.8 mmol) solution was added. The reaction mixture was stirred at room temperature for 48 hr in the dark. DMSO was removed by vacuum distillation and the remaining solid was dissolved in 30 ml of dichloromethane and centrifuged at 4 °C for 30 min. The clear solution which was present at the lower part of the centrifuge tube was carefully withdrawn by pasteur pipett and added to 10 fold excess dioxane and stored at 4 °C overnight. The white precipitate was isolated by centrifugation, washed with cold dioxane and dried. The yield was 50%. The same procedure was used to produce C16O-PBLG3 and polydisperse C16O-PBLGs with comparable reaction yields. ^{1}H NMR ($CDCl_3$) δ 0.9 (3H,-CH_3), 1.4 (26H, -CH_2-), 1.8 (2H, β-CH_2 of hexadecyl group), 2.1-2.8 (4H, β– and γ-CH_2 of glutamate), 3.8 (2H, -OCH_2-), 4.0 (1H, α-CH_2 of glutamate), 4.7-5.1 (2H, benzylic CH_2), 6.8 (2H Ar-H), 7.2 (2H, Ar-H), 8.4 (1H, amide H).

4.2.6 Polarized Light Optical Microscopy

An Olympus BH-2 optical microscope and a Linkam THMS600/HFS91 stage were used for recording polarized light optical micrographs. Temperature of the samples was controlled within ±0.2°C by Linkam TMS91 temperature controller Typically, the samples were placed in between two glass cover slips and photomicrographs were recorded with × 200 magnification.

4.2.7 Differential Scanning Calorimetry

A TA Instruments DSC 2910 was used for differential scanning calorimetry experiments. DSC thermograms were recorded at 10°C/min heating and cooling rates under nitrogen flow.

4.2.8 X-ray Diffraction

The 1 mm quartz capillary tube was filled with the sample and placed inside a heating unit which was connected to a temperature controller. The heating unit was placed inside an evacuated flat-plate Statton camera and the X-ray diffraction pattern was recorded with pin-hole collimation and Ni-filtered Cu Kα radiation. The temperature of the heating unit was controlled to within ±3°C.

4.3 Results and Discussion

4.3.1 Synthesis of Poly(γ-4-(hexadecyloxy)benzyl α,L-glutamate)

We have employed diazoalkane chemistry, the same type of chemistry used for benzylation of the PLGAs in the previous chapter, for the synthesis of poly(γ-4-(hexadecyloxy)benzyl α,L-glutamate) (Fig. 4.1 and 4.2). 4-(Hexadecyloxy)benzaldehyde was synthesized by the reaction of 4-hydroxybenzaldehyde with cesium carbonate to prepare the cesium salt derivative, which was then reacted with hexadecyl iodide. The ^{1}H NMR (Fig. 4.3) and IR (Fig. 4.4) spectra are in good agreement with the expected structure of the product. Reaction of 4-(hexadecyloxy)benzaldehyde with hydrazine gave 4-(hexadecyloxy)benzaldehyde hydrazone and the structure was confirmed by ^{1}H NMR (Fig. 4.5) and IR (Fig. 4.6) spectra.

Synthesis of 4-(hexadecyloxy)phenyl diazomethane from 4-(hexadecyloxy) benzaldehyde hydrazone was carried out in benzene solution with HgO and a catalytic amount of KOH. Addition of base to this reaction has been reported to facilitate the formation of the diazo compound, however, the exact role of the base remains to be determined[18]. 4-(Hexadecyloxy)phenyl diazomethane was unstable and was deactivated in the reaction system soon after it was synthesized. This was evidenced by the disappearance of the red color of the solution after longer reaction times (typically 45 min). By analyzing the intensity of its absorption band (λmax=500) at different reaction times, 15-20 min was

chosen to be the optimum reaction time. However, there were variations in the optimum reaction time from run to run.

The target polymers, poly(γ-4-(hexadecyloxy)benzyl α,L-glutamate)s were prepared by reaction of PLGAs with 4-(hexadecyloxy)phenyl diazomethane (Fig. 4.2). Four different polymers were synthesized from their PLGA precursor polymers: polydisperse (PDI=1.2) samples with DP=55 (C16O-PBLG-55) and 98 (C16O-PBLG-98), and monodisperse samples derived from biosynthesized PLGAs, C16O-PBLG-3 (DP=58) and C16O-PBLG-4 (DP=76). The structure and purity of these polymers were confirmed by ^{1}H NMR spectroscopy (Figure 4.7-4.10); the integration indicated more than 95% substitution of the side chains (Table 4.1).

4.3.2 Characterization of Poly(γ-4-(hexadecyloxy)benzyl α,L-glutamate)s

The DSC thermograms of the synthesized polymers are shown from Figures 4.11 to 4.14 and the latent heats related to the phase transitions are summarized in Table 4.1. All four polymers show strong endotherms at around 40°C. Additional weak endotherms are also present at around 90-100°C for all the polymers except C16O-PBLG-55. All transitions are reversible and appear also in the cooling curves. After the first transition, the polymers became elastic but were not liquid like - samples did not flow between the two glass plates. However, after the second transition the polymers became liquid as evidenced by the fluidity of the samples. When analyzed with polarized light optical microscopy (POM), the second transition was marked by the disappearance of birefringence of the samples. Polarized light optical micrographs are shown in Figures 4.15 to 4.18. The samples were first heated above the isotropization temperature (110 °C), then cooled down to the preset temperature and annealed for 3-5 hr before acquiring the photomicrographs. When investigated with POM, C16O-PBLG-55 (polydisperse DP=55), C16O-PBLG-3 (monodisperse DP=58), and C16O-PBLG-4 (monodisperse, DP=76) showed similar

phase transition behavior and optical textures. When cooled from isotropic phase, small birefringent islands slowly appeared. The rate of nucleation of the birefringent spots and final birefringences after 5 hr of annealing at 70°C varied in increasing order from the C16O-PBLG-3 (Figure 4.17), the C16O-PBLG-55 (Figure 4.15) and the C16O-PBLG-4 (Figure 4.18). In the case of C16O-PBLG-98 (polydisperse) there was a distinct phase transition at around 100 °C and an unusual sheath-like texture appeared (Figure 4.16 b). This phase was stable up to 105 °C above which it became isotropic. When the sheath-like textured phase was cooled to 70 °C, plate-like textures appeared and eventually made the whole field of view birefringent (Fig. 4.16 a). The unique texture observed in C16O-PBLG-98 at 100 °C may have come from the LC ordering of higher molecular weight portion of the polydisperse samples.

Figure 4.19 shows the X-ray diffraction patterns of C16O-PBLG-4 recorded at room temperature. At room temperature, strong reflections with Bragg spacings of 3.75 Å (strong) and 4.17 Å (very strong) are present in the wide-angle diffraction pattern. These spacings are similar to those of 100 and 010 reflections of the two-dimensional crystal lattices formed by alkane chains of 10 or more methylene groups in poly(alkyl α,L-glutamate)s. These two-dimensional lattices are believed to resemble the subunit cell attained by c-axes projection of the triclinic unit cell in crystals of low molecular weight alkanes[6]. In the smaller angle region, a very intense reflection at 37.2 Å and corresponding second order reflection at 18.9 Å are present. This large layer spacings are likely to originate from the distance between the polymeric backbone which is separated by the long alkyl side chains. Presence of well-defined second order suggest that the chains are packed in a regularly arranged layer-like structure. In addition, weak but distinct reflection of spacing 12.9 Å is also seen in the diffraction pattern. This spacing is very close to the interchain distance of PBLG rod in solid state. From the diffraction patterns, it is reasonable to suggest that the rods are arranged in a layer like structure as shown in Figure 4.22. This structure is similar to the structure proposed by Watanabe and co-worker[6] for

the solid state of poly(alkyl α,L-glutamate)s. The X-ray experiments on poly(γ-alkyl α,L-glutamic acid) with alkyl chain longer than dodecyl group performed by these workers did not show a clear reflection corresponding to the interchain spacing. However, from the calculation of density, they estimated the interchain spacing to be 12.3 Å which is very close to the spacing we have assigned to the interchain distance of C16O-PBLG-4. The origin of the 47.6 Å spacing is not known at this point. When the diffraction pattern is recorded at 70°C, the interlayer spacing is changed to 35.8 Å and the interchain spacing is changed to 14.1 Å (Figure 4.20). The wide angle reflections, 3.75 Å and 4.17 Å are still present but with reduced intensities compared to room temperature diffraction pattern. At 70°C, a broad scattering at a spacing around 4.5~5 Å is seen which was not observed in the diffraction pattern recorded at room temperature. The spacing of this diffuse scattering is close to the spacing of first layer line of typical α-helical diffraction pattern (5.4 Å for a perfect α-helix, but it is more likely that this diffuse intensity originates from the amorphous part of the side alkyl chains. At 70°C, part of the side chain crystals are melted which has provided flexibility to the interlayer part of the polymer assembly allowing contraction of the interlayer distance. Such contraction in the interlayer distance is compensated by the increased interchain distances. A small-angle X-ray diffraction yielded no reflection suggesting smectic-like arrangement of rods in the solid state. However, a complete description of the molecular structure can only be assessed from the oriented diffraction pattern. When the sample was heated above 100°C no Bragg reflection rings were observed (Figure 4.21). However the diffuse scattering with spacing between 4.5~5 Å was still present. At this temperature, the side chain crystallites are melted and the polymers are in isotropic liquid state. This is also apparent from the disappearance of birefringence from polarized light optical microscopy. All of these results suggest that for C16O-PBLG-4, there is no molecular ordering present after the phase transition to the liquid state. It is likely that the long alkyl side chain has increased the effective diameter of the helix and reduced the aspect ratio to a point that the polymer is no longer liquid

crystalline. From the rough calculation following the results of Iizuka (Table 4.1)[12] the aspect ratio of C16O-PBLG-4 can be estimated to be 3.5. Flory's rod-ordering theory predicts the critical aspect ratio for liquid crystalline phase formation to be 7. Therefore, it is possible that we can only expect the liquid crystalline phase with C16O-PBLG-X where X is more than 8 (DP=148). Synthesis of C16O-PBLG-9 and 10 are currently in progress.

Table 4.1 Thermal Properties of C16O-PBLGs

	Aspect Ratio (L/D)[a]	% Substitution of Side Chains	Transition Temperatures (Enthalpy Changes)	
			1st Transition	2nd Transition
C16O-PBLG-55		95.3%	38.8°C (6.5 cal/g)	-
C16O-PBLG-98		95.4%	38.4°C (5.3 cal/g)	94.6°C (0.67 cal/g)
C16O-PBLG-3	1.8	94.9%	44.9°C (6.5 cal/g)	85.8°C (0.20 cal/g)
C16O-PBLG-4	3.5	95.5%	46.9°C (11.2 cal/g)	87.9°C (0.29 cal/g)

a. L=1.5 Å x number of repeating units.
D=32.4 Å (From Ref. 12)

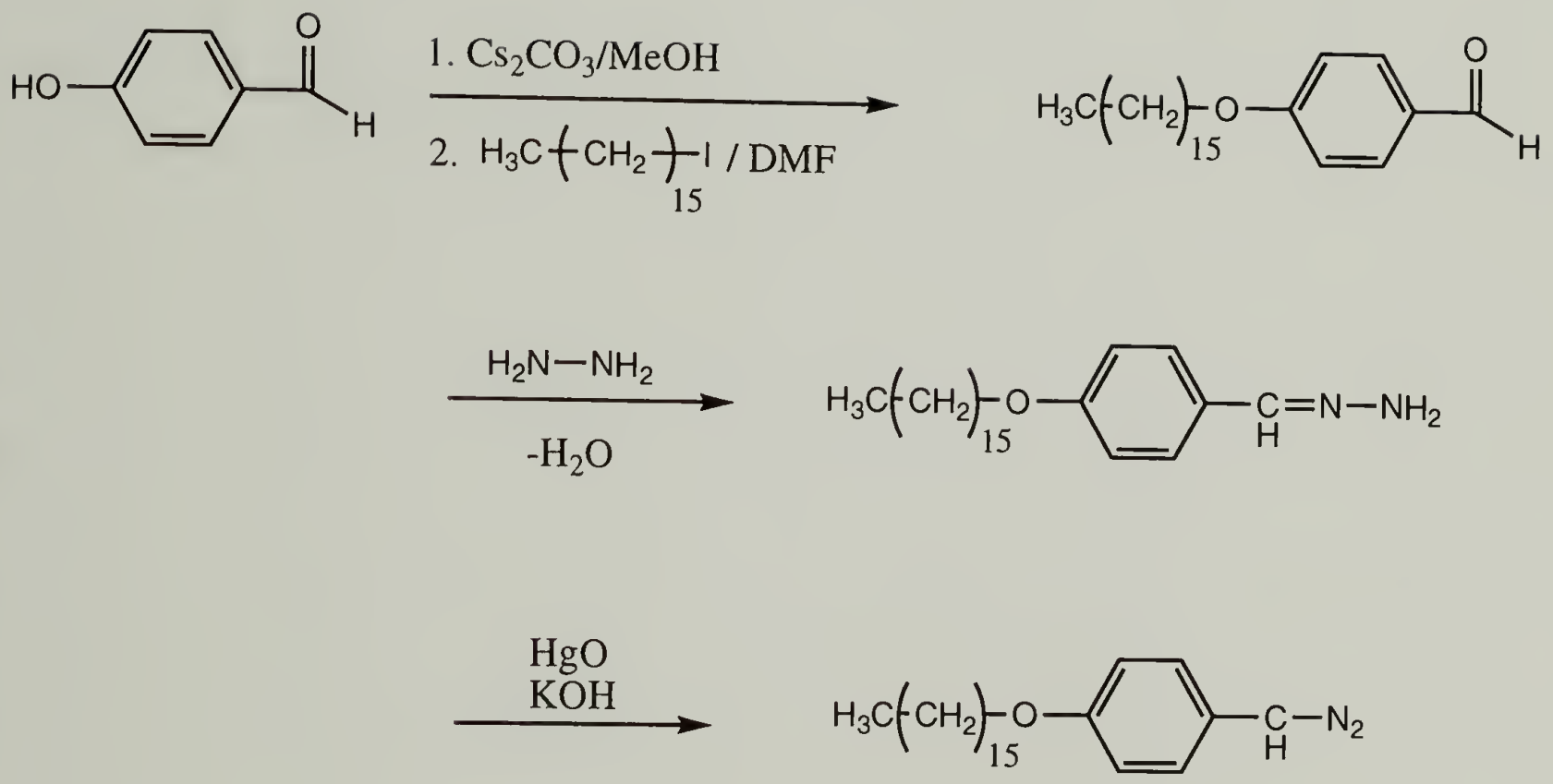

Figure 4.1 Synthetic scheme for the preparation of 4-(hexadecyloxy)phenyl diazomethane.

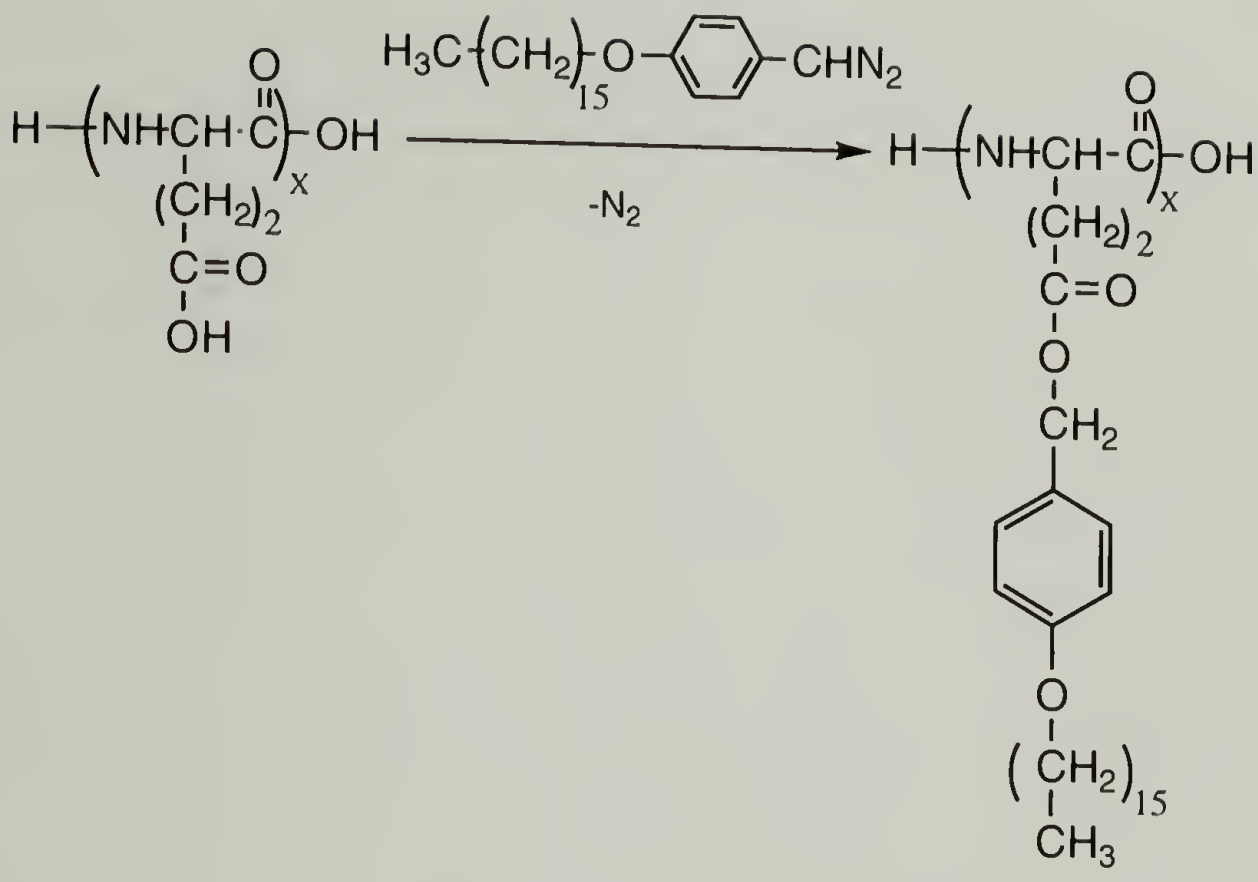

Figure 4.2 Synthetic scheme for converting poly(α,L-glutamic acid) to poly(γ-4-(hexadecyloxy)benzyl α,L-glutamate).

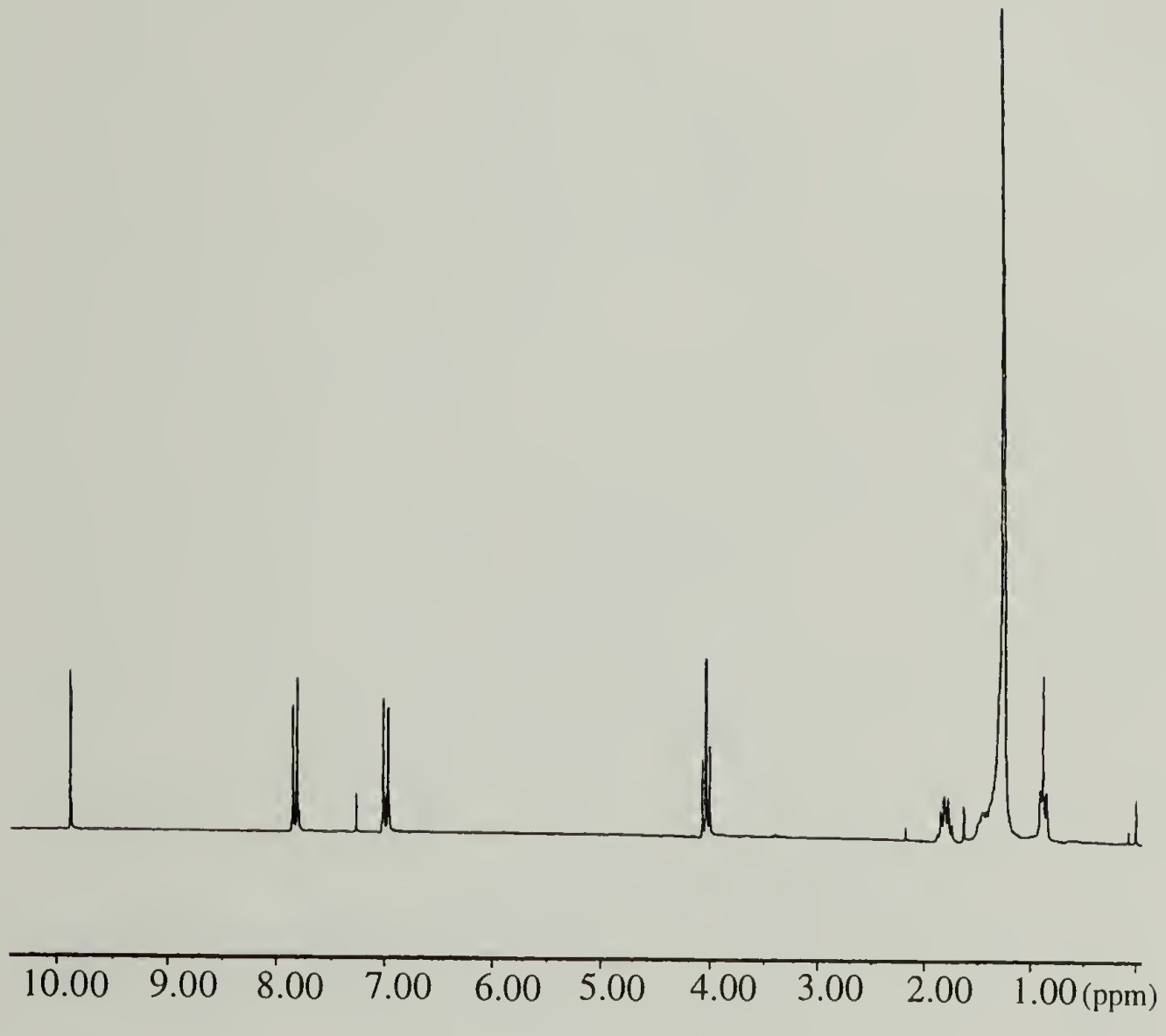

Figure 4.3 ^{1}H NMR spectrum (200 MHz) of 4-(hexadecyloxy) benzaldehyde in $CDCl_3$.

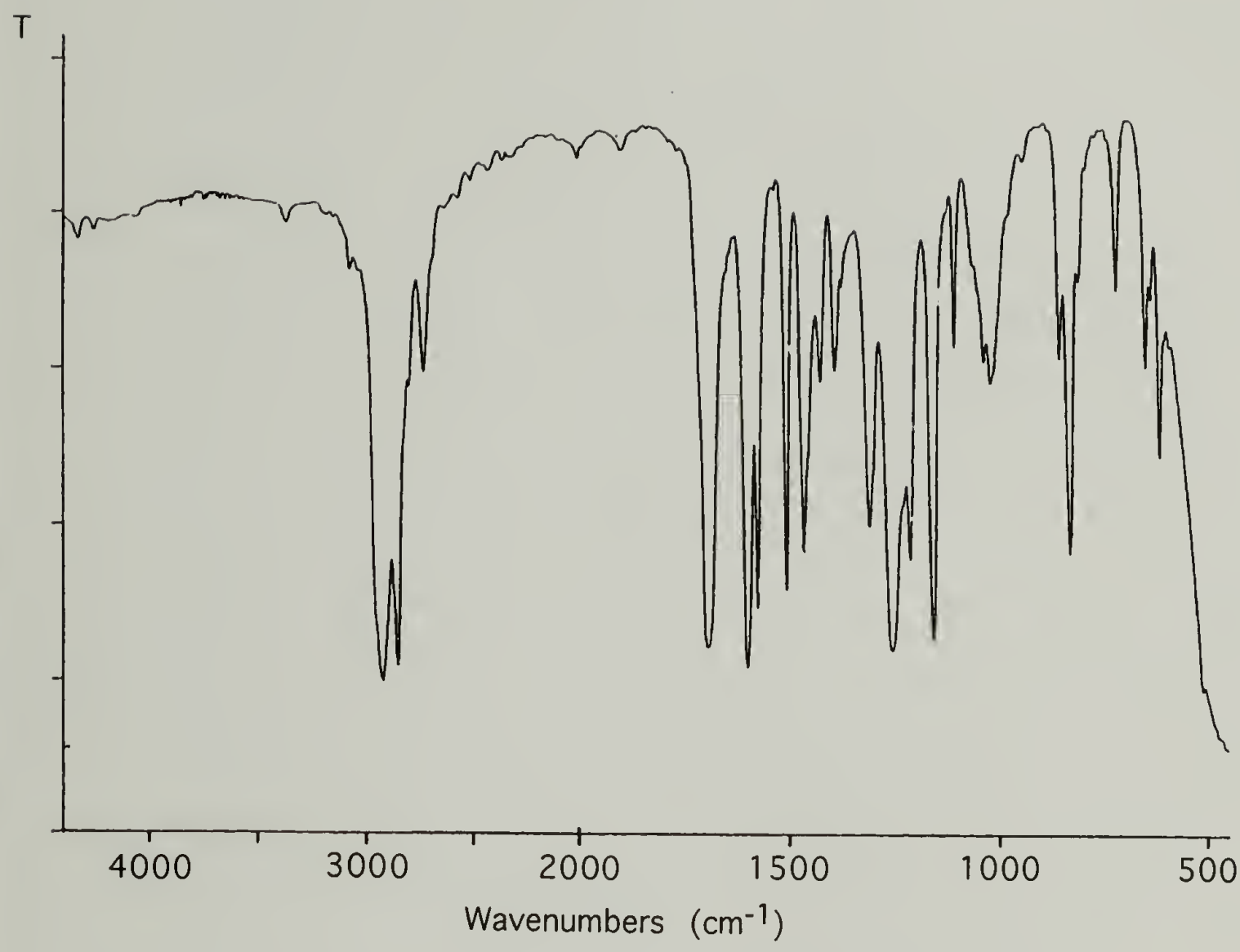

Figure 4.4 Fourier transform infrared spectrum of 4-(hexadecyloxy)benzaldehyde.

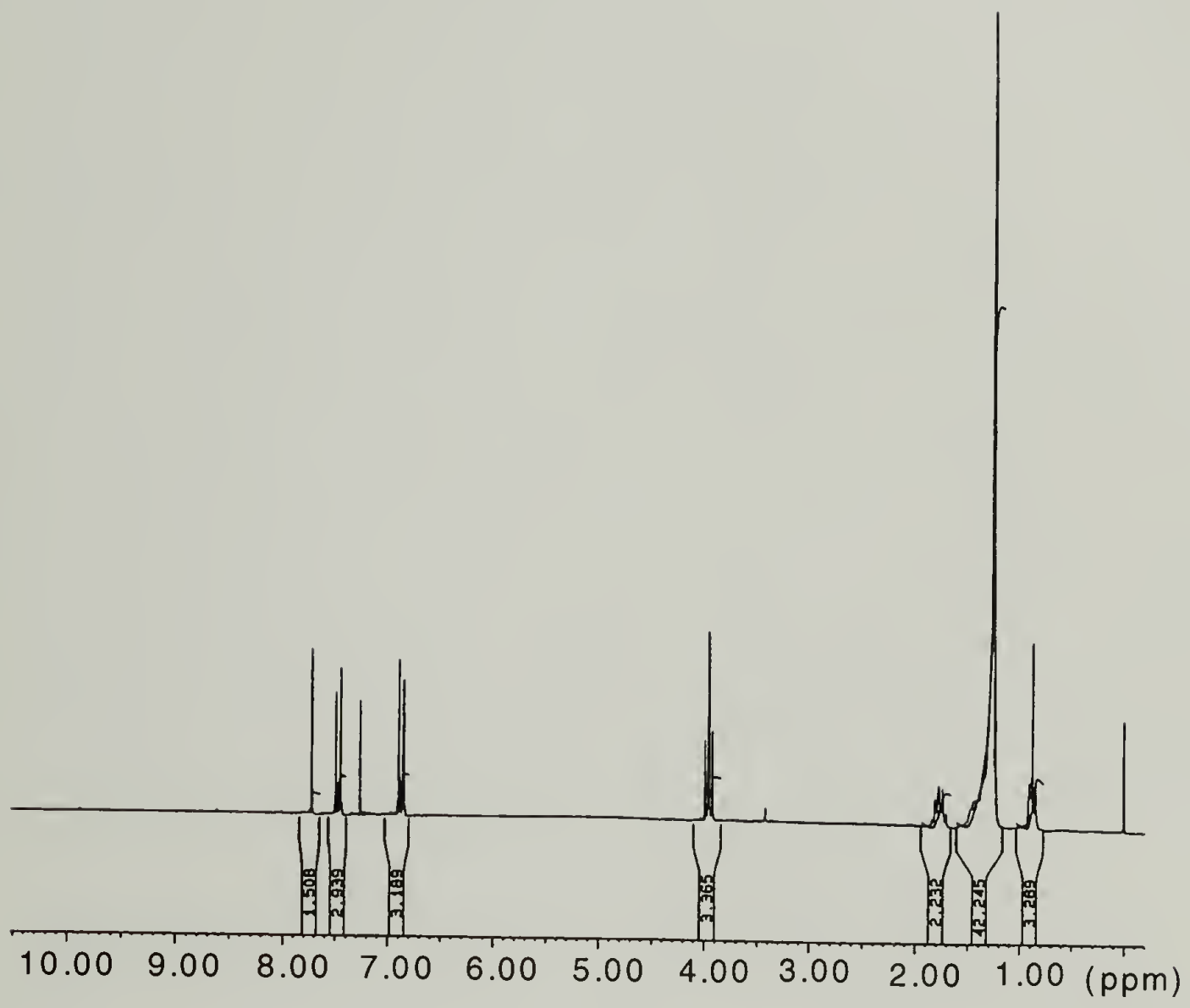

Figure 4.5 ^{1}H NMR spectrum (200 MHz) of 4-(hexadecyloxy)benzaldehyde hydrazone in $CDCl_3$.

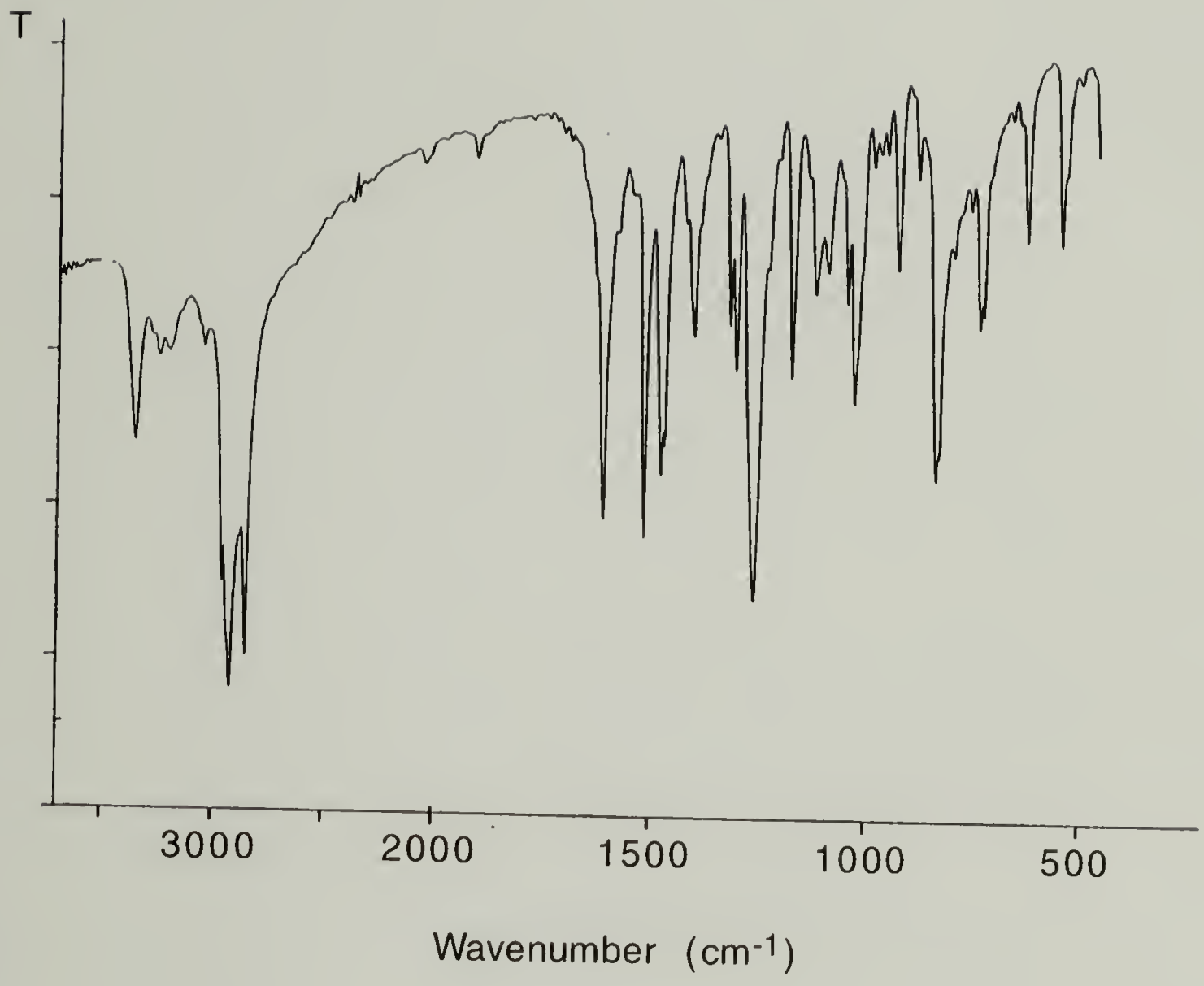

Figure 4.6 Fourier transform infrared spectrum of 4-(hexadecyloxy)benzaldehyde hydrazone.

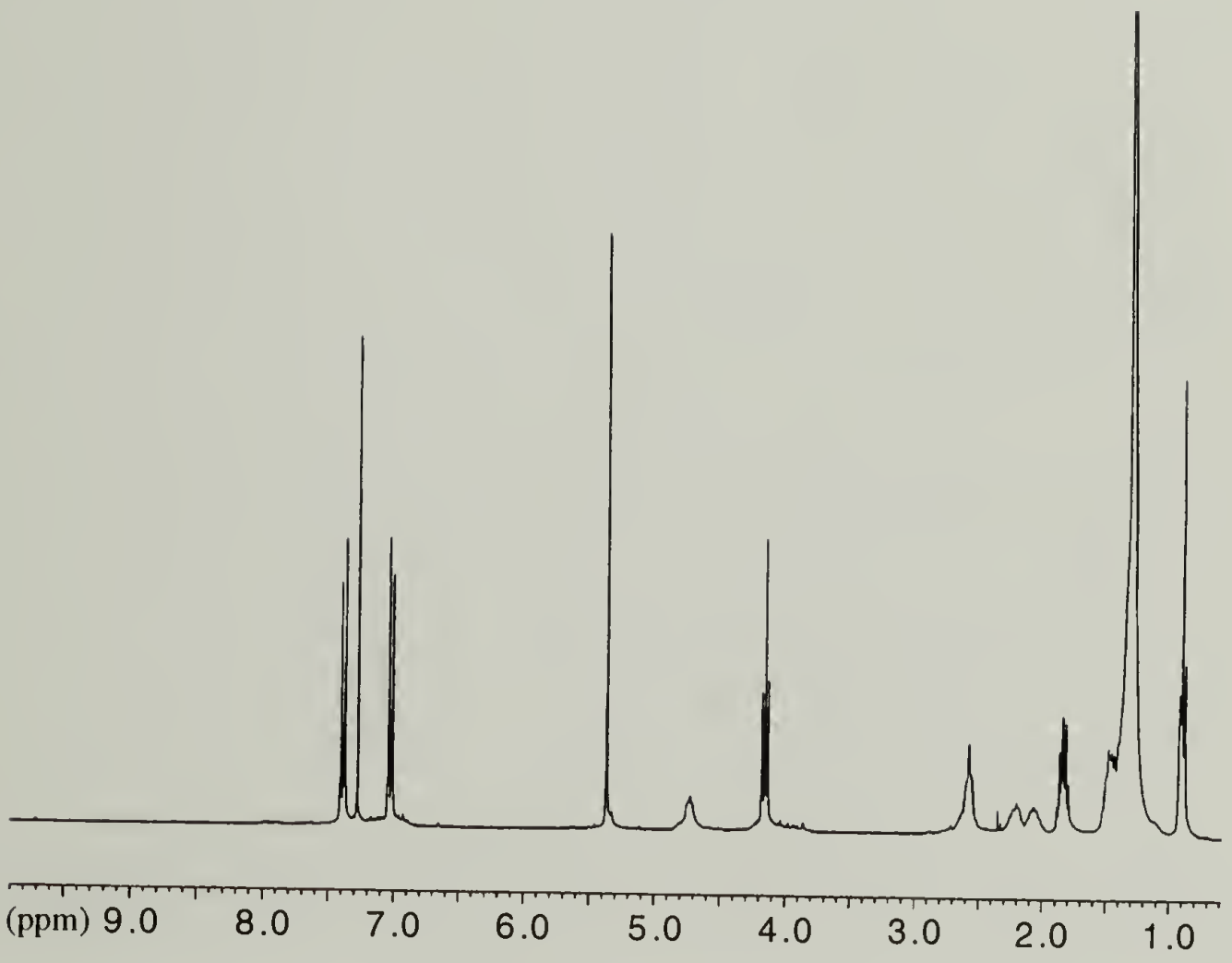

Figure 4.7 ^{1}H NMR spectrum (300 MHz) of polydisperse C16O-PBLG (DP=55, PDI=1.2) in $CDCl_3$/TFA.

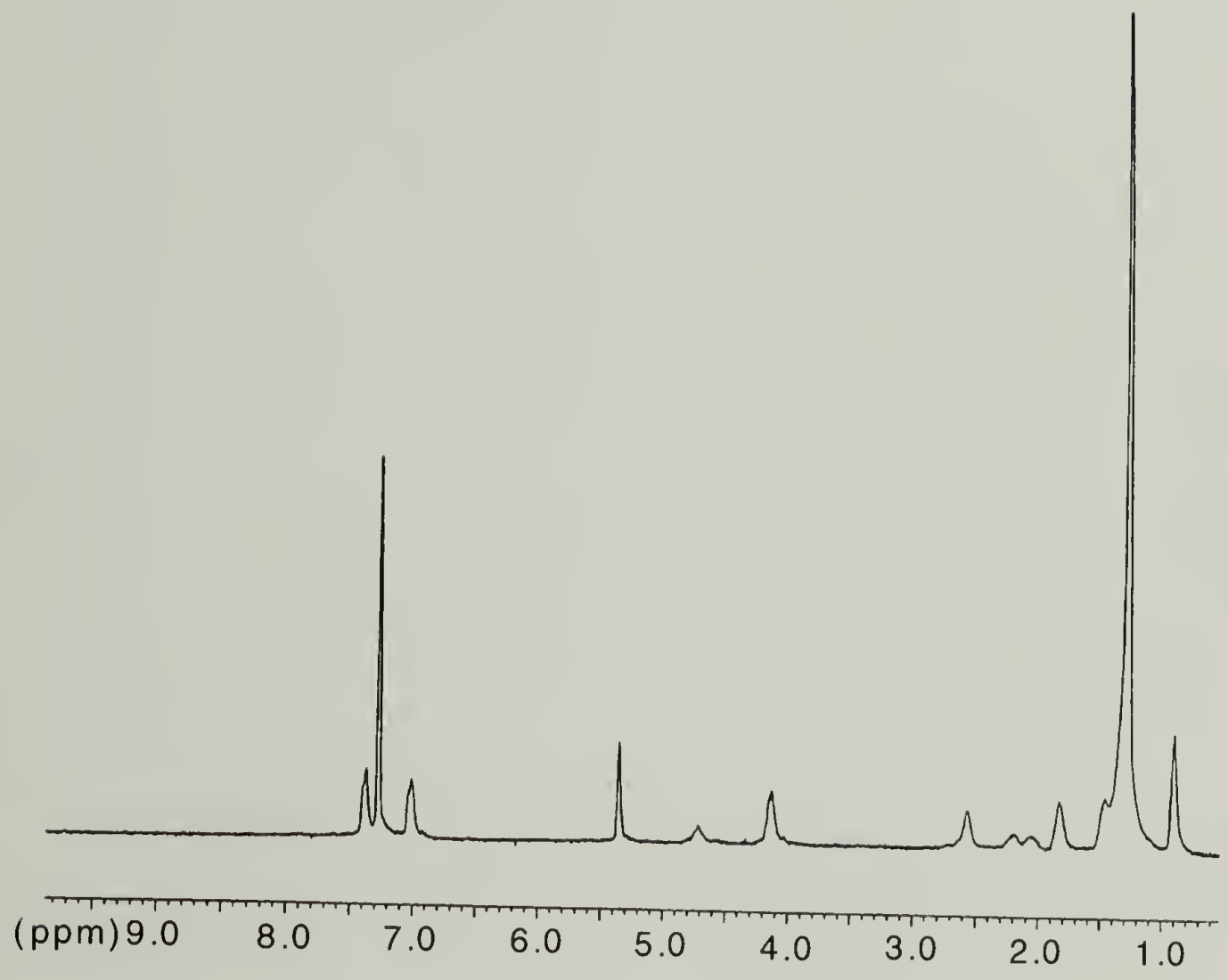

Figure 4.8 ^{1}H NMR spectrum (300 MHz) of polydisperse C16O-PBLG (DP=98, PDI=1.2) in $CDCl_3$/TFA.

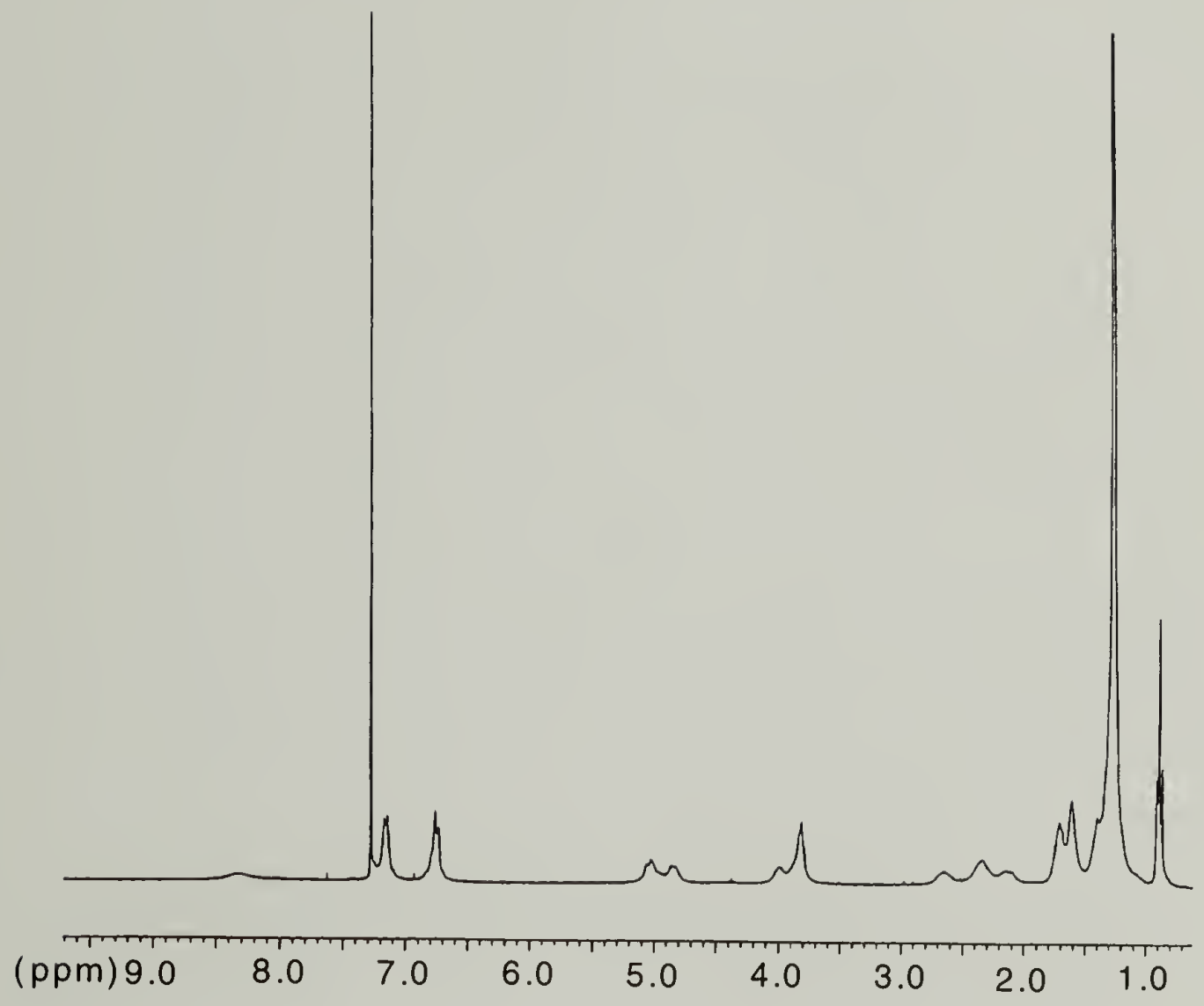

Figure 4.9 ^{1}H NMR spectrum (300 MHz) of C16O-PBLG-3 in $CDCl_3$.

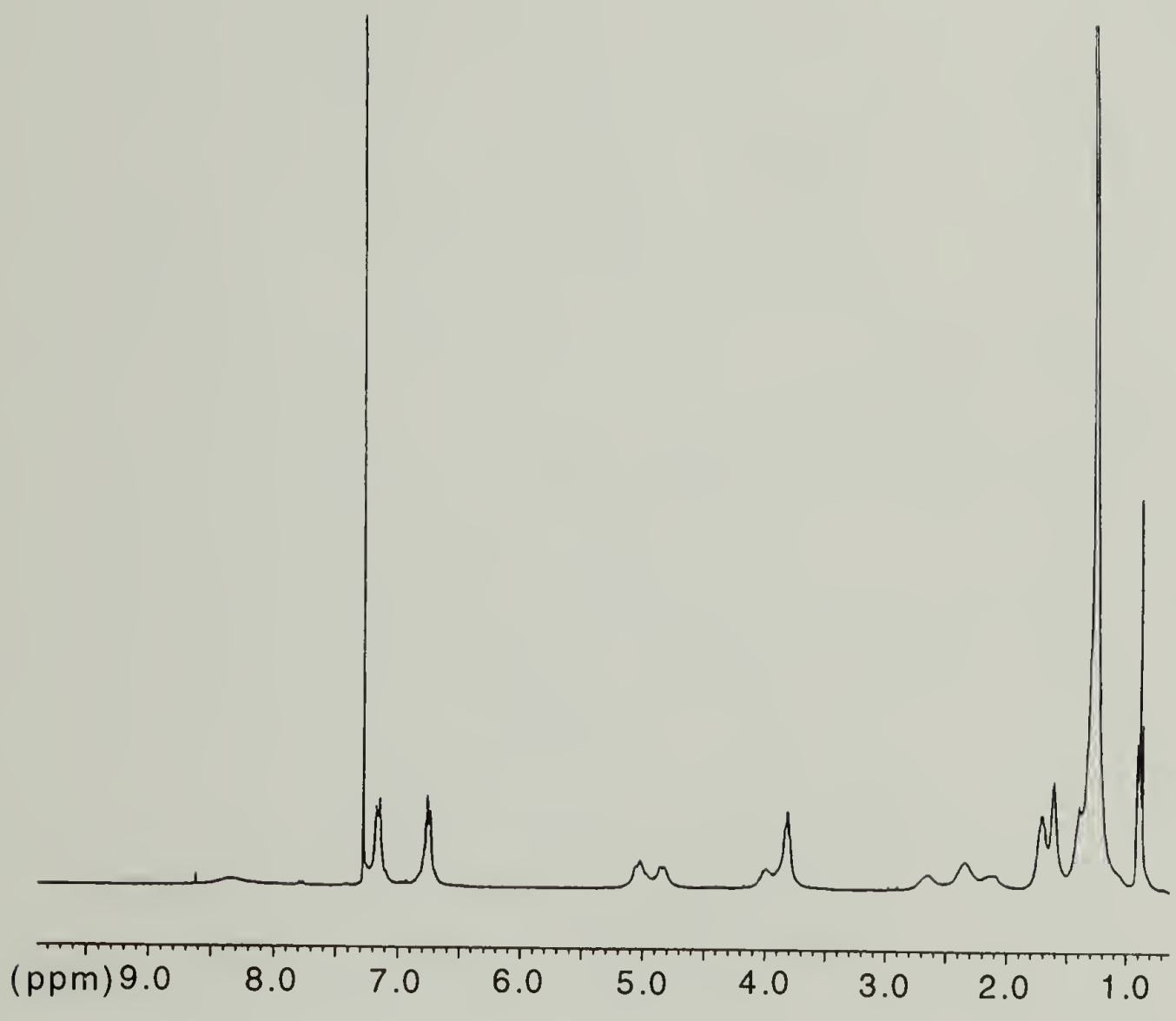

Figure 4.10 ^{1}H NMR spectrum (300 MHz) of C16O-PBLG-4 in $CDCl_3$.

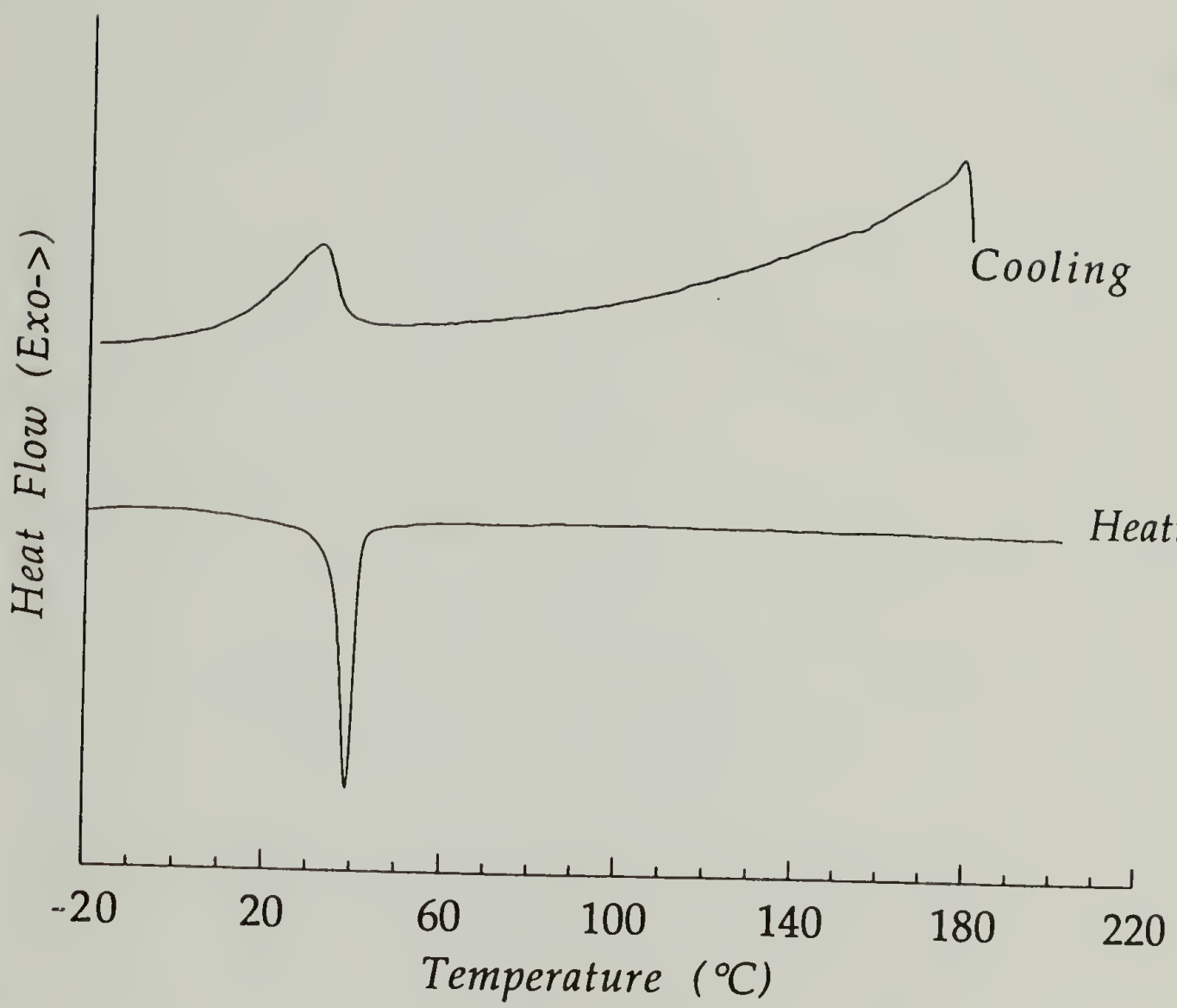

Figure 4.11 DSC thermograms of polydisperse C16O-PBLG (DP=55, PDI=1.2).

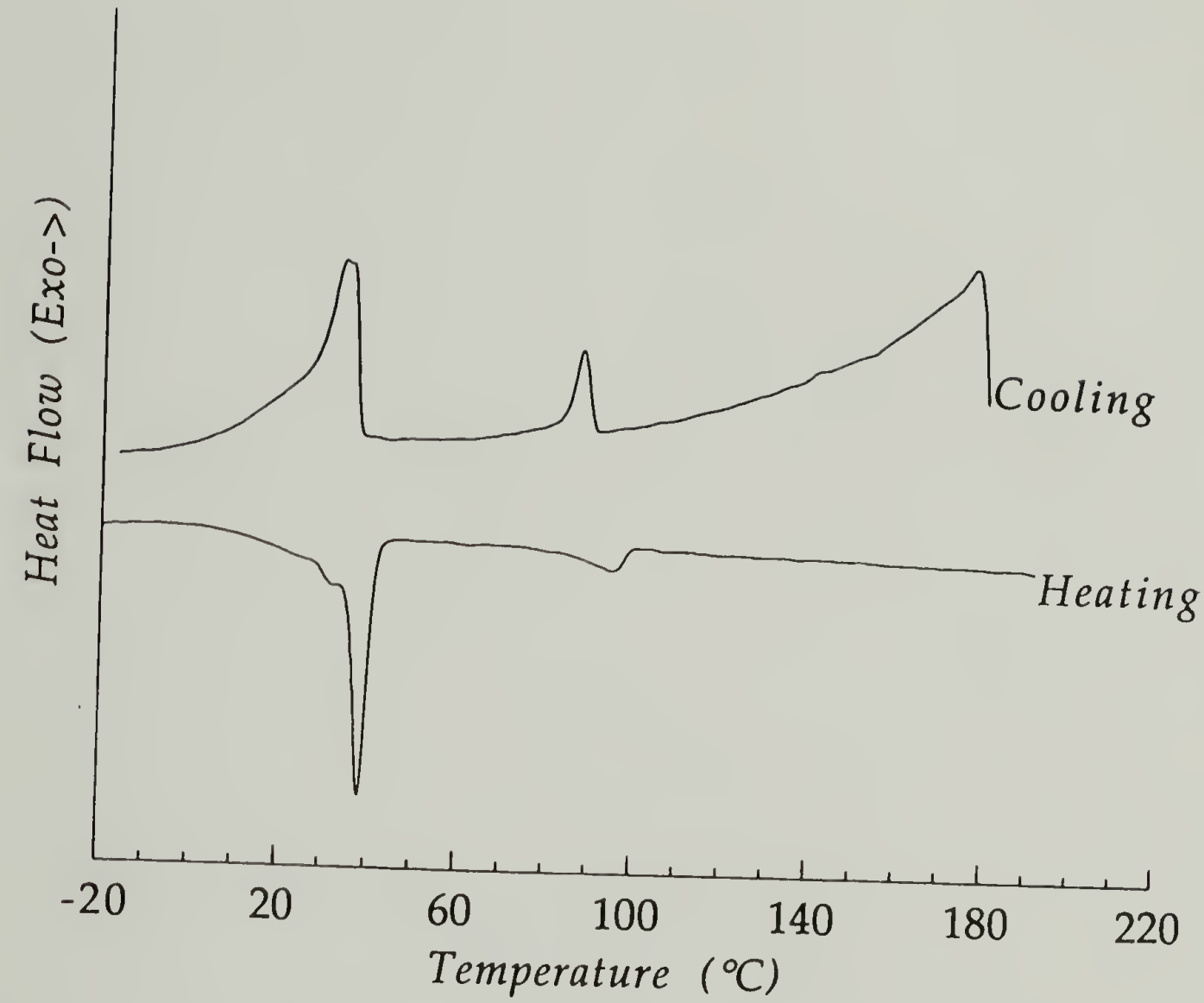

Figure 4.12 DSC thermograms of polydisperse C16O-PBLG (DP=98, PDI=1.2)

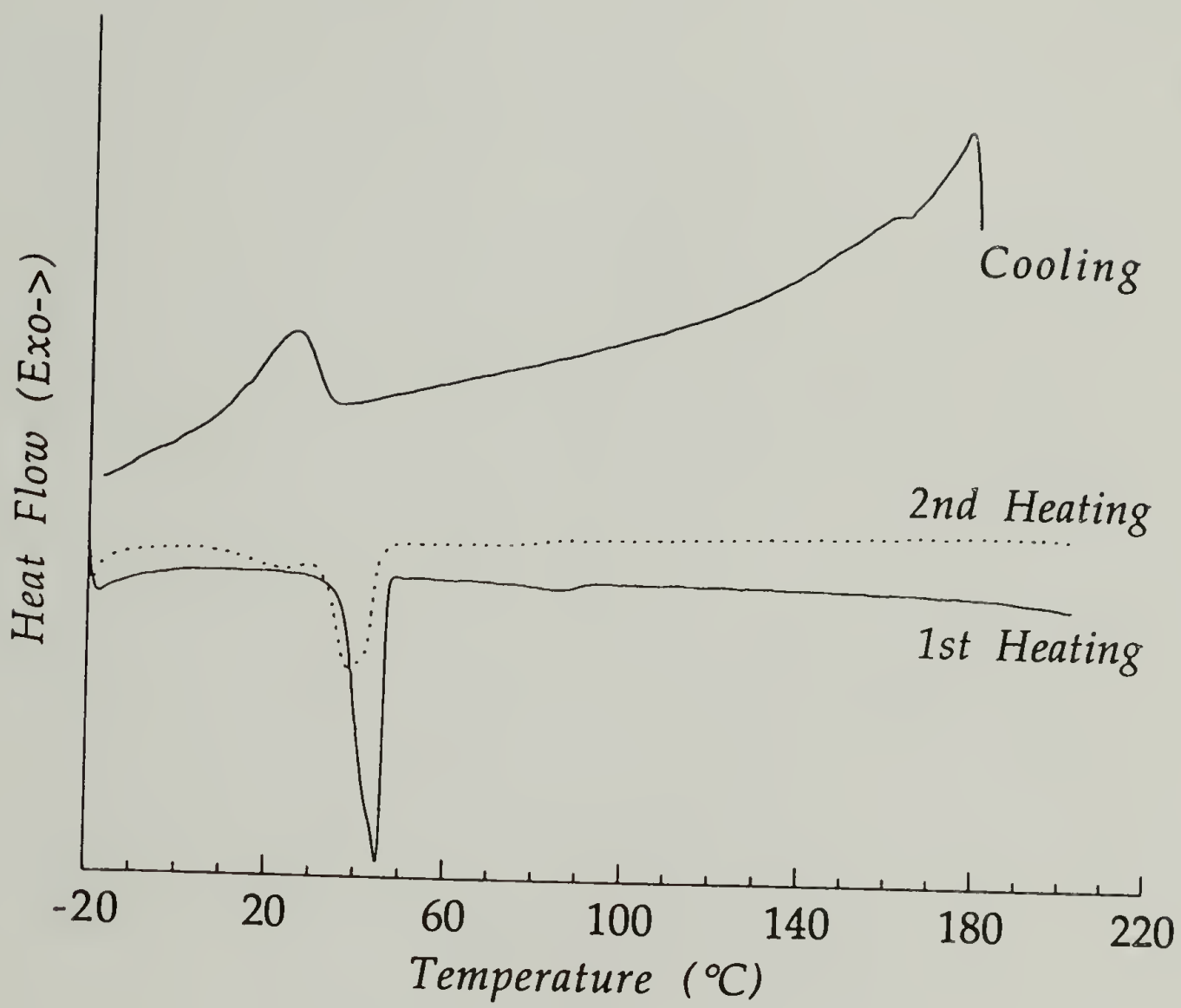

Figure 4.13 DSC thermograms of C16O-PBLG-3.

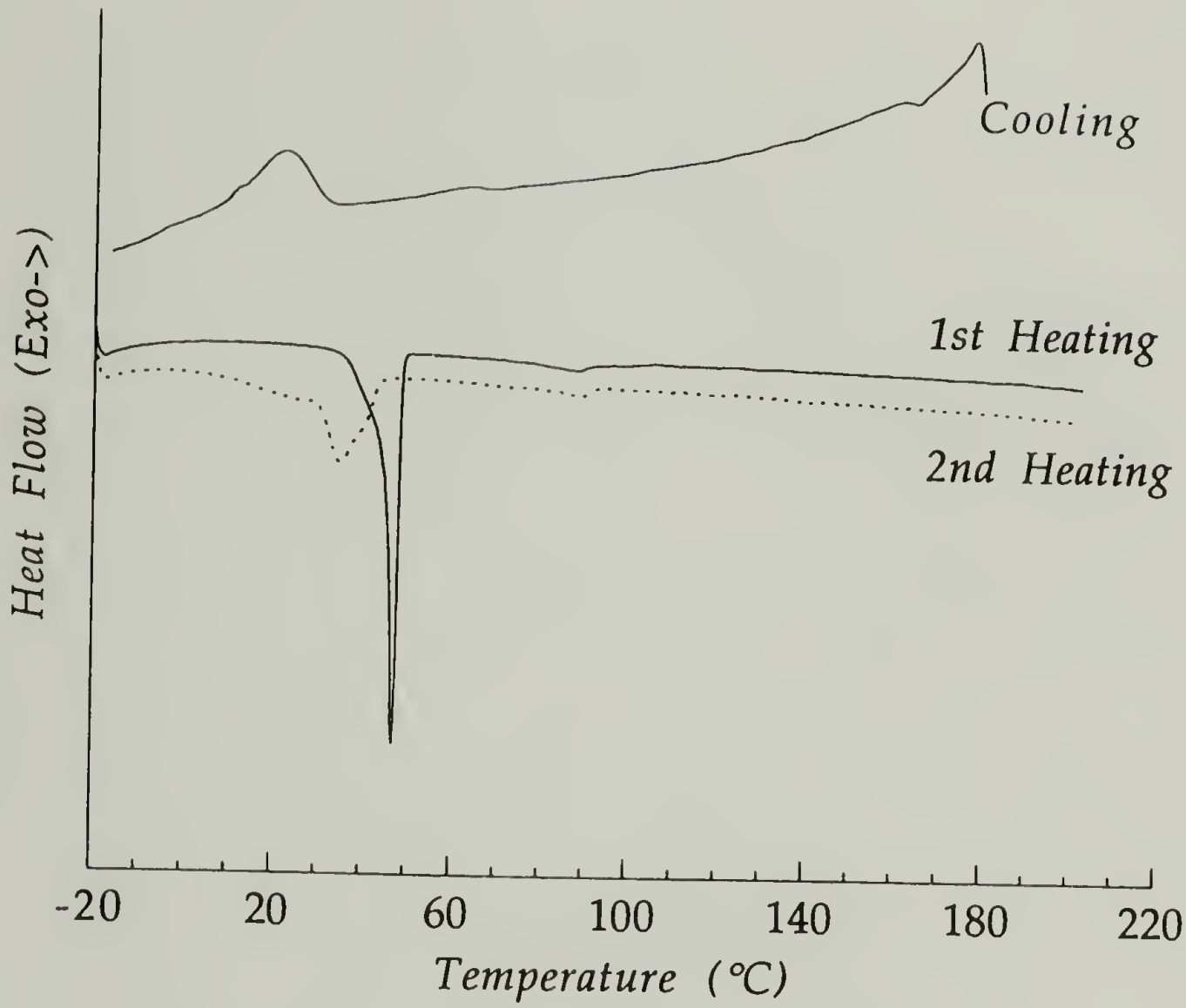

Figure 4.14 DSC thermograms of C16O-PBLG-4.

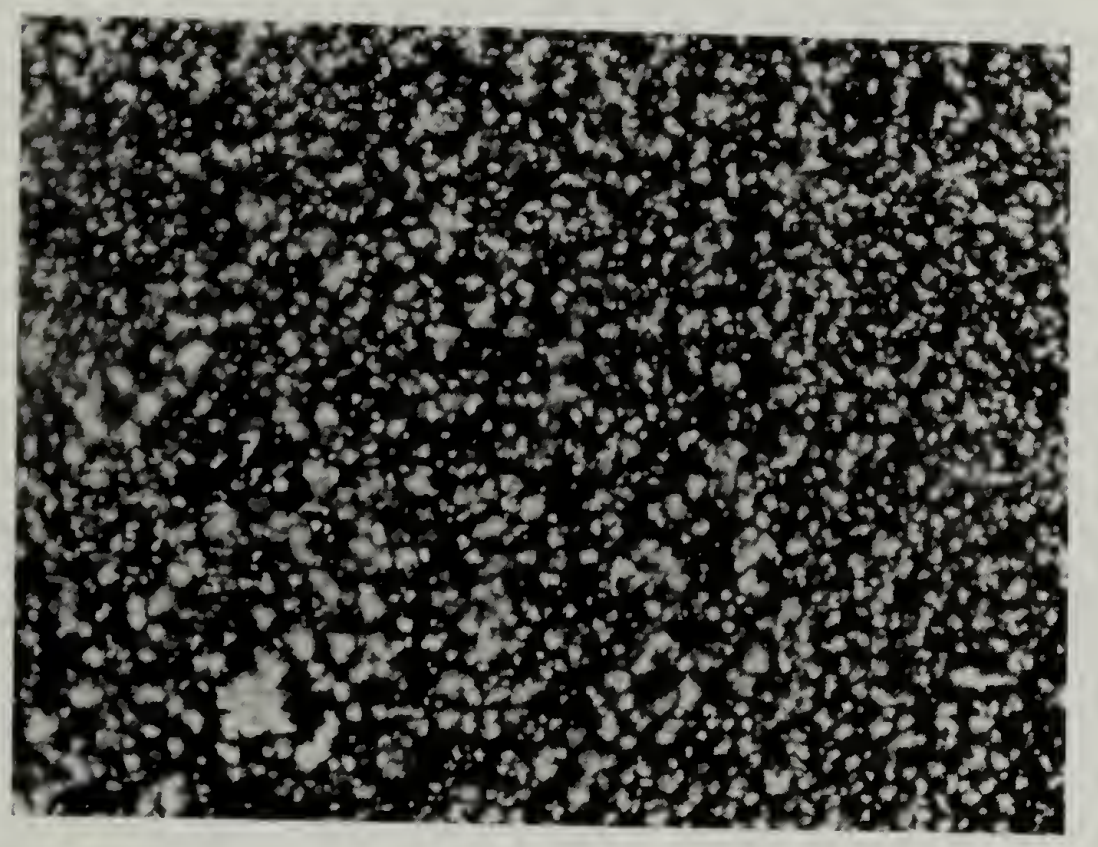

Figure 4.15 Polarized light optical micrograph (mag. x200) of polydisperse C16O-PBLG (DP=55, PDI=1.2) after annealing at 70 °C for 5 hr.

(a)

(b)

Figure 4.16 Polarized light optical micrographs (mag. x200) of polydisperse C16O-PBLG (DP=98, PDI=1.2) after annealing at 70°C for 5 hr (a) and after annealing at 101°C for 3 hr (b).

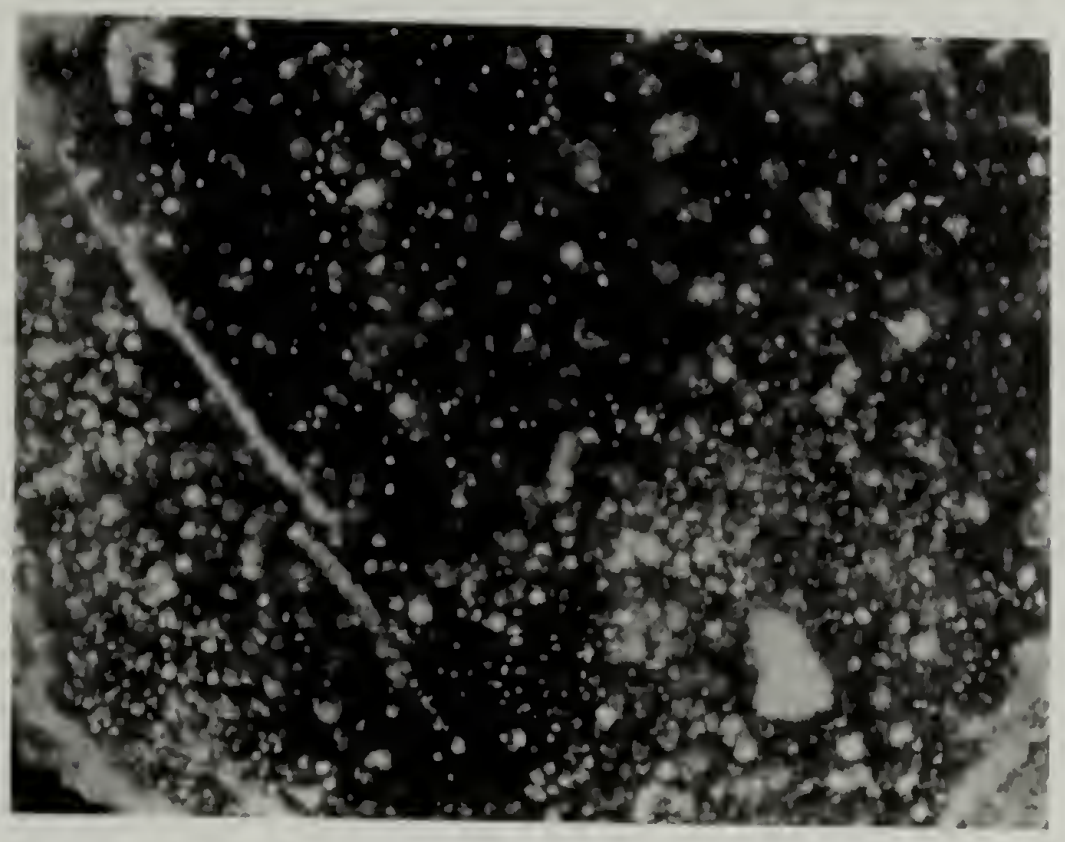

Figure 4.17 Polarized light optical micrograph (mag. x200) of C16O-PBLG-3 after annealing at 70°C for 5 hr.

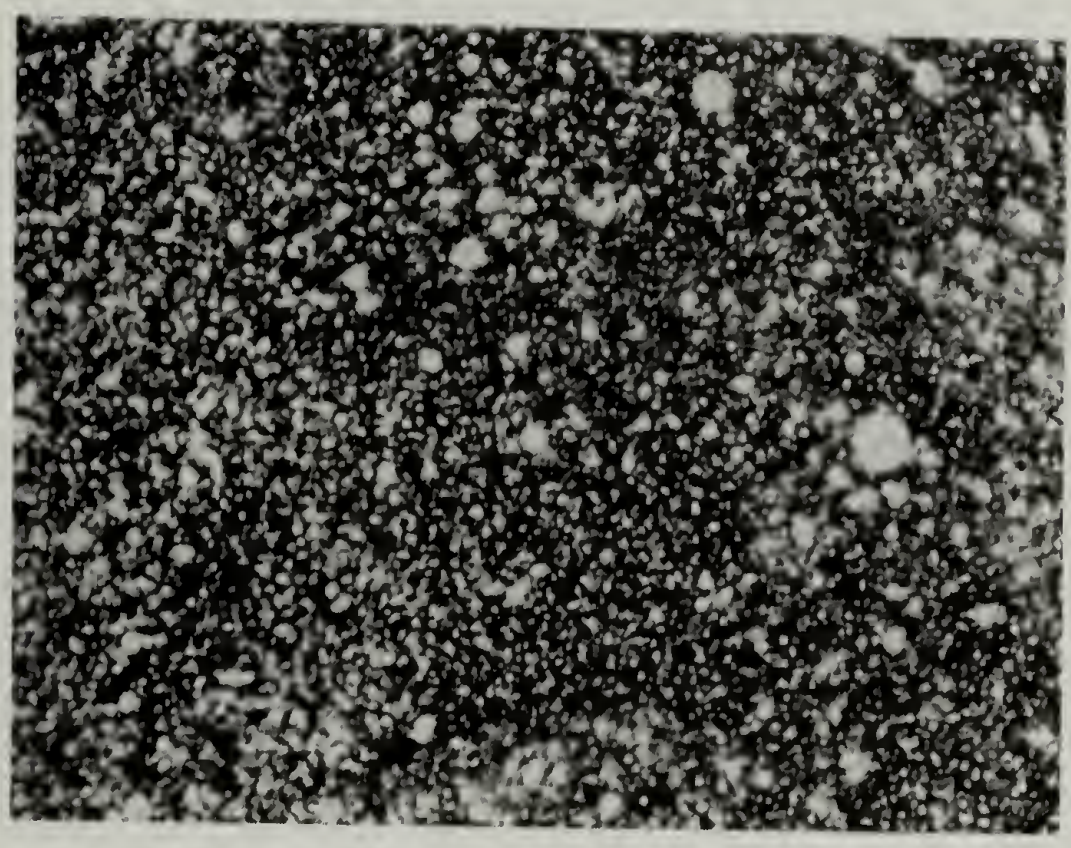

Figure 4.18 Polarized light optical micrograph (mag. x200) of C16O-PBLG-4 after annealing at 70°C for 5 hr.

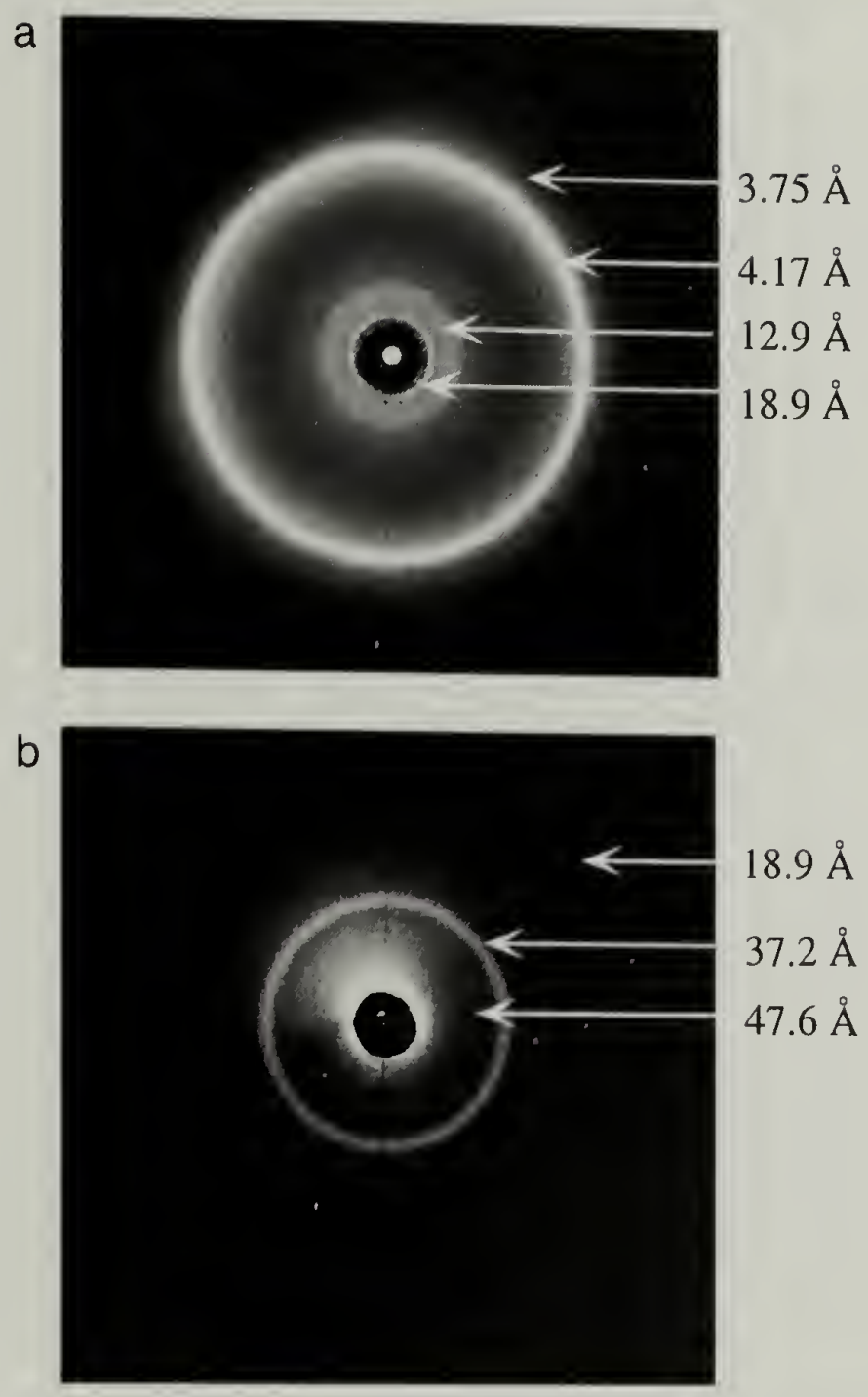

Figure 4.19 X-ray diffraction patterns of C16O-PBLG-4 recorded at 25°C with camera distances of 5.01 cm (a) and 29. 01 cm (b).

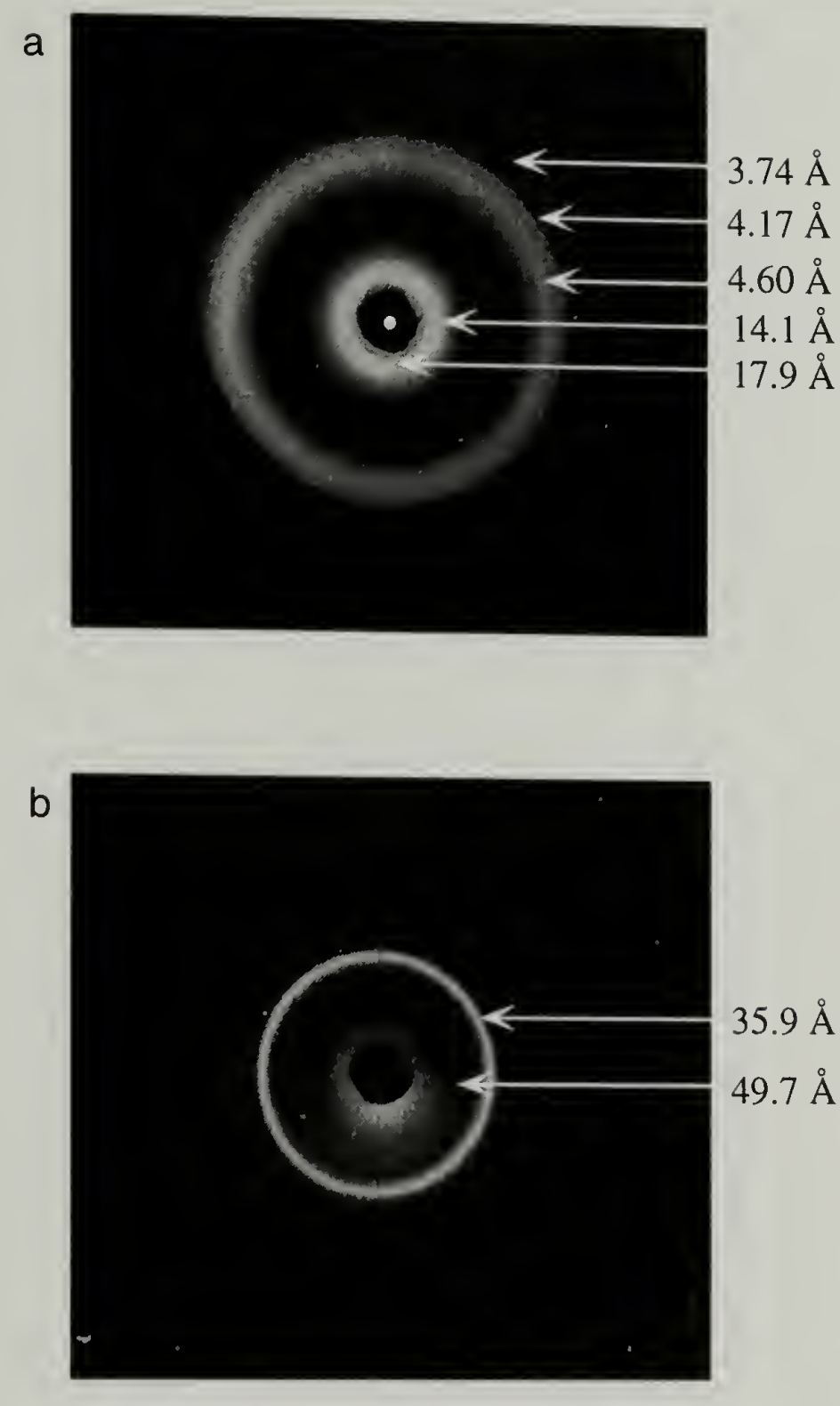

Figure 4.20 X-ray diffraction patterns of C16O-PBLG-4 recorded at 70°C with camera distances of 5.01 cm (a) and 29.01 cm (b).

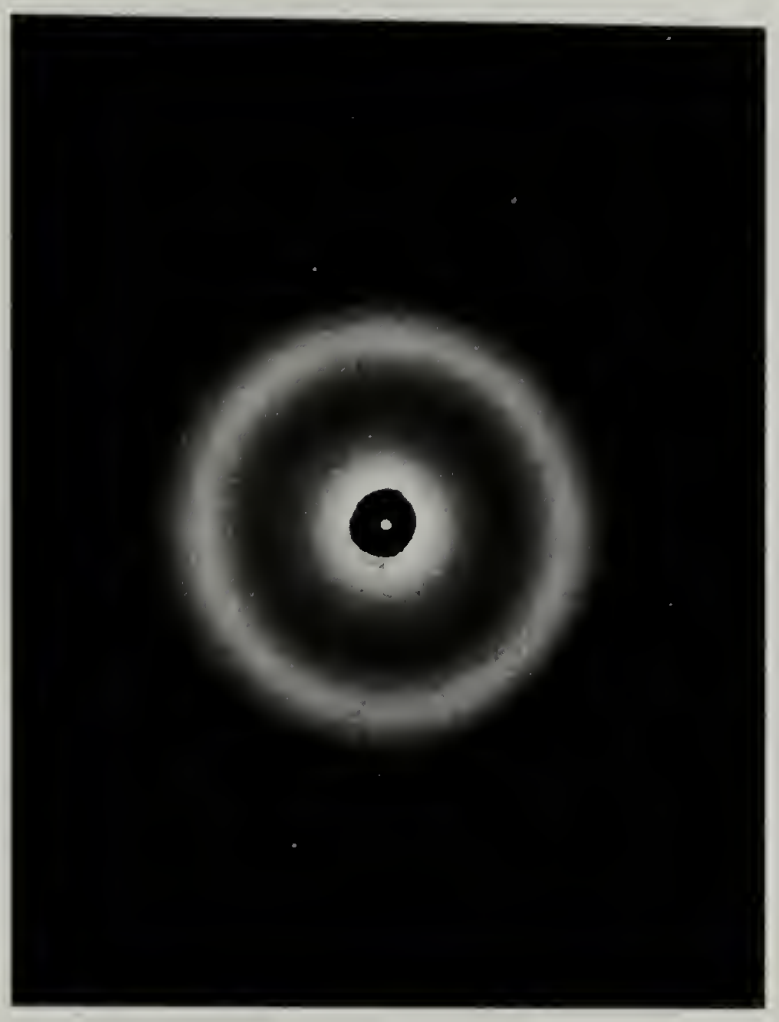

Figure 4.21 X-ray diffraction pattern of C16O-PBLG-4 recorded at 110°C with camera distance of 5.01 cm.

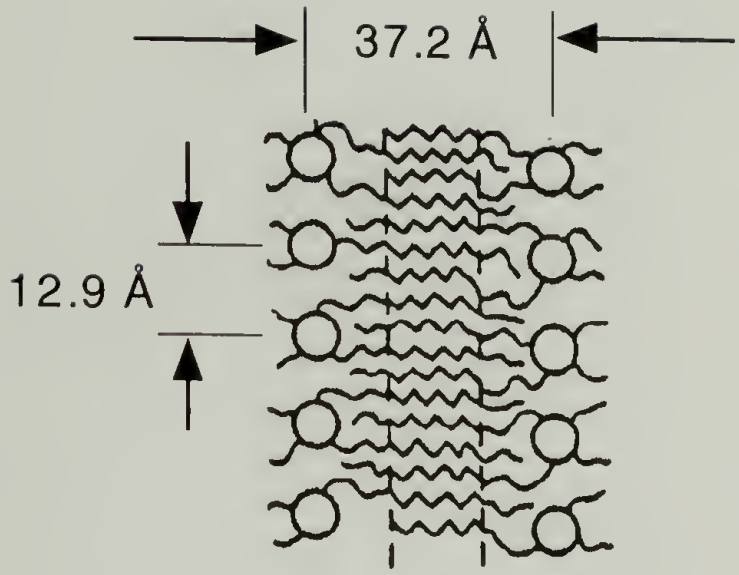

Figure 4.22 Schematic diagram of layer-like structure of C16O-PBLG-4 at 25°C showing the origin of 37.2 Å and 12.9 Å spacings.

4.4 References

1. Sohn, D.; Yu, H.; Nakamatsu, J.; Russo, P. S.; Daly, W. H. *J. Polym. Sci.: Polym. Phys.* **1996**, 34, 3025.

2. Ober, C. K.; Jin, J.-I.; Lenz, R. W. *Adv. Polym.Sci.* **1984**, 59, 103.

3. Smith, J. C.; Woody, R. W. *Biopolymers* **1973**, 12, 2657.

4. Mathy, A.; Mathauer, K.; Wegner, G.; Bubeck, C. *Thin Solid Films* **1992**, 215, 98.

5. Vogel, A.; Hoffmann, B.; Schwiegk, S.; Wegner, G. *Sensors Actuators* **1991**, B4, 65.

6. Watanabe, J.; Ono, H.; Uematsu, I.; Abe, A. *Macromolecules* **1985**, 18, 2141.

7. Watanabe, J. in *Ordering in Macromolecular Systems*; Teramoto, A.; Kobayashi, M.; Norisuye, T., Eds.; Springer: Berlin, 1993.

8. Mathauer, K.; Schmidt, A.; Knoll, W.; Wegner, G. *Macromolecules* **1995**, 28, 1214.

9. Ponomarenko, E. A.; Waddon, A. J.; Bakeev, K. N.; Tirrell, D. A.; MacKnight, W. J. *Macromolecules* **1996**, 29, 4340.

10. Ponomarenko, E. A.; Waddon, A. J.; Tirrell, D. A.; MacKnight, W. J. *Langmuir* **1996**, 12, 2169.

11. Hanabusa, K.; Sato, M.; Shirai, H.; Takemoto, K. *J. Polym. Sci.: Polym. Lett.* **1984**, 22, 559.

12. Iizuka, E.; Abe, K.; Hanabusa, K.; Shirai, H. *Current Topics in Polymer Science* **1987**, 1, 235.

13. Kricheldorf, H. R. *α-Aminoacid-N-Carboxy-Anhydrides and Related Heterocycles*; Springer: New York, 1987.

14. Ponomarenko, E. A.; Waddon, A. J.; Tirrell, D. A.; MacKnight, W. J. *Macromolecules* **1996**, 29, 8751.

15. Ponomarenko, E. A.; Waddon, A. J.; Tirrell, D. A.; MacKnight, W. J. *Macromolecules* **1998**, 131, 1584.

16. Block, H. *Poly(γ-benzyl-L-glutamate) and Other Glutamic Acid Containing Polymers;* Gordon & Breach: New York, 1993.

17. Steigman, J.; Verdini, A. S.; Montagner, C.; Strasorier, L. *J. Am. Chem. Soc.* **1969**, 91, 1829.

18. Zollinger, H. *Diazo Chemistry II*; VCH publishers: New York, 1995.

BIBLIOGRAPHY

Albrecht, C.; Lieser, G.; Wegner, G. *Prog. Colloid Polym. Sci.* **1993**, 92, 111.

Ambler, R. P. *Biochem. Soc. Trans.* **1991**, 19, 517.

Anakkar, A.; Daoudi, A.; Buisine, J.-M.; Isaert, N.; Bougrioua, F.; Nguyen, H. T. *Liq. Cryst.* **1996**, 20, 411.

Bamford, C. H.; Elliott, A.; Hanby, W. E. *Synthetic Polypeptides*; Academic Press: New York, 1956.

Beguin, A.; Billard, J.; Bonamy, F.; Buisine, J. M.; Cuvelier, P.; Dubois, J. C.; Le Barny, P. *Mol. Cryst. Liq. Cryst.* **1984**, 115, 9.

Berreman, D. W.; Meiboom, S.; Zasadzinski, J. A.; Sammon, M. J. *Phys. Rev. Lett.* **1986**, 57, 1737.

Block, H. *Poly(γ-benzyl-L-glutamate) and Other Glutamic Acid Containing Polymers*; Gordon & Breach: New York, 1993.

Bujard, H.; Gentz, R.; Lanzer, M.; Stueber, D.; Mueller, M.; Ibrahimi, I.; Haeuptle, M.-T.; Dobberstein, B. *Meth. Enzymol.* **1987**, 155, 416.

Bula, C.; Wilcox, K. W. *Protein Expression Purif.* **1996**, 7, 92.

Bunning, T. J. *Liq. Cryst.* **1994**, 16, 769.

Burlatsky, S.; Deutch, J. *Science* **1993**, 260, 1782.

Cabani, S.; Paci, A.; Rizzo, V. *Biopolymer* **1976**, 15, 113.

Cappello, J.; Crissman, J.; Dorman, M.; Mikolajczak, M.; Textor, G.; Marquet, M.; Ferrari, F. *Biotechnol. Prog.* **1990**, 6, 198.

Chandrasekhar, S. *Liquid Crystals*; Cambridge University Press: New York, 1977.

Chen, J. T.; Thomas, E. L.; Ober, C. K.; Mao, G.-p. *Science* **1996**, 273, 343.

Conticello, V. P.; Zhang, G.; Fournier, M. J.; Mason, T. L.; Tirrell, D. A. manuscript in preparation.

De Gennes, P. G.; Prost, J. *The Physics of Liquid Crystals*; Clarendon Press: Oxford, 1993.

Deming, T. J. *Nature* **1997**, 390, 386.

Deming, T. J. *J. Am. Chem. Soc.* **1998**, 119, 2759.

Demus, D.; Richter, L. *Textures of Liquid Crystals*; Chemie: Weinheim, 1978.

Doty, P.; Bradbury, J. H.; Holtzer, A. M. *J. Am. Chem. Soc.* **1956**, 78, 947.

Doty, P.; Wada, A.; Yang, J. T.; Bout, E. R. *J. Polym. Sci.* **1957**, 23, 851.

Duke, R. W.; Du Pre, D. B.; Hines, W. A.; Samulski, E. T. *J. Am. Chem. Soc.* **1976**, 98, 3094.

Du Pre, D. B.; Samulski, E. T. in *Liquid Crystals The Fourth State of Matter*; Saeva F. D., Ed.; Dekker: New York, 1979; pp 203.

Elliot, A. E.; Ambrose, E. J. *Discuss. Faraday Soc.* **1950**, 9, 246.

Enriquez, E. P.; Gray, K. H.; Guarisco, V. F.; Linton, R. W.; Mar, K. D.; Samulski, E. T. *J. Vac. Sci. Technol. A*, **1992**, 10, 2775.

Fasman, G. D. *Poly(α-amino acid)*; Marcel and Dekker: New York, 1967.

Flory, P. J. *Principles of Polymer Chemistry*; Cornell University Press: New York, 1953.

Flory, P. J. *Proc. Roy. Soc. (London)* **1956**, A234, 73.

Gibson, H. W. in *Liquid Crystals The Fourth State of Matter*; Saeva, F. D., Ed.; Macel Dekker, Inc: New York, 1979.

Goodby, J. W.; Waugh, M. A.; Stein, S. M.; Chin, E.; Pindak, R.; Patel, J. S. *J. Am. Chem. Soc.* **1989**, 111, 8119.

Goodby, J. W.; Waugh, M. A.; Stein, S. M.; Chin, E.; Pindak, R.; Patel, J. S. *Nature* **1989**, 337, 449.

Gray, G. W.; Goodby, J. W. G. *Smectic Liquid Crystals*; Heyden & Son, Inc: Philadelphia, 1984.

Hanabusa, K.; Sato, M.; Shirai, H.; Takemoto, K. *J. Polym. Sci.: Polym. Lett.* **1984**, 22, 559.

Horton, J. C.; Donald, A. M.; Hill, A. *Nature* **1990**, 346, 44.

Iizuka, E.; Abe, K.; Hanabusa, K.; Shirai, H. *Current Topics in Polymer Science* **1987**, 1, 235.

Inglis, A. S. *Meth. Enzymol.* **1983**, 91, 324.

Jaworek, T.; Neher, D.; Wegner, G.; Wieringa, R. H.; Schouten, A. J. *Science* **1998**, 279, 57.

Jones, R.; Tredgold, R. H. *J. Phys. D.* **1988**, 21, 449.

Karasz, F. E.; Gajinos, G. E. *Biopolymers* **1974**, 13, 725.

Kelman, M. in *Liquid Crystals, Magnetic Systems and Various Ordered Media*; John Wiley & Sons Ltd.: New York, 1983.

Kiss, G.; Porter, R. S.; *Mol. Cryst. Liq. Cryst.* **1980**, 60, 267.

Kleina, L. G.; Masson, J.-M.; Normanly, J.; Abelson, J.; Miller, J. H. *J. Mol. Biol.* **1990**, 213, 705.

Kresheck, G. C.; Kierleber, D.; Albers, R. J. *J. Am. Chem. Soc.* **1972**, 94, 8889.

Kricheldorf, H. R. *α-Aminoacid-N-Carboxy-Anhydrides and Related Heterocycles*; Springer: New York, 1987.

Kuliopulos, A.; Walsh, C. T. *J. Am. Chem. Soc.* **1994**, 116, 4599.

Lavrentovich, O. D.; Nastishin, Y. A.; Kulishov, V. I.; Narkevich, Y. S.; Tolochko, A. S.; Shiyanovski, S. V. *Europhys. Lett.* **1990**, 13, 313.

Le Grice, S. F. J.; Gruninger-Leitch, F. *Eur. J. Biochem.* **1990**, 187, 307.

Leninger, A. L. *Biochemistry*; Worth Publisher, Inc.: New York, 1970.

Lewin, B. *Genes V*; Oxford University Press: Oxord, 1994.

Lubensky, T. C.; *Renn, S. R. Phys. Rev. A* **1990**, 41, 4392.

Machidas, S.; Urano, T. I.; Sano, K.; Kawata, Y.; Sunohara, K.; Sasaki, H.; Yoshiki, M.; Mori, Y. *Langmuir* **1995**, 11, 4838.

Mahajan, S. K. in *Genetic Recombination*; Kucherlapati, R.; Smith, G. R., Eds.; American Society for Microbiology: Washington D.C., 1998; Ch. 3.

Makrides, S. C. *Microbiol. Rev.* **1996**, 60, 512.

Malcolm, B. R. *Proc. Roy. Soc. Ser. A* **1968**, 21, 449.

Markley, J. L.; Meadows, D. H.; Jardetzky, O. *J. Mol. Biol.* **1967**, 27, 25.

Mathauer, K.; Schmidt, A.; Knoll, W.; Wegner, G. *Macromolecules* **1995**, 28, 1214.

Mathy, A.; Mathauer, K.; Wegner, G.; Bubeck, C. *Thin Solid Films* **1992**, 215, 98.

Mawn, M. V.; Tirrell, D. A.; Mason, T. L. manuscript in preparation.

Mcardle, C. B. *Side Chain Liquid Crystal Polymers*; Blackie and Sons: Glasgow, 1989, 5.

McGrath, K. P.; Fournier, M. J.; Mason, T. L.; Tirrell, D. A. *J. Am. Chem. Soc.* **1992**, 114, 728.

McGrath, K. P.; Tirrell, D. A.; Kawai, M.; Mason, T. L.; Fournier, M. J. *Biotechnol. Prog.* **1990**, 6, 188.

Mckinnon, A. J.; Tobolsky, A. V. *J. Phys. Chem.* **1966**, 70, 1453.

McMaster, T. C.; Carr, H. J.; Miles, M. J.; Carins, P.; Morris, V. J. *Macromolecules* **1991**, 24, 1428.

McMillan, W. L. *Phys. Rev.* **1971**, A4, 1238.

Miller, W. *Liquid Crystals and Ordered Fluids*; Plenum: New York, 1993.

Nakamura, H.; Husimi, G.; Jones, P.; Wada, A. *J. Chem. Soc. Faraday II* **1977**, 73, 1178.

Nakano, K.; Fujita, Y.; Maeda, M.; Takagi, M. *Polymer* **1992**, 33, 3997.

Nguyen, H. T.; Bouchta, A.; Navailles, L.; Barois, P.; Isaert, N.; Twieg, R. J.; Maaroufi, A.; Destrade, C. *J. Phys. II* **1992**, 2, 1889.

Normanly, J.; Masson, J.-M.; Kleina, L. G.; Abelson, J.; Miller, J. H. *Proc. Natl. Acad. Sci.* **1986**, 83, 6548.

Ober, C. K.; Jin, J.-I.; Lenz, R. W. *Adv. Polym. Sci.* **1984**, 59, 103.

Papkov, S. P. *Advances in Polymer Science* **1984**, 59, 75.

Papkov, S. P.; Kulichikhin, V. G.; Kalmykova, V. D. *J. Polym. Sci., Polym. Phys. Ed.* **1974**, 12, 1753.

Parsons, D. F.; Martius, U. *J. Mol. Biol.* **1964**, 10, 530.

Peterson, H. T.; Matire, D. E. *J. Chem. Phys.* **1974**, 61, 3547.

Piszkiewics, D.; Landon, M.; Smith, E. L. *Biochem. Biophys. Res. Commun.* **1970**, 40, 1173.

Poland, D.; Scherga, H. A. *Theory of Helix-coil Transitions in Biopolymers*; Academic Press: New York, 1970.

Ponomarenko, E. A.; Waddon, A. J.; Bakeev, K. N.; Tirrell, D. A.; MacKnight, W. J. *Macromolecules* **1996**, 29, 4340.

Ponomarenko, E. A.; Waddon, A. J.; Tirrell, D. A.; MacKnight, W. J. *Langmuir* **1996**, 12, 2169.

Ponomarenko, E. A.; Waddon, A. J.; Tirrell, D. A.; MacKnight, W. J. *Macromolecules* **1996**, 29, 8751.

Ponomarenko, E. A.; Waddon, A. J.; Tirrell, D. A.; MacKnight, W. J. *Macromolecules* **1998**, 131, 1584.

Powers, J. C. Jr.; Peticolas, W. L. *Advances in Chemistry* #63; American Chemical Society: Washington D.C., 1967.

Powers, J. C. Jr.; Peticolas, W. L. *Biopolymers* **1970**, 9, 195.

Preston, J. In *Liquid Crystalline Order in Polymers* ; Blumstein, A., Ed.; Academic Press: New York, 1978; pp 141.

Price, C.; Harris, P. A.; Holton, T. J.; Stubbersfield, R. B. *Polymer* **1975**, 16, 69.

Rajan, V. T.; Woo, C.-W. *Phys. Rev. A* **1980**, 21, 990.

Renn, S. R.; Lubensky, T. C. *Phys. Rev. A* **1988**, 38, 2132.

Robinson, C. *Trans Faraday Soc.* **1956**, 52, 571.

Robinson, C.; Ward, J. C. *Nature* **1957**, 180, 1183.

Robinson, C.; Ward, J. C.; Beever, R. B. *Discuss. Faraday Soc.* **1958**, 25, 29.

Rosewell, D. F.; White, E. H. *Meth. Enzymol.* **1978**, 57, 409.

Rybnikar, F.; Geil, P. H. *Makromol. Chem.* **1972**, 158, 39.

Sambrook, J.; Fritsch, E. F.; Maniatis, T. *Molecular Cloning: A Laboratory Manual*, 2nd ed.; Spring Harbor Laboratory Press: New York, 1989.

Samulski, E. T.; Tobolsky, A. V. in *Liquid Crystals & Plastic Crystals*; Gray, G. W.; Winsor, P. A., Eds.; John Wiley & Sons Inc.: New York, 1974; pp 175.

Samulski, E. T.; Tobolsky, A. V. *Nature* **1967**, 216, 997.

Samulski, E. T.; Tobolsky, A. V. *Mol. Cryst. Liq. Cryst.* **1969**, 7, 433.

Samulski, E. T.; Tobolsky, A. V. *Biopolymers* **1971**, 10, 1013.

Samulski, E. T.; Tobolsky, A. V. in *Liquid Crystalline and Ordered Fluids*; Johnson, J. F.; Porter, R. S., Eds.; Plenum Press: New York, 1970; pp 111.

Schwartz, G. *Biopolymers* **1968**, 6, 873.

Smith, J. C.; Woody, R. W. *Biopolymers* **1973**, 12, 2657.

Sohn, D.; Yu, H.; Nakamatsu, J.; Russo, P. S.; Daly, W. H. *J. Polym. Sci.: Polym. Phys.* **1996**, 34, 3025.

Sorenson, M. A.; Pedersen, S. *J. Mol. Biol.* **1991**, 222, 265.

Steigman, J.; Verdini, A. S.; Montagner, C.; Strasorier, L. *J. Am. Chem. Soc.* **1969**, 91, 1829.

Stephens, R. M.; Bradbury, E. M. *Polymer* **1976**, 17, 563.

Straley, J. P. *Mol. Cryst. Liq. Cryst.* **1973**, 22, 333.

Stroobants, A.; Lekkerkerker, H. N. W. *Phys. Rev.* **1987**, A36, 2929.

Subramanian, R. J.; Wittebort, R. J.; DuPre, D. B. *Mol. Cryst. Liq. Cryst* **1982**, 97, 325.

Sugimoto, Y.; Yatsunami, K.; Tsujimoto, M.; Khorana, H. G. *Proc. Natl. Acad. Sci. USA* **1991**, 88, 3116.

Szwarc, M.; Van Beylen, M. *Ionic Polymerization and Living Polymers*; Chapman & Hall: New York, 1993.

Tsung, C. M.; Fraenkel-Conrat, H. *Biochemistry* **1965**, 4, 793.

Urano, T. K.; Machida, S.; Sano, K. *Chem. Phys. Lett.* **1995**, 242, 471.

Voet, D.; Voet, J. G. *Biochemstry*; John Wiley & Sons: New York, 1990.

Vogel, A.; Hoffmann, B.; Schwiegk, S.; Wegner, G. *Sensors Actuators* **1991**, B4, 65.

Vorlander, E. *Trans. Faraday Soc.* **1933**, 29, 907.

Wada, A. *J. Chem. Phys.* **1959**, 30, 328.

Watanabe, J. in *Ordering in Macromolecular Systems*; Teramoto, A.; Kobayashi, M.; Norisuye, T., Eds.; Springer: Berlin, 1993.

Watanabe, J.; Ono, H.; Uematsu, I.; Abe, A. *Macromolecules* **1985**, 18, 2141.

Wee, E. L.; Miller, W. G. *J. Phys. Chem.* **1970**, 75, 1446.

Wen, X.; Meyer, R. B.; Caspar, D. L. D. *Phys. Rev. Lett.* **1989**, 63, 2760.

Willcox, P. J.; Gido, S. P.; Muller, W.; Kaplan, D. L. *Macromolecules* **1996**, 29, 5106.

Wulfman, D. S.; Yousefian, S.; White, J. M. *Synth. Commun.* **1988**, 18, 2349.

Yu, S. M.; Conticello, V. P.; Zhang, G.; Kayser, C.; Fournier, M. J.; Mason, T. L.; Tirrell, D. A. *Nature* **1997**, 389, 167.

Zhang, G.; Fournier, M. J.; Mason, T. L.; Tirrell, D. A. *Macromolecules* **1992**, 35, 3601.

Zollinger, H. *Diazo Chemistry II*; VCH publishers: New York, 1995.